

SUPPORTING INFORMATION

Intensified Continuous Flow Synthesis of Oxazolidones

*Lionel Crane,^{1,2} Thomas Habets,¹ Bruno Grignard,^{1,3} Jean-Christophe Monbaliu,^{*2,4} Pierre Stiernet,^{*1}
Christophe Detrembleur^{*1,4}*

¹ Center for Education and Research on Macromolecules (CERM), CESAM Research Unit, University of Liège, Sart-Tilman B6a, 4000 Liege, Belgium.

² Center for Integrated Technology and Organic Synthesis, MolSys Research Unit, University of Liège, Sart-Tilman B6a, 4000 Liege, Belgium.

³ FRITCO2T Platform, CESAM Research Unit, University of Liege, Sart-Tilman B6a, 4000 Liège, Belgium.

⁴WEL Research Institute, avenue Pasteur, 6, 1300 Wavre, Belgium.

Number of pages: 55 pages

Number of tables: 3 tables

Number of figures: 10 figures

TABLE OF CONTENTS

1. Materials and instrumentation	2
2. Experimental procedures	6
3. DFT methodology	10
4. Supplementary figures and tables	11
5. Calculation of conversions and selectivities	24
6. Structural characterisation	30
7. References	54

1. Materials and instrumentation

Materials

1,8-diazabicyclo[5.4.0]undec-7-ene (DBU) (99%), polystyrene-supported DBU, heptylamine (99%), cyclohexylamine (>99%), 2-ethyl-1-hexylamine (98%), allylamine (98%), oleylamine (98%), 3-amino-1-propanol (99%), benzylamine (99%), furfurylamine (99%), aniline (99%), 4-(aminomethyl)pyridine (98%), 3-(Dimethylamino)-1-propylamine (99%), 1-(3-aminopropyl)imidazole (97%), 2-phenylbut-3-yn-2-ol (98%), 2-methyl-3-butyn-2-ol (98%) and p-Anisidine (99%) were purchased from Sigma-Aldrich. Dimethyl sulfoxide (DMSO) (>99%), and propargylamine (97%) was supplied by Fluorochem. 1-Ethynyl-1-cyclohexanol (99%) was purchased by Fisher Scientific. 2-methoxyethylamine (98%), 3,5-Dimethyl-1-hexyn-3-ol (98%), and 3-methyl-1-penten-4-yn-3-ol (98%) were acquired by Merck. Propylamine (99%) was provided by Fluka Chemika. Acetic acid glacial (>99%) and acetonitrile (>99%) were purchased from VWR, while deuterated dimethyl sulfoxide (DMSO-*d*₆) (>99%) was supplied by Eurisotop.

Characterization methods

Nuclear magnetic resonance (NMR) spectroscopy. NMR analyses were performed on Bruker 400 MHz spectrometers. Conversion and selectivity were determined by ¹H NMR. The structure of the products was determined by ¹H NMR and ¹³C NMR spectroscopy (400 MHz Bruker Avance spectrometer) in DMSO-*d*₆. Chemical shifts are reported in ppm relative to TMS as internal standard or to reagent residual peak.

High resolution mass spectrometry (HRMS). ESI-MS data were acquired on a Waters Synapt G2-Si mass spectrometer (Waters, UK) equipped with an Electrospray ionization source used in the positive ion mode. Samples were prepared as followed, 1mg/mL solution in Acetonitrile solution were diluted 500 times to reach a final concentration of 2.10⁻⁶ g/mL. For the mass spectrometer parameters, the Electrospray ionization (ESI) conditions were capillary voltage 3.1 kV; cone voltage 30 V; source temperature 120 °C; desolvation temperature 150 °C. Dry nitrogen, the desolvation gas, is used as the ESI gas with a flow rate of 500 L.h⁻¹. Mass accuracy measurement (HRMS) was performed by using lock spray unit, available on the source ion block, by infusing NaI solution as reference to perform internal calibration.

Fourier Transform Infrared Spectra (FT-IR). FTIR measurements were carried out on a Nicolet IS5 spectrometer (Thermo Fisher Scientific) equipped with a diamond attenuated transmission reflectance (ATR) device. 32 scans were recorded for each sample over the range 4000-500 cm⁻¹ with a normal resolution of 4 cm⁻¹.

Microfluidic setup

The continuous-flow setup was composed of PFA tubing 1/16 (1.58 mm outer diameter, 762 μm internal diameter) connected using super flangeless PEEK connectors and ferrule fitting for 1/16" OD tubing. Injekt™ Syringe 20 mL Luer Lock were used for the feed solutions, which were connected to each other using a PEEK T-mixer. The whole setup was carried by a Chemyx Fusion 4000-X independent dual-channel infusion and was thermocontrolled with a heating magnetic stirrer serie MR Hei Model Hei-Tec with a PT 1000 temperature sensor. To enhance the mixing, the column of supported DBU was immersed in the Branson 1510 Ultrasonic bath (frequency of 40 kHz) at 70 °C. A thermometer was immersed in the ultrasonic bath to monitor the effective temperature of the system.

<i>Item</i>	<i>Details</i>	<i>Vendor</i>	<i>Reference</i>
Connectors	Super Flangless Nuts, natural PEEK 1/4-28 thread for 1/16" OD tubing	IDEX/Upchurch Scientific	P-255X
	Super Flangeless Ferrule Tefzel (ETFE), SS ring 1/4-28 thread for 1/16" OD tubing	IDEX/Upchurch Scientific	P-259X
Mixers	T-mixer, natural PEEK 1/4-28 thread for 1/16" o.d. tubing, 0.02" through hole	IDEX/Upchurch Scientific	P-712
Tubings	High-purity PFA tubing, 1.58 mm outer diameter, 762 μm internal diameter	VICI (Valco Ins. Co. Inc.)	JR-T-4002-M25
Syringes	B. BRAUN Injekt™ syringes 20 mL Luer Lock	Lab Unlimited carl stuart group	4AJ-6702740
	20cc stainless steel syringe with 1/16th and 1/8th Swagelok fitting	KR Analytical Ltd	SS020
Syringe pump	High force Chemyx Fusion 4000-X independent motors dual syringe pumps	KR Analytical Ltd	74000-X
BPR	Back Pressure Regulator P-785, 40 psi (2,8 bar), volume of 131 μl, PEEK	Upchurch Scientific	554-3197

Calculation of the fluidic metrics:

1) Daily output (g d⁻¹)

$$\text{Daily output} = \text{Flow rate} * \text{Conc.} * \text{MM} * 1.44 * \frac{\text{yield}}{100}$$

Where the flow rate corresponds to the individual feeding flow rate of reactant (αCC) (ml min⁻¹), Conc. is the concentration of the corresponding αCC (in mol L⁻¹) and MM is the molar mass of the formed oxazolidone (g mol⁻¹). 1.44 is a factor to obtain the value in the final metric (g d⁻¹).

2) Space-time yield (STY) (kg L⁻¹ h⁻¹)

$$\text{STY} = m_p * (T_R * V_R)^{-1} \Rightarrow \text{STY} = \frac{\text{Flow rate} * \text{Conc.} * \text{MM} * 0.06}{V_R} * \frac{\text{yield}}{100}$$

Where m_p is the amount of product formed within the residence time (T_R) and V_R is the volume of the reactor. m_p, T_R, and V_R are expressed in kg, hour, liter respectively. The flow rate corresponds to the individual feeding flow rate of reactant (αCC) (ml min⁻¹), Conc. is the concentration of the αCC 1a (mol L⁻¹) and MM is the molar mass of the formed oxazolidone 3a (g mol⁻¹). We considered the yield obtained before purification.

3) Productivity per catalyst amount ($\text{mmol h}^{-1} \text{mmol}_{\text{cat}}^{-1}$)

$$\text{Productivity per catalyst amount} = \frac{\text{Flow rate} * \text{Conc.} * 60}{n(\text{Cat})} * \frac{\text{yield}}{100}$$

Where the flow rate corresponds to the individual feeding flow rate of reactant (αCC) (mL min^{-1}), Conc. is the concentration of the corresponding αCC (in mmol mL^{-1}) and $n(\text{cat})$ is the molar amount of the catalyst loaded in the packed column ($\text{mmol}_{\text{cat}}^{-1}$). 60 is a factor to obtain the value in the final metric ($\text{mmol h}^{-1} \text{mmol}_{\text{cat}}^{-1}$).

4) E-factor

$$E - \text{factor} = \frac{\sum m_{\text{input}} - m_{\text{product}}}{m_{\text{product}}}$$

Where “m” corresponds to the mass (expressed in g).

Considering a 30 min run:

Condition A for 3a		Condition B for 3c	
- DMACC	1.50 g	- DMACC	2.28 g
- Amine	1.35 g	- Amine	2.30 g
- DMSO	4.66 g	- Acetonitrile	2.45 g
- DBU	0.09 g	- DBU	0.14 g
- Diethyl Ether	214.20 g	- Diethyl Ether	
	107.10 g		
- Hexane	65.90 g	- Hexane	32.95 g
- Silica	50 g	- Silica	25 g
- 3a	2.10 g	- 3c	2.80 g
E- factor	160	E-factor	61

For **3p**, and **3r**, a precipitation was performed as purification using diethyl ether (21.42 g) and hexane (6.59 g).

5) Process Mass Intensity (PMI)

$$PMI = \frac{\sum m_{\text{input}}}{m_{\text{product}}}$$

Where “m” corresponds to the mass (expressed in g).

Considering a 30 min run:

Condition A for 3a		Condition B for 3c	
- DMACC	1.50 g	- DMACC	2.28 g
- Amine	1.35 g	- Amine	2.30 g
- DMSO	4.66 g	- Acetonitrile	2.45 g
- DBU	0.09 g	- DBU	0.14 g
- Diethyl Ether	214.20 g	- Diethyl Ether	
	107.10 g		

- Hexane	65.90 g	- Hexane	32.95 g
- Silica	50 g	- Silica	25 g
- 3a	2.10 g	- 3c	2.80 g
PMI	161	PMI	62

6) Atom economy (AE)

$$AE = \frac{\text{Molecular weight product}}{\sum \text{Molecular weight reagents}}$$

Considering the formation of **3a**:

Molecular weight of α CC (**1a**): 128.13 g.mol⁻¹

Molecular weight of heptylamine (**A1**): 115.22 g.mol⁻¹

Molecular weight of hydroxy-oxazolidone **3a**: 243.35 g.mol⁻¹

The process displays an atom economy of 100%.

7) Calculation of the amount (equivalent) of DBU in the supported system vs α CC

α CC syringe concentration: 1.95 mol/L

- α CC flow rate: 0.0173 mL/min
- Amine flow rate: 0.0050 mL/min
- Total flow: 0.0223 mL/min

The effective α CC concentration in the column is therefore:

$$C_{\alpha\text{CC, column}} = 1.95 \times 0.0173 / 0.0223 = 1.51 \text{ mol/L}$$

With an internal column volume of 0.332 mL, the instantaneous amount of α CC is:

$$n_{\alpha\text{CC, column}} = 1.51 \times 0.000332 \text{ L} = 0.502 \text{ mmol}$$

Accordingly, the supported DBU amounts (0.352–0.586 mmol) correspond to 0.70–1.17 equivalents, which we reported in the manuscript as 0.7–1.2 equiv.

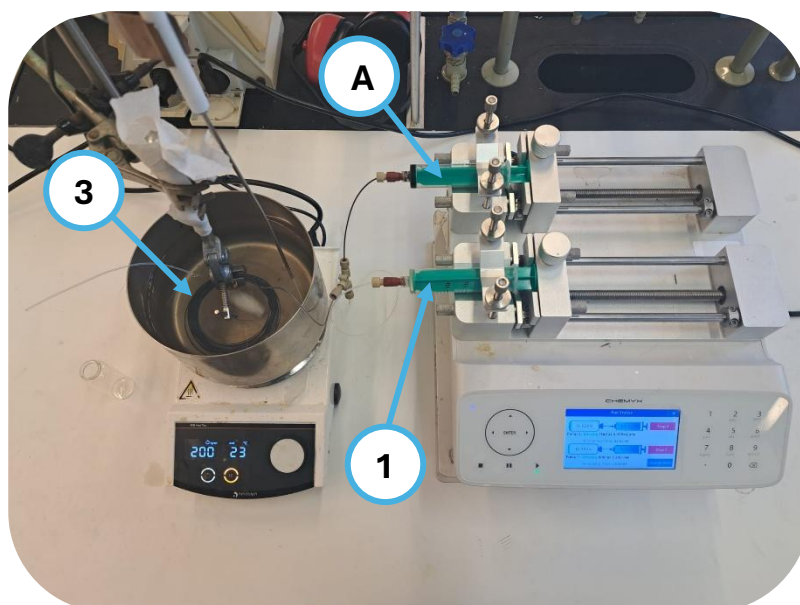
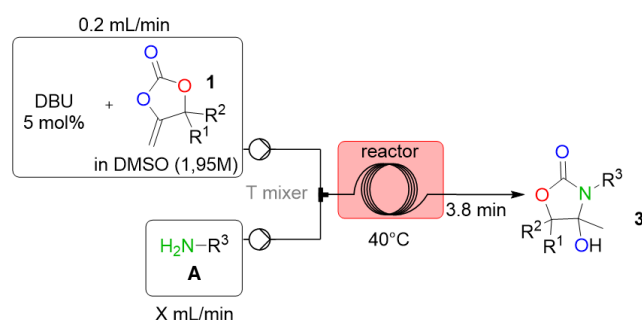
2. Experimental procedures

General procedure for the continuous flow synthesis of oxazolidones in DMSO (Condition A)

A solution of α CC (**1**) at 1.95 M in dry DMSO, with DBU at 5 mol% was prepared and the pure liquid primary amine are inserted into two distinct 20 mL syringes. The α CC solution was injected within the reactor via a T-shape mixer at a flow rate of 0.200 mL.min⁻¹. The amine flow rate varied for each amine in order to be inject 1 equivalent vs α CC, that can be calculated using this equation:

$$\text{Amine flow rate} = \frac{\text{Conc.}_{\alpha\text{CC}} \left(\frac{\text{mol}}{\text{L}}\right) * \text{Flow rate}_{\alpha\text{CC}} \left(\frac{\text{L}}{\text{min}}\right) * \text{Molar Mass}_{\text{amine}} \left(\frac{\text{g}}{\text{mol}}\right)}{\text{Density}_{\text{amine}} \left(\text{g/mL}\right)}$$

The reaction took place a 0.9860 mL PFA reactor thermostabilized at 40°C, the retention time (Tr) slightly depends on the total flow rate (α CC + amine) and varied between 3.0 and 4.3 min. After 1.5 * Tr, the solution was collected for 1 min into 600 μ L of DMSO-*d*₆ for analysis by ¹H-NMR. Then, the solution (about 30 min of collection) was collected directly in a vessel containing 20 mL of hexane and 20 mL of diethyl ether under strong agitation. The oxazolidones were purified by column chromatography on silica gel using Hexane/Diethyl ether as eluent (from 100/0 to 25/75 in volume) to give the products.



The procedure was adapted for p-anisidine which is solid at room temperature. A solution of α CC (**1a**) at 2.60 M in dry DMSO, with DBU at 5 mol%, and the second solution with p-Anisidine at 3.28

M in dry DMSO were prepared and inserted into two distinct 20 mL syringes. The α CC solution was injected within the reactor via a T-shape mixer at a flow rate of 0.150 mL.min⁻¹, while the amine was injected at a flowrate of 0.119 mL.min⁻¹. The reaction took place a 0.9860 mL PFA reactor thermostabilized at 40°C. After 1.5 * Tr, the solution was collected for 1 min into 600 μ L of DMSO-*d*₆ for analysis by ¹H-NMR.

General procedure for the continuous flow synthesis of oxazolidones in ACN (Condition B)

Solution of α CCs (**1**) at 3.5 M in ACN, with DBU at 5 mol% were prepared and then inserted in a 20 mL syringe. The pure liquid primary amines (**A**) were placed in another 20 mL syringe. The solution of α CC was injected within the reactor via a T-shape mixer at 0.17 mL.min⁻¹, while the amine was injected at a flow rate that varies depending on the amine to inject an equimolar amount vs the α CCs. The reaction took place in a 1.6630 mL PFA reactor thermostabilized at 80°C. The retention time slightly depended on the total flow rate (α CC + amine) and varied between 4.6 and 7.5 min. After 1.5 * Tr, the solution was collected during 1 min into 600 μ L of DMSO-*d*₆ to be analyzed by ¹H-NMR without purification. Then, the reactor output dropped the rest of the solution (about 30 min of collection) directly in a vessel containing 20 mL of hexane and 20 mL of diethyl ether under strong agitation. Then, the products were purified by column chromatography on silica gel (Hexane/Diethyl ether) (from 100/0 to 25/75) to give the products as yellowish oils or a white solids depending on the amine used. **3n**, **3p**, and **3r** were purified just by precipitation in 50/50 mixture of Hexane/Diethyl ether and then washed with cold diethyl ether.

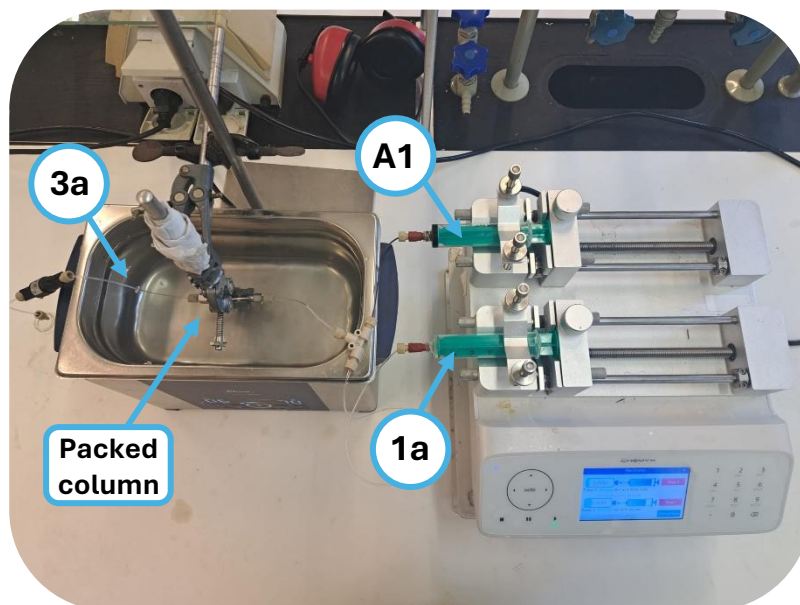
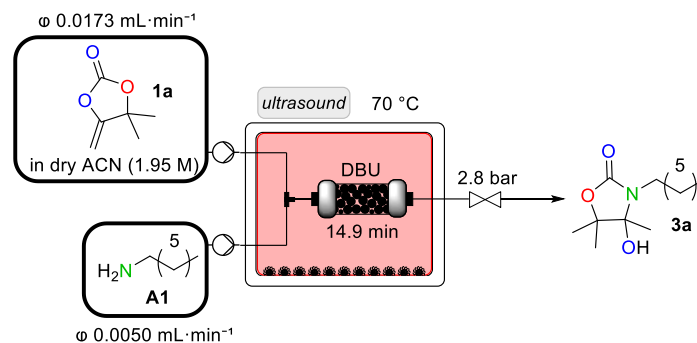
The procedure was adapted for p-anisidine which is solid at room temperature. Solution of α CC (**1a**) at 4.96 M in ACN, with DBU at 5 mol% were prepared and then inserted in a 20 mL syringe. Another solution with p-Anisidine (**A16**) at 5.00 M was prepared and placed in another 20 mL syringe. The solution of α CC was injected within the reactor via a T-shape mixer at 0.120 mL.min⁻¹, while the amine was injected at 0.119 mL.min⁻¹. The reaction took place in a 1.6630 mL PFA reactor thermostabilized at 80°C. After 1.5 * Tr, the solution was collected during 1 min into 600 μ L of DMSO-*d*₆ to be analyzed by ¹H-NMR without purification. Then, the reactor output dropped the rest of the solution (about 30 min of collection) directly in a vessel containing 20 mL of hexane and 20 mL of diethyl ether under strong agitation. Then the products were purified by column chromatography on silica gel (Hexane/Diethyl ether) (from 100/0 to 25/75) to give a white solid.

General procedure for the continuous flow synthesis of oxazolidones in 28.3 min (Condition C)

Solution of α CC (**1a**) at 4.96 M in ACN, with DBU at 5 mol% were prepared and then inserted in a 20 mL syringe. Another solution with p-Anisidine (**A16**) at 5.00 M was prepared and placed in another 20 mL syringe. The solution of α CC was injected within the reactor via a T-shape mixer at 0.060 mL.min⁻¹, while the amine was injected at 0.060 mL.min⁻¹. The reaction took place in a 3.396 mL PFA reactor thermostabilized at 80°C. After 1.5 * Tr, the solution was collected during 1 min into 600 μ L of DMSO-*d*₆ to be analyzed by ¹H-NMR without purification.

Continuous flow preparation of hydroxy-oxazolidones using supported DBU.

Pictures of the set-up:



Synthesis of oxazolidones in flow using solvent free conditions.

A liquid α CC (**1c** or **1d**) and liquid amine (**A1** or **A9**) were placed into two distinct 20 mL syringes. The α CC solution was injected within the reactor via a T-shape mixer at a flow rate of 0.16 mL·min⁻¹, while the amine flowrate was set to inject an equimolar amount compared to the α CC. The reaction took place with residence time t_r between 47 and 55 sec in a 0.2773 mL PFA reactor thermostabilized at 120°C. After 1.5 minutes, the solution was collected during 1 min into 600 μ L of DMSO-*d*₆ for analysis by ¹H-NMR.

α CC	Amine	ϕ Amine (mL/min)	t_r (sec)
1c	A1	0.153	51
1c	A9	0.130	55
1d	A1	0.188	47
1d	A9	0.160	52

Monitoring the exothermicity of batch reactions

Concentration of 1.95 M: In a glass vial were introduced 0.75 g of **1a** (5.86 mmol, 1 eq), 43.7 μL of DBU (0.293 mmol, 0.05 eq) and then DMSO until the total volume reaches 3 mL. The sensor of the RS PRO 1384 4-input Data Logging Thermometer was dipped into the solution. Then to this vial was added 869 μL of **A1** (5.86 mmol, 1 eq).

Concentration of 3.5 M: In a glass vial were introduced 1.34 g of **1a** (10.5 mmol, 1 eq), 78.4 μL of DBU (0.525 mmol, 0.05 eq) and then ACN/DMSO until the total volume reaches 3 mL. The sensor of the RS PRO 1384 4-input Data Logging Thermometer was dipped into the solution. Then to this vial was added 1.56 mL of **A1** (10.5 mmol, 1 eq).

Hydrolysis of **1a**.

In a glass vial were introduced 1.34 g of **1a** (10.5 mmol, 1 eq), 78.4 μL of DBU (0.525 mmol, 0.05 eq) and then DMSO until the total volume reached 3 mL. To this vial was added 189 μL of deionized water (10.5 mmol, 1 eq). Then, the reaction was run at 80 or 140 $^{\circ}\text{C}$ and the hydrolysis rate monitored over time. Conversions were determined by ^1H NMR spectroscopy by monitoring the apparation of the signal characteristic of the hydroxyketone **2** at 2.19 ppm

Kinetic monitoring of aminolysis of **1a** with different amines.

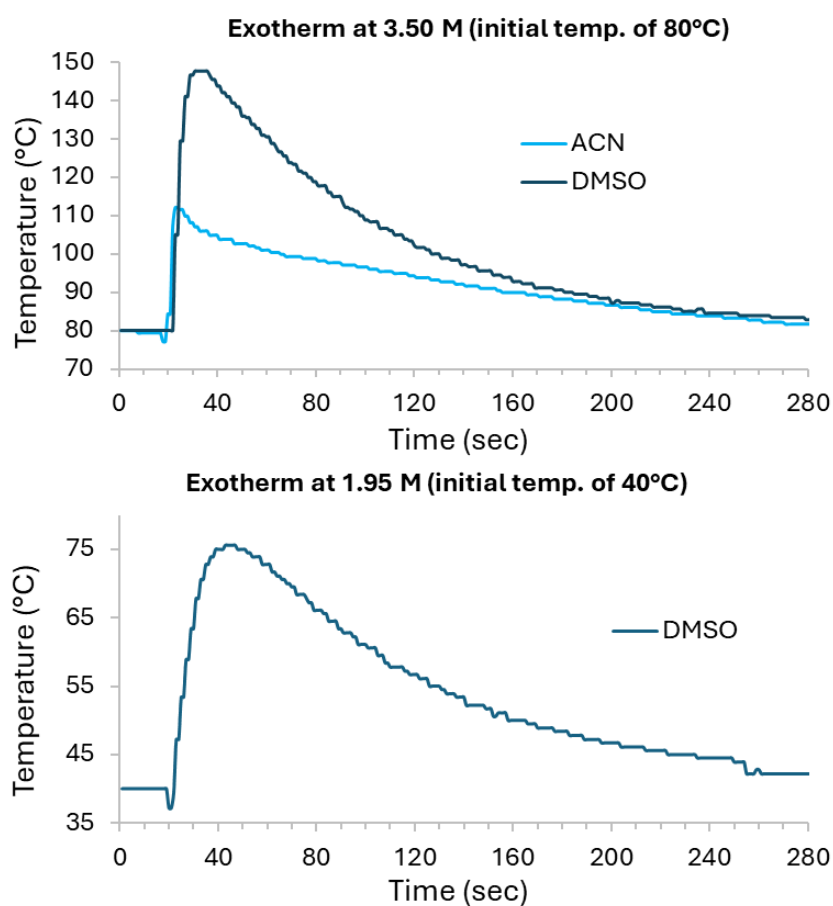
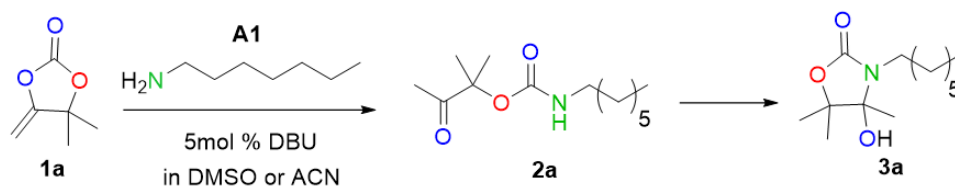
In a glass vial were introduced 192 mg of **1a** (1.5 mmol, 1 eq), 11.2 μL of DBU (0.075 mmol, 0.05 eq) and then ACN until the total volume reaches 3 mL. To this vial was added either, 123 μL of **A2** (1.5 mmol, 1 eq), or 172 μL of **A4** (1.5 mmol, 1 eq), or 137 μL of **A15** (1.5 mmol, 1 eq). The reaction was realized at 25 $^{\circ}\text{C}$ and the kinetic was monitored by ^1H NMR over 4 h.

3. DFT methodology

The aminolysis α CC has been previously studied with and without the addition of a catalyst. It revealed that catalyst-free aminolysis works fine but is as expected much slower than the catalyzed reaction.¹ In this work, we studied the aminolysis in presence of DBU as the catalyst. Propylamine, cyclohexylamine and aniline were selected as the reference amines to react with DMACC.

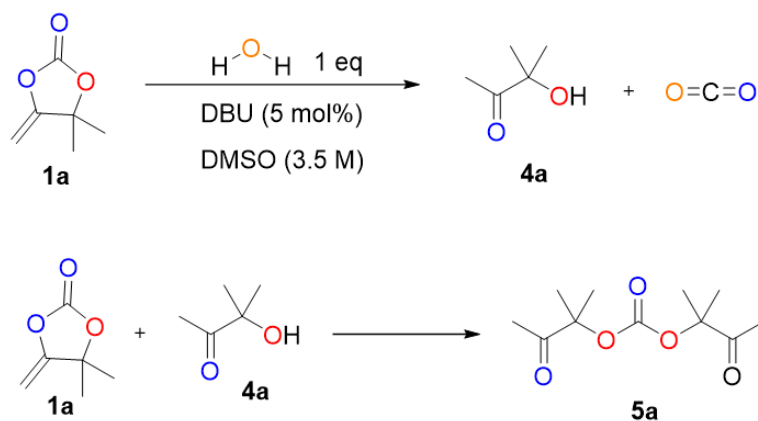
Methodology. All calculations were performed using the quantum chemistry package Gaussian (version 16, Revision C.01).² All geometry optimizations and transition state (TS) searches were done using the range-separated hybrid functional $wB97X-D$,³ consistent with previously reported work on similar molecules.^{4,5,6} This is a hybrid functional which accounts for non-covalent interactions through an adjusted Grimme D2 dispersion scheme. It is used in combination with a triple- ζ basis set adding polarization and diffuse functions to accurately describe TSs and anionic species (6-311++G(d,p)). Furthermore, this functional has given reliable results for medium sized organic molecules and was reviewed as one of the hybrid functionals to use in atomistic calculations by Mardirossian et al.⁷ The conductor-like polarizable continuum model (CPCM)⁸ was used with acetonitrile as the solvent, providing implicit representation of the matrix environment. Transition-, reactant- and product states are identified by means of a frequency analysis which results in a single negative frequency for a TS and all positive frequencies for reactant - and product states. Additionally intrinsic reaction coordinate (IRC) calculations are performed to assess the correctness of the transition state and obtain corresponding pre- and post-reactive complexes which were then further optimized.^{9,10,11,12} To consider enthalpic and entropic effects, the energies mentioned in this study correspond to the Gibbs free energy. A conformational analysis for reactant -, product - and transition states, has been performed manually using chemical instinct and to best fit with the reaction path and mechanism. Only the most favorable conformations are shown and discussed in this work. Pre- and post-reactive complexes were only optimized starting from the IRC results and were hence not further conformationally analyzed. Electronic energies were computed (Single point energy) at the M08-HX/6-311+G(d,p) level¹³ with CPCM model (acetonitrile) to better estimate the barriers' energy. Concentration (3.5 M), temperature (353.15 K) and quasi-harmonic factors (Grimme method for entropy and Head-Gordon method for enthalpy correction, scaling factor = 1) were included using the open-access Python toolkit Goodvibes v3.0.1.¹⁴ To carried out this work, we followed best-practices described in the following work: Best-Practice DFT Protocols for Basic Molecular Computational Chemistry.¹⁵

4. Supplementary figures and tables



*

Figure S1. Temperature profiles monitored during the batch reaction of **1a** with **A1** in presence of 5 mol% of DBU in DMSO or ACN at different concentrations and bath temperatures.



Entry	Temp. (°C)	Time (min)	Conv. of 1a (%)	4 (%)	5 (%)
1	80	0.5	8	>7	<1
2	80	1	11	>10	<1
3	80	2	14	13	1
4	140	0.5	38	35	3
5	140	1	52	46	6
6	140	2	62	52	10

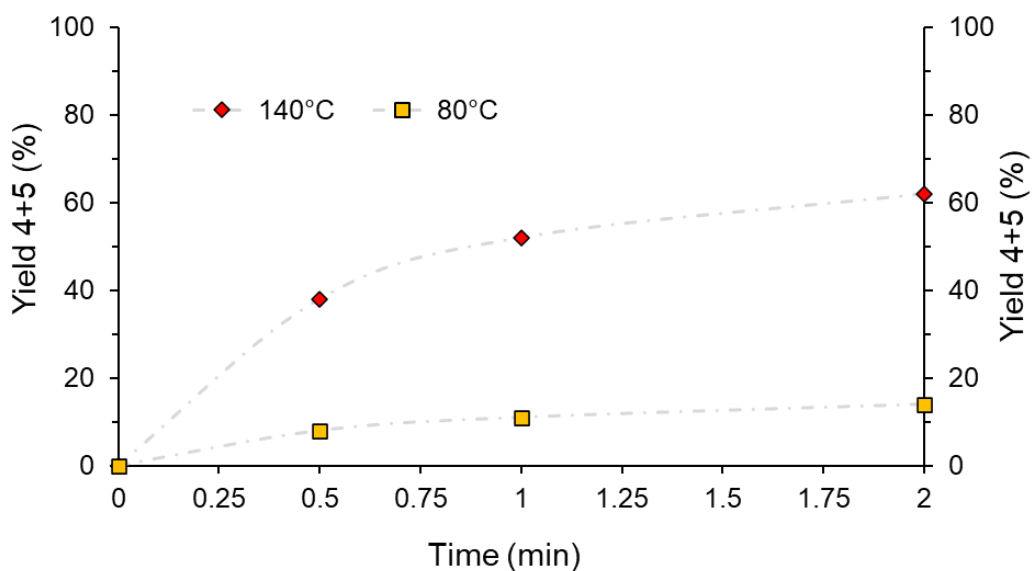


Figure S2: Hydrolysis of **1a** with 1 equiv. of water at 80 and 140 °C in DMSO (3.5 M) and with 5 mol% DBU. The formation of product **2** and the side-product **3** was monitored by ^1H NMR.

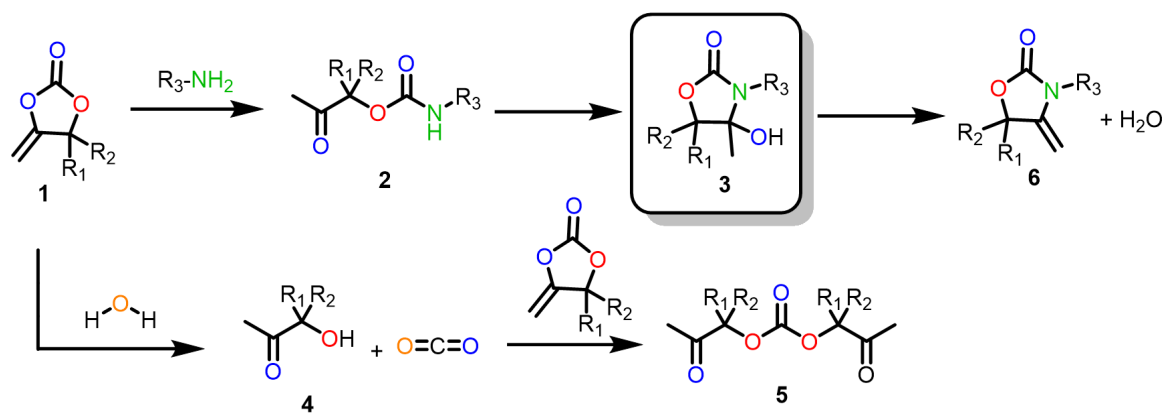


Figure S3. Scheme of all the different species that can be found in the crude reaction mixtures besides the expected hydroxyoxazolidone (3).

Table S1. Oxazolidone scope along with the different metrics reported in the main document.

<i>Entry</i>	<i>Product</i>	<i>Cond.</i>	<i>Conv. (%)</i>	<i>Selec. (%)</i>	<i>Isolated yield (%)</i>	<i>STY (kg L⁻¹ h⁻¹)</i>	<i>Production (g day⁻¹)</i>	<i>E-Factor</i>	<i>PMI</i>
1	3a	A	98	>99	74	5.64	133	160	161
2		B	>99	98	--	5.11	204	--	--
3	3b	A	96	>99	70	4.26	101	219	220
4		B	--	--	--	--	--	--	--
5	3c	A	82	70	--	3.49	83	--	--
6		B	>99	96	61	5.30	212	61	62
7	3d	A	62	49	20	1.62	38	636	637
8		B	--	--	--	--	--	--	--
9	3e	A	>99	>99	--	6.73	159	--	--
10		B	>99	>99	98	6.08	243	34	35
11	3f	A	89	93	--	5.57	132	--	--
12		B	95	99	94	5.76	230	35	36
13	3g	A	>99	>99	--	6.02	142	--	--
14		B	96	>99	94	5.26	210	39	40
15	3h	A	>99	98	--	7.10	168	--	--
16		B	>99	>99	04	6.56	262	--	--
17	3i	A	92	99	76	4.00	95	203	204
18		B	--	--	--	--	--	--	--
19	3j	A	93	>99	54	4.02	95	290	291
20		B	--	--	--	--	--	--	--
21	3k	A	92	91	--	7.82	185	--	--
22		B	98	99	75	8.24	329	32	33
23	3l	A	83	99	--	3.98	94	--	--
24		B	>99	>99	86	4.36	174	54	55
25	3m	A	99	>99	--	5.42	128	--	--
26		B	>99	>99	40	4.94	197	104	105
27	3n	A	>99	65	--	3.11	74	--	--
28		B	--	--	--	--	--	--	--
29	3o	A	63	98	61	3.32	79	209	210
30		B	--	--	--	--	--	--	--
31	3p	A	94	99	--	5.60	132	--	--
32		B	96	97	93	5.06	202	7	8
33	3q	A	81	96	--	4.35	103	--	--
34		B	98	>99	49	4.95	198	82	83
35	3r	A	95	97	--	5.16	122	--	--
36		B	96	>99	95	4.87	194	8	9
37	3s	A	05	>99	--	0.25	6	--	--
38		B	14	>99	--	0.66	27	--	--
39	3t	A	24	93	--	1.30	31	--	--
40		B	29	74	30	1.16	46	127	128
41		C	31	87	--	0.50	41	--	--

Condition A = reactions performed in dry DMSO 1.95 M, 40 °C, 5 mol% DBU, 3.0 – 4.3 min; Condition B = reactions performed in ACN 3.5 M, 80 °C, 5 mol% DBU, 4.6 – 7.5 min; Condition C = reactions performed in ACN 3.5 M, 80 °C, 5 mol% DBU, 28.3 min.

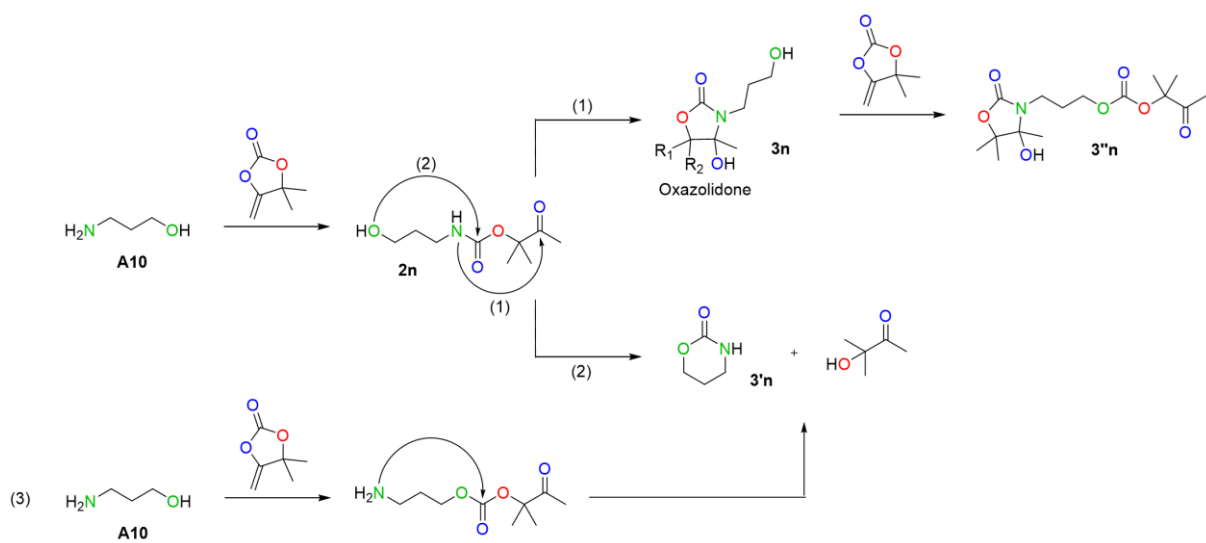
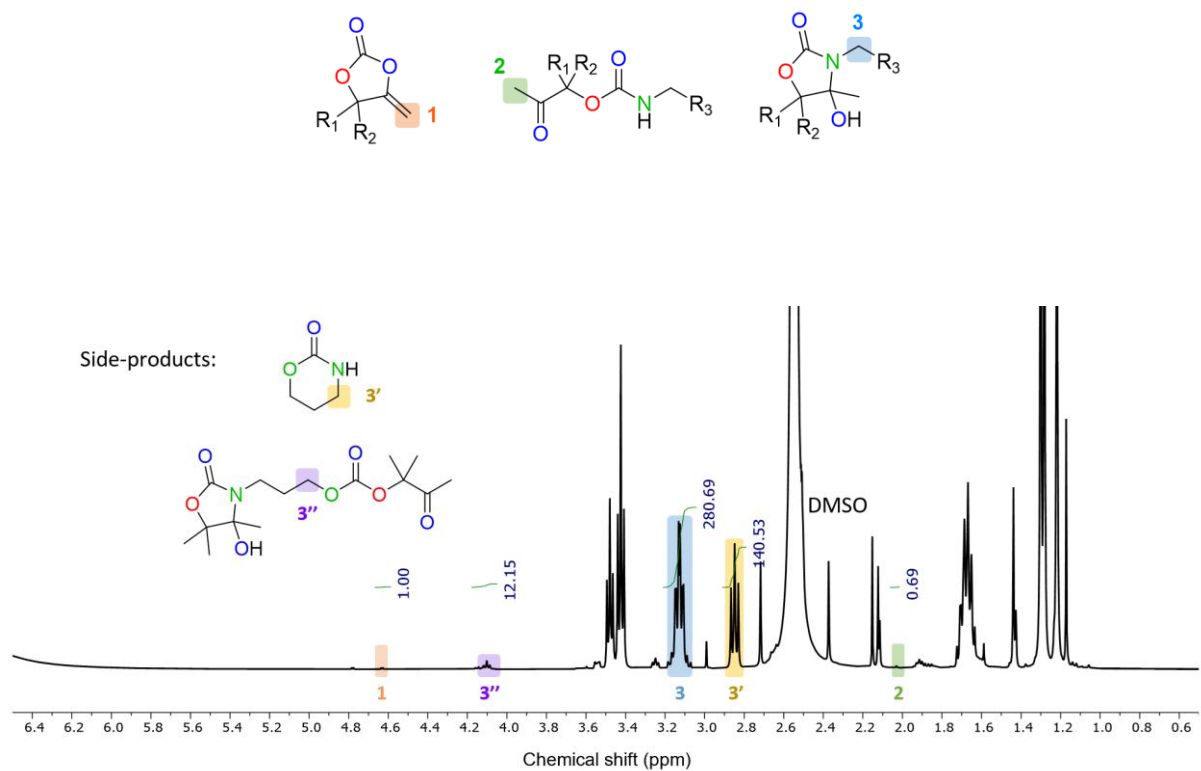


Figure S4. ^1H NMR spectrum of the crude reaction mixture of **1a** and **A10** affording 66 % of the desired product **3n** along with side-products **3'n** and **3''n**.

Table S2. DFT calculated energies corrected with Goodvibes (see DFT section)

	propyl	cyclohexyl	phenyl	propyl	Cyclohex	phenyl
	Hartree			kcal mol ⁻¹		
	Delta G			Delta G		
Amine	-174.401989	-291.086287	-287.519601			
αCC	-459.012929	-459.012929	-459.012929			
DBU	-461.887515	-461.887515	-461.887515			
Reagents +cata.	-1095.302433	-1211.986731	-1208.420045	0.00	0.00	0.00
reverse	-1095.29185	-1211.974971		6.64	7.38	
TS0	-1095.274665	-1211.957153		17.42	18.56	
forward	-1095.278004	-1211.958793		15.33	17.53	
reverse	-1095.278416	-1211.958766	-1208.411341	15.07	17.55	5.46
TS1	-1095.278313	-1211.958284	-1208.383680	15.14	17.85	22.82
forward	-1095.283492	-1211.963636	-1208.396698	11.89	14.49	14.65
reverse	-1095.290015	-1211.971663	-1208.404007	7.79	9.46	10.06
TS2	-1095.289761	-1211.971658	-1208.401148	7.95	9.46	11.86
forward	-1095.301374	-1211.985956	-1208.410855	0.66	0.49	5.77
reverse	-1095.307484	-1211.990424	-1208.426368	-3.17	-2.32	-3.97
TS3	-1095.299549	-1211.982659	-1208.408245	1.81	2.56	7.40
forward	-1095.32318	-1212.007244	-1208.432309	-13.02	-12.87	-7.70
Isolated oxo-urethane	-633.441348	-750.124707	-746.548062			
Iso. oxo-urethane+DBU	-1095.328863	-1212.012222	-1208.435577	-16.58	-16.00	-9.75
reverse	-1095.315346	-1211.99514	-1208.421451	-8.10	-5.28	-0.88
TS4	-1095.306667	-1211.985499	-1208.415972	-2.66	0.77	2.56
forward	-1095.310012	-1211.986437	-1208.427857	-4.76	0.18	-4.90
reverse	-1095.308595	-1211.990015	-1208.427073	-3.87	-2.06	-4.41
TSS	-1095.301093	-1211.983294	-1208.421702	0.84	2.16	-1.04
forward	-1095.323183	-1212.001229	-1208.423895	-13.02	-9.10	-2.42
reverse	-1095.32976	-1212.004171	-1208.437615	-17.15	-10.94	-11.03
TS6	-1095.331754	-1212.006237	-1208.439844	-18.40	-12.24	-12.42
forward	-1095.336213	-1212.012438	-1208.443798	-21.20	-16.13	-14.91
Final product isolated	-633.447193	-750.128042	-746.551807			
Final prod. +DBU isolated	-1095.334708	-1212.015557	-1208.439322	-20.25	-18.09	-12.10

Table S3. Relative kinetics of the rate-limiting steps (ring opening and ring closing)

Substituent	Ring Opening free. energy (ΔG_1^\ddagger , kcal mol ⁻¹)	Ring Closing free energy (ΔG_2^\ddagger , kcal mol ⁻¹)	Relative kinetic Ring Opening	Relative kinetic Ring Closing
propyl	17.4	13.9	1	1
cyclohexyl	18.6	16.8	2.02E-01	1.84E-02
phenyl	22.8	12.3	5.06E-04	1.37E+01

Relative kinetic: $\frac{k_{\text{substituent}}}{k_{\text{propyl}}}$ with $k = \frac{\kappa * k_b * T}{h} * e^{\frac{-\Delta G^\ddagger}{RT}}$

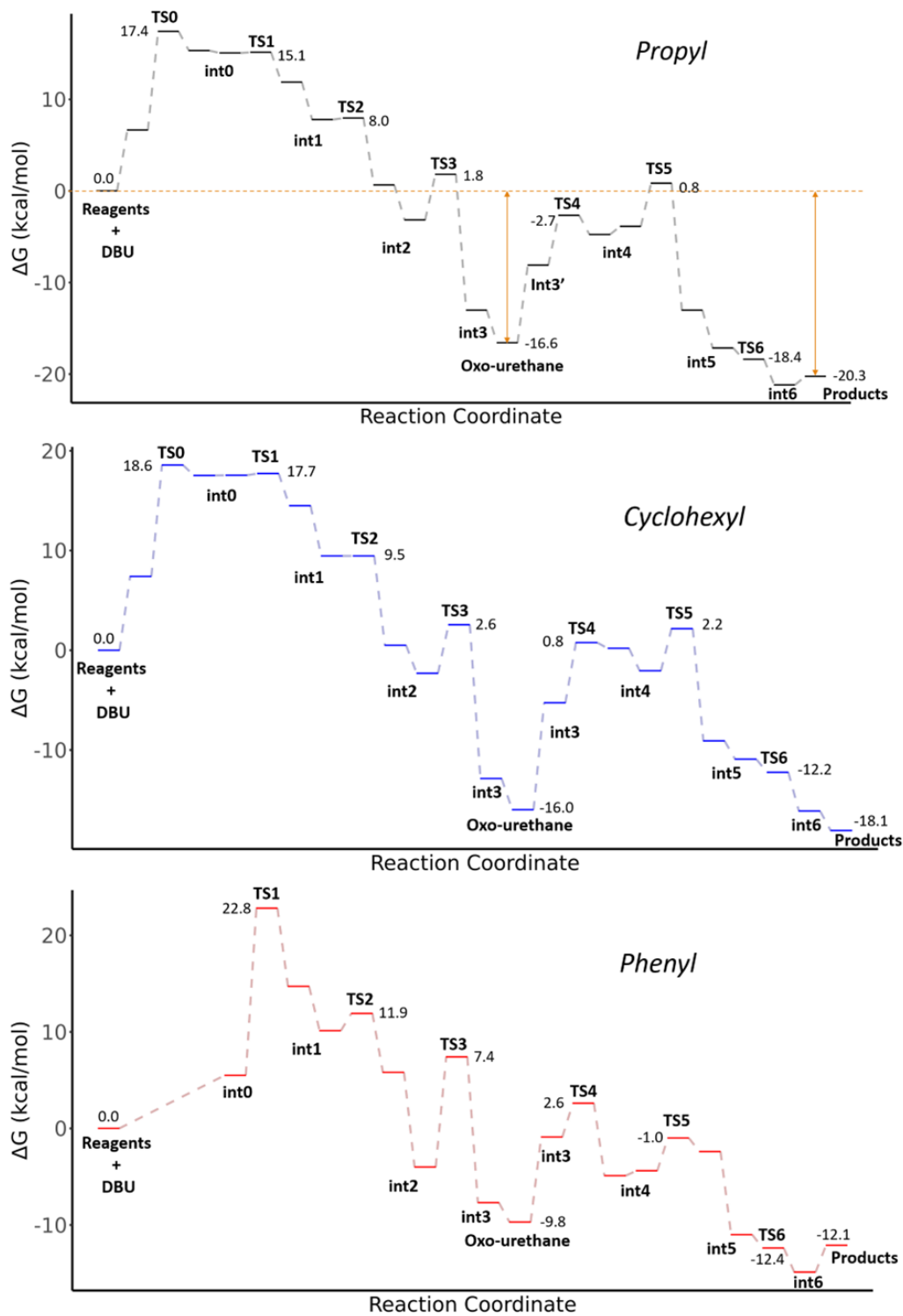


Figure S5. Gibbs free energy profiles for the aminolysis of 1a with propylamine, cyclohexylamine and aniline.

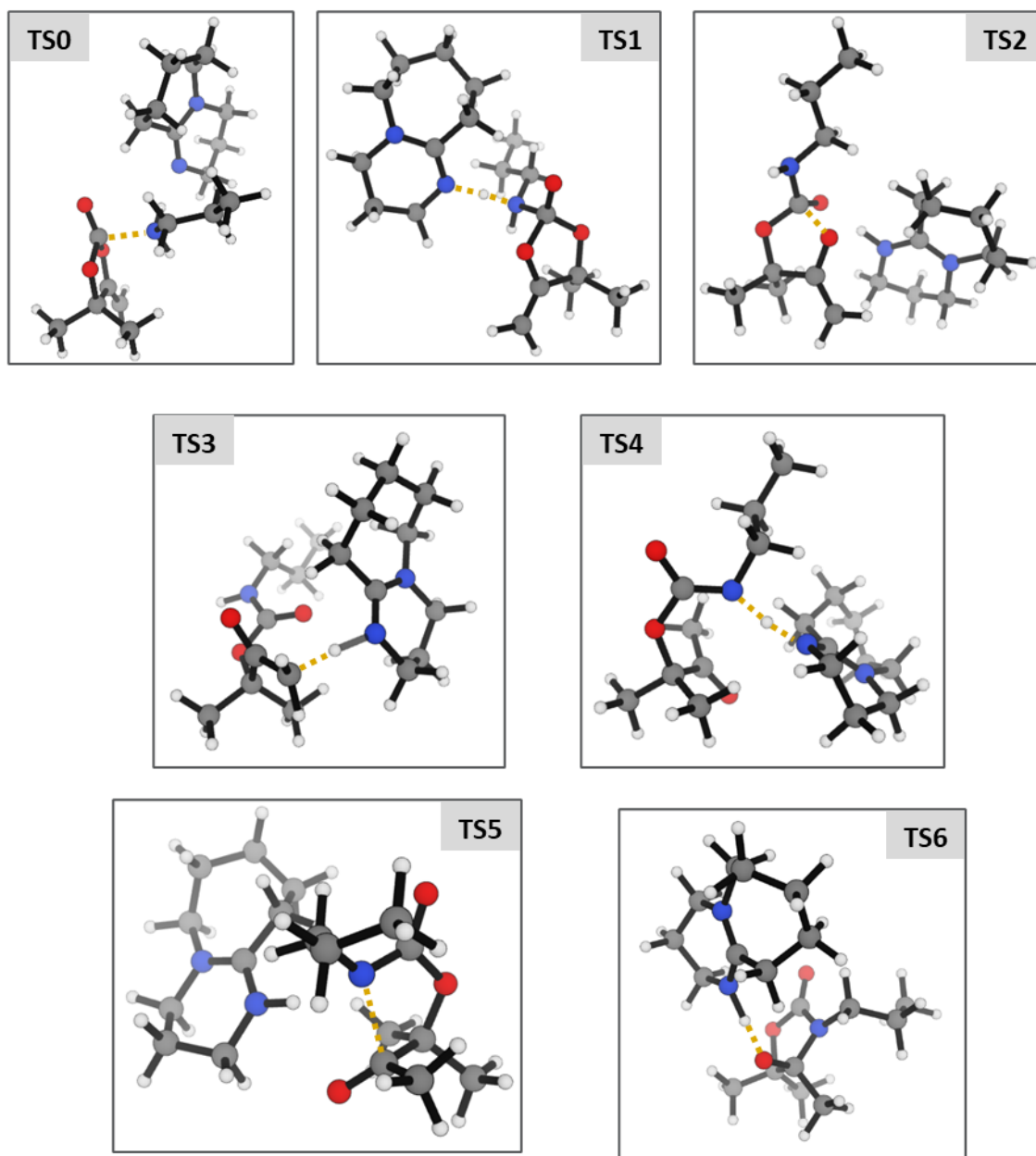


Figure S6. Molecular structures of the optimized geometries of each transition state found for the reaction of **1a** with propylamine.

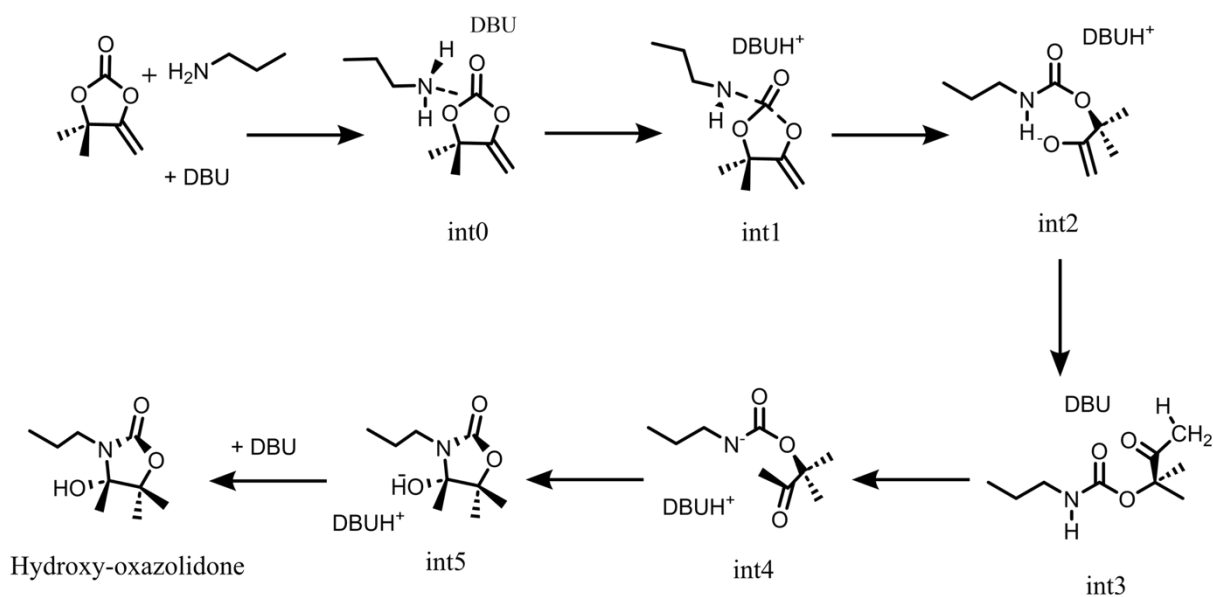


Figure S7. 2D representation of the aminolysis mechanism with each intermediate found for the reaction of **1a** with propylamine. $\text{mol}\cdot\text{L}^{-1}$

The reaction mechanism progresses through a series of key transition states. For propylamine and cyclohexylamine, **TS0** corresponds to the initial approach of the amine toward the carbon of the carbonyl. No **TS0** was identified for aniline, and this will be explained later. **TS1** is the deprotonation of the amine by DBU, facilitating the formation of the carbon-nitrogen bond. Following this, **TS2** depicts the opening of the oxo-carbonate ring, leading to the generation of the enolate intermediate (**int2**). In the next step, **TS3** corresponds to the protonation by the protonated DBU of the sp^2 carbon in α position of the enolate to afford the ketone. Subsequently, **TS4** involves the deprotonation of the nitrogen of the urethane. **TS5** represents the cyclization process and marks the formation of a new nitrogen-carbon bond. Finally, **TS6** describes the protonation of the resulting alkoxide, converting it into an alcohol and yielding the final hydroxy-oxazolidone product.

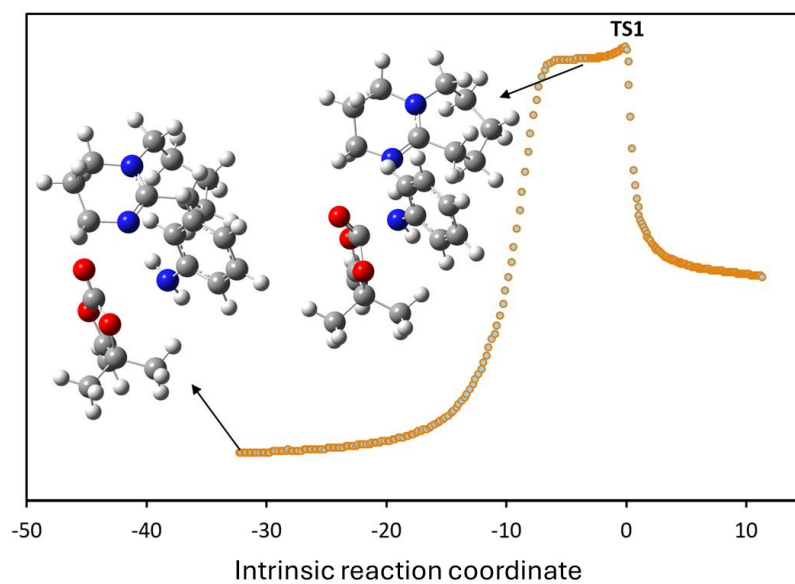


Figure S8. IRC of TS1 for the reaction of **1a** and aniline.

Intrinsic Reaction Coordinate (IRC) calculation exhibits no stationary point corresponding to **int0**. Instead, IRC showed that the path was directly leading to the separate reagents with no stationary point. However, we observed a loss of inflection. This unexpected finding highlights a distinct mechanistic behavior for aniline compared to propylamine and cyclohexylamine. Such an observation was reported for similar nucleophilic attack of amine on cyclic compounds.¹⁶

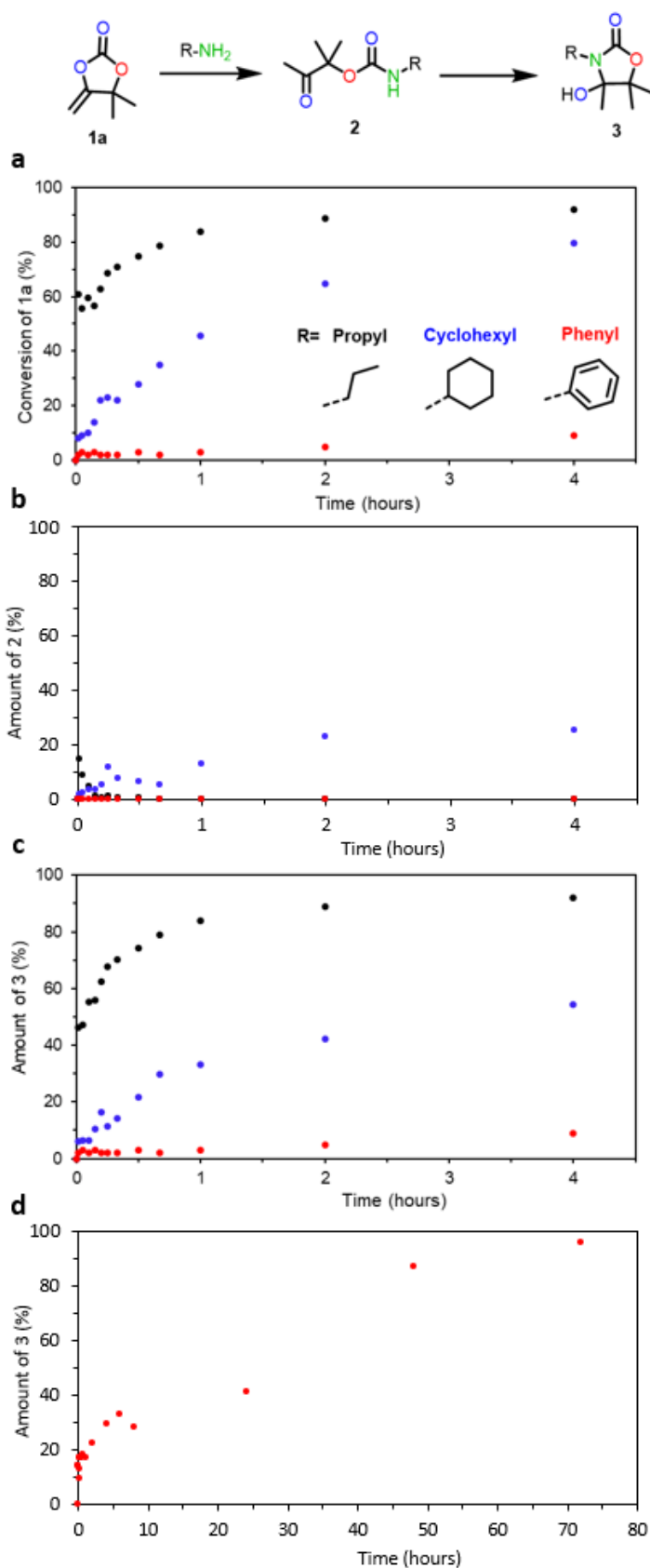


Figure S9. Kinetic profiles of the reaction between **1a** and different amines (propylamine, cyclohexylamine and aniline) carried out at 25 °C in acetonitrile (0.5 M). The conversion of **1a** (a) and the appearance of intermediates **2** (b) and final products **3** (c) were followed

by ^1H NMR. Additionally, the reaction of **1a** with aniline at higher concentration (3.5 M, 25 °C) was analyzed, following the formation of final products **3** (d) by ^1H NMR.

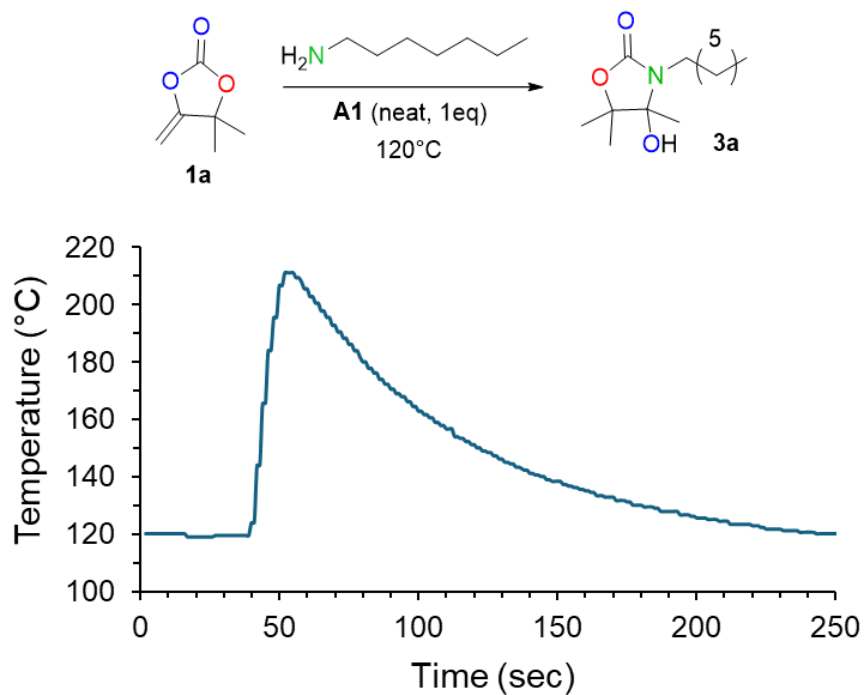
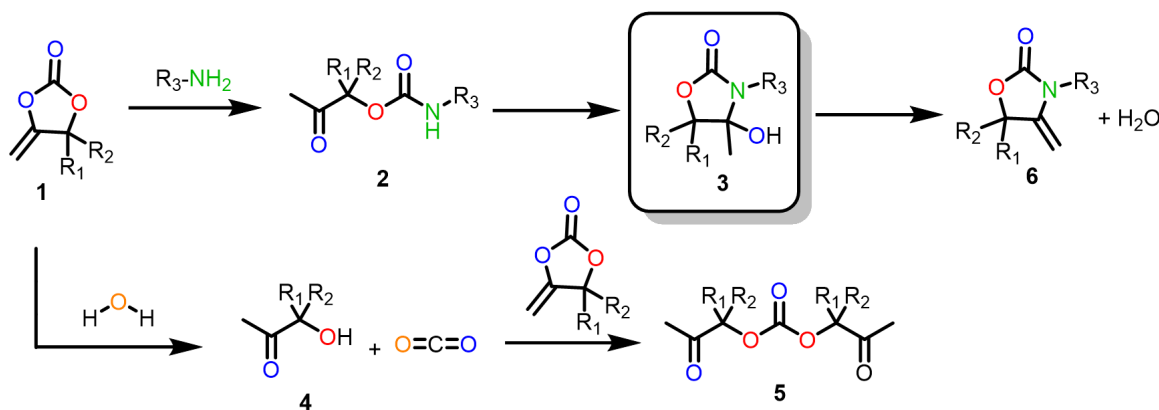


Figure S10. Temperature profile monitored during the neat reaction of **1a** with **A1** in presence with an initial temperature of 120 °C.

5. Calculation of conversions and selectivities

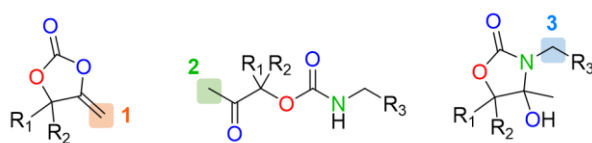
The conversions and selectivities are calculated based on the NMR spectra of the crude reaction mixture according to the following general equations relying on the different possible reactions.



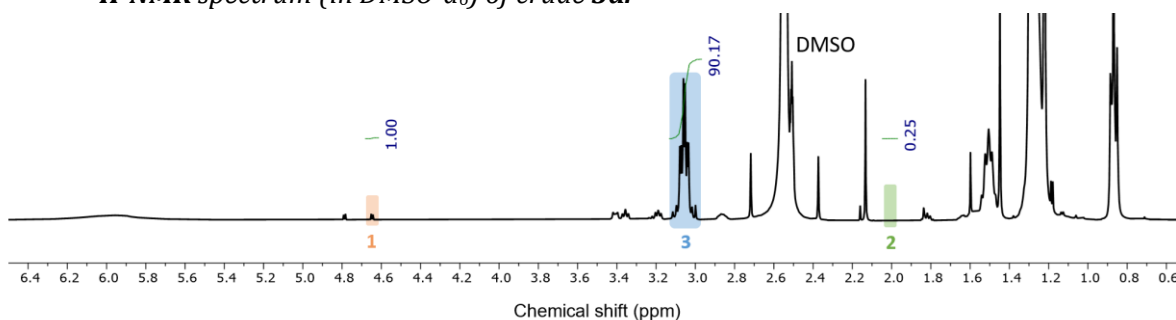
$$Conversion = \frac{2 + 3}{1 + 2 + 3} \times 100$$

$$Selectivity (product composition) = \frac{3}{2 + 3} \times 100$$

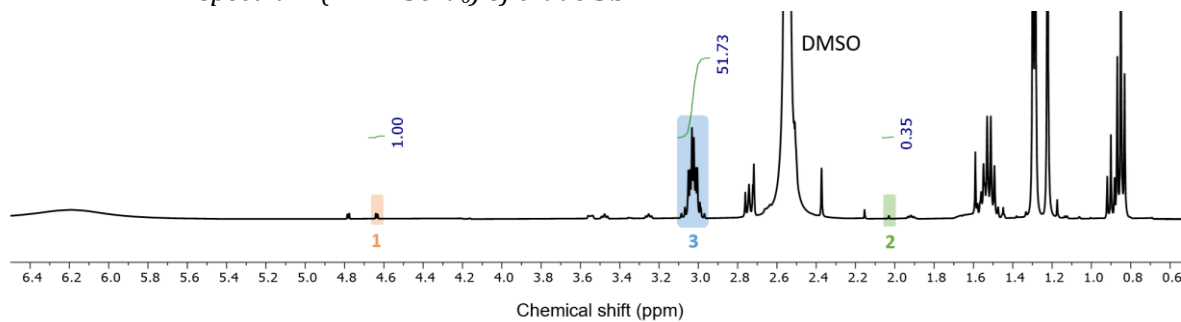
Note that, depending on the amine, not all products are detected. A distinct signal for each species must be identified and integrated for the calculation. The chemical shifts of the signals vary for the different amines.



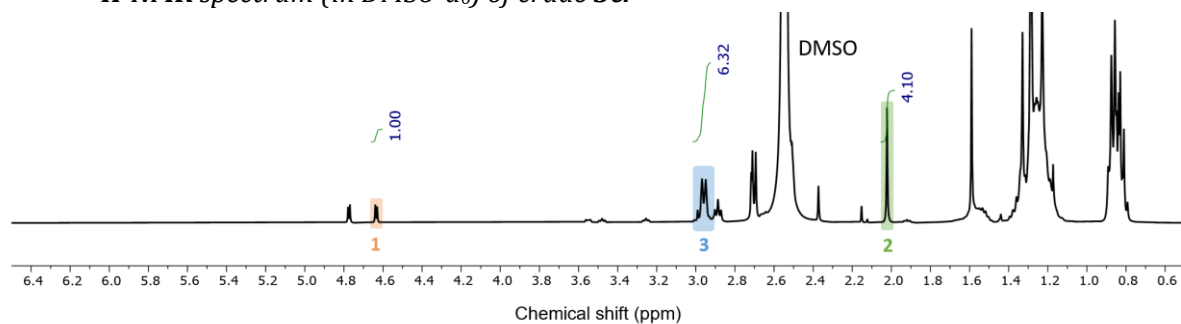
- 1H -NMR spectrum (in $DMSO-d_6$) of crude **3a**.



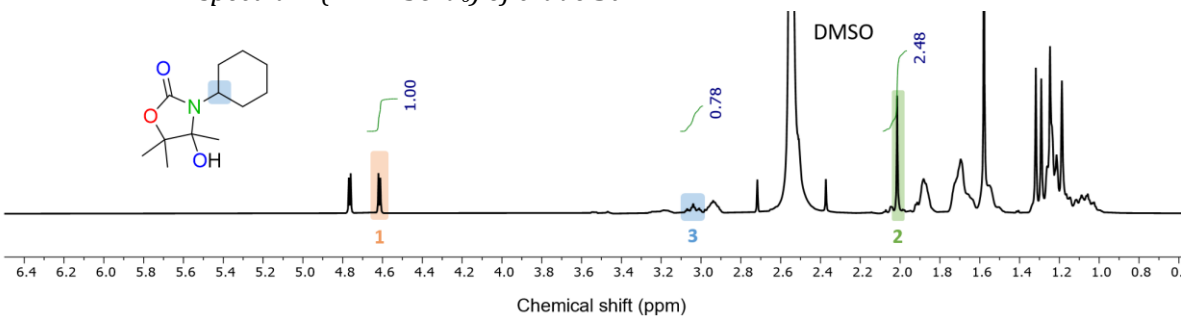
- $^1\text{H-NMR}$ spectrum (in DMSO-d_6) of crude **3b**.



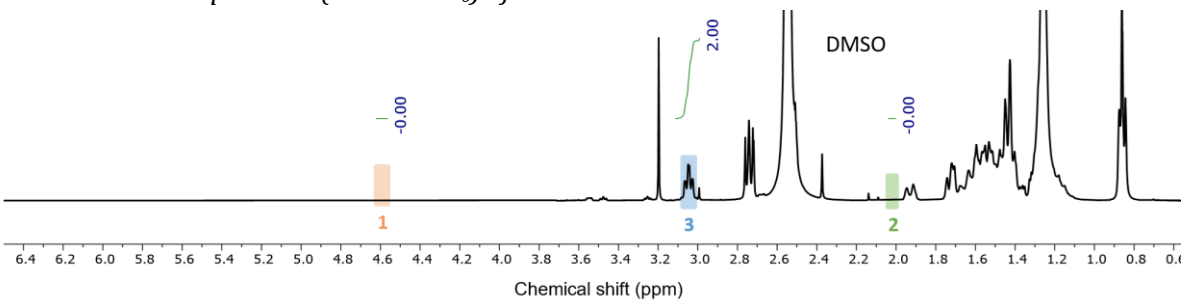
- $^1\text{H-NMR}$ spectrum (in DMSO-d_6) of crude **3c**.



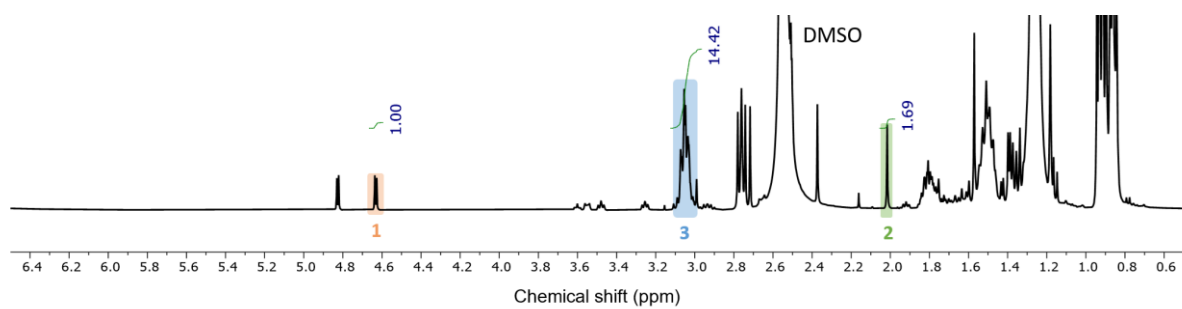
- $^1\text{H-NMR}$ spectrum (in DMSO-d_6) of crude **3d**.



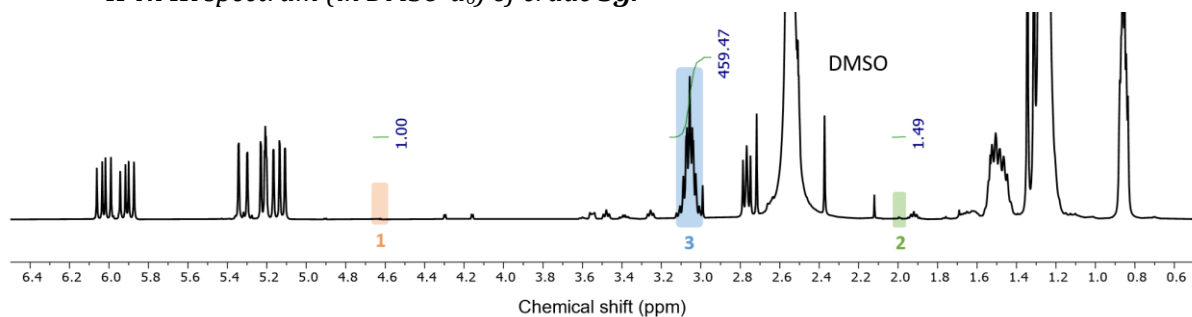
- $^1\text{H-NMR}$ spectrum (in DMSO-d_6) of crude **3e**.



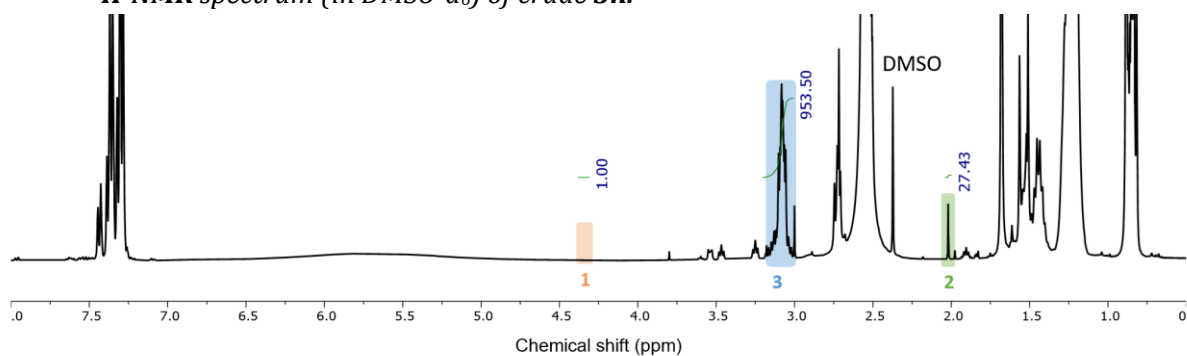
- $^1\text{H-NMR}$ spectrum (in DMSO-d_6) of crude **3f**.



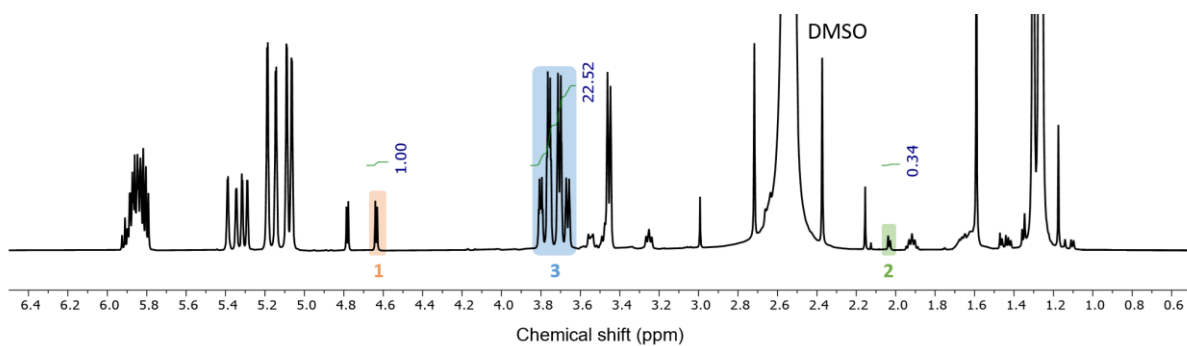
- *¹H-NMR spectrum (in DMSO-d₆) of crude **3g**.*



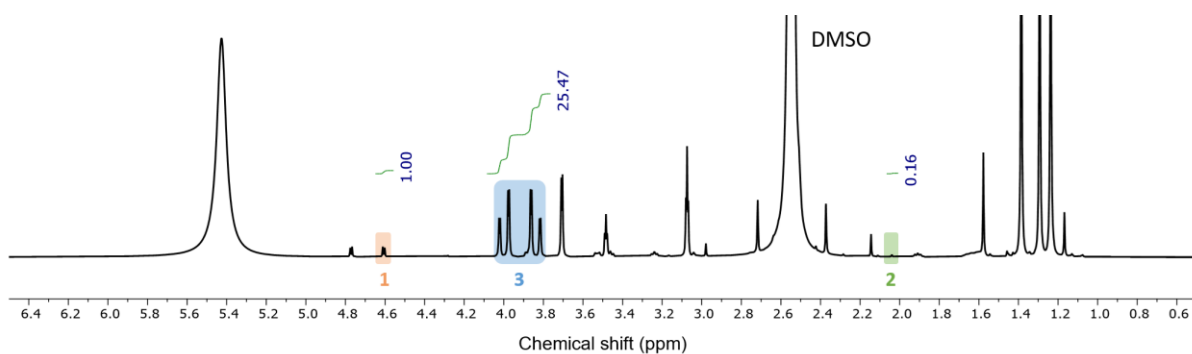
- *¹H-NMR spectrum (in DMSO-d₆) of crude **3h**.*



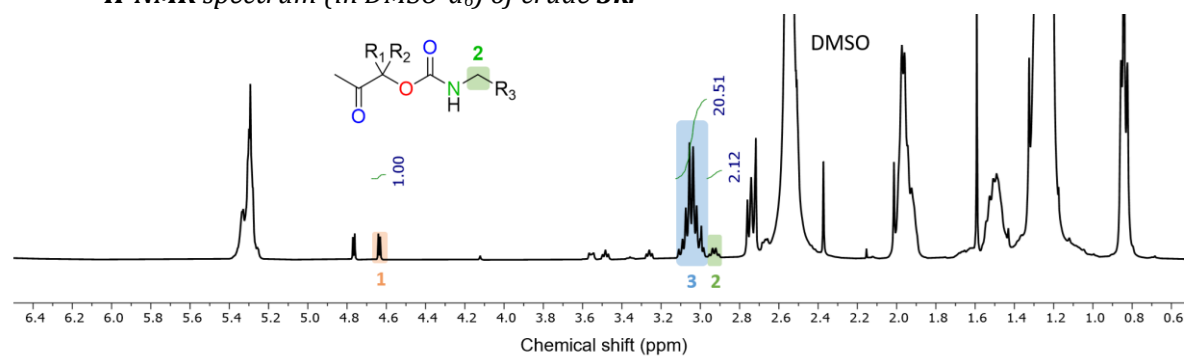
- *¹H-NMR spectrum (in DMSO-d₆) of crude **3i**.*



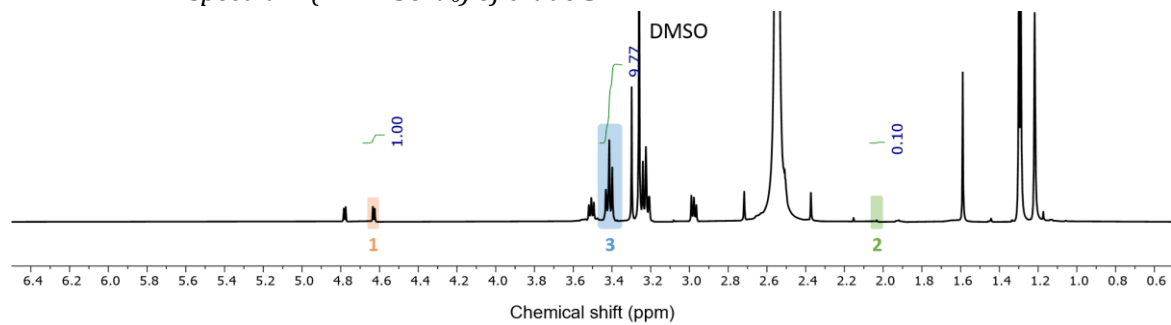
- *¹H-NMR spectrum (in DMSO-d₆) of crude **3j**.*



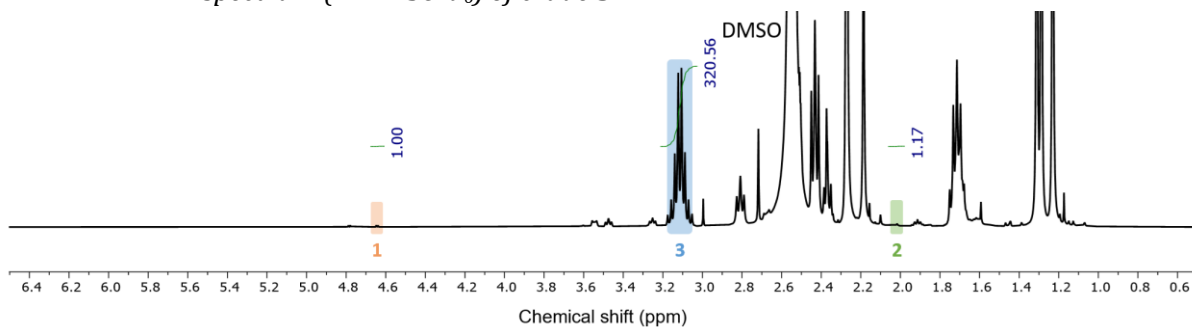
- $^1\text{H-NMR}$ spectrum (in DMSO-d_6) of crude **3k**.



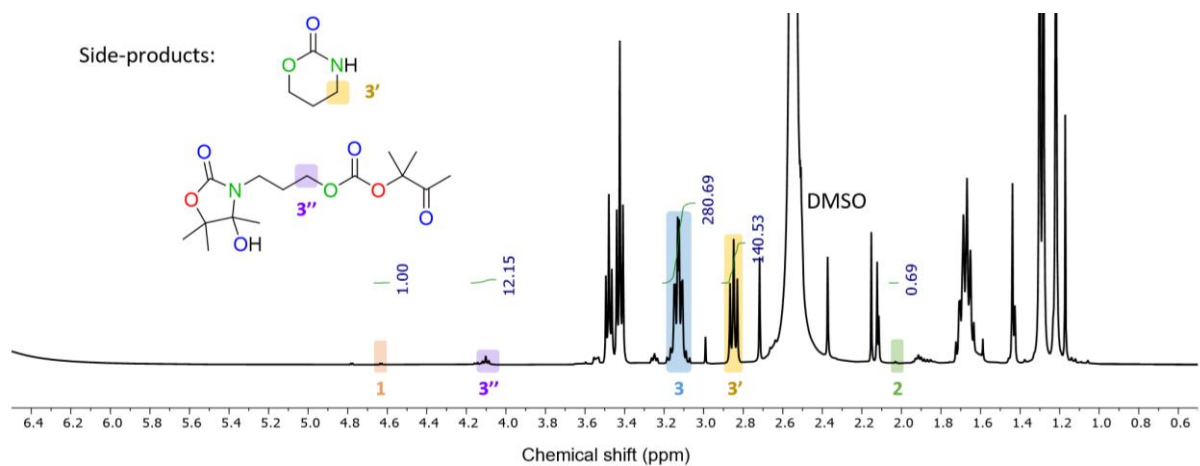
- $^1\text{H-NMR}$ spectrum (in DMSO-d_6) of crude **3l**.



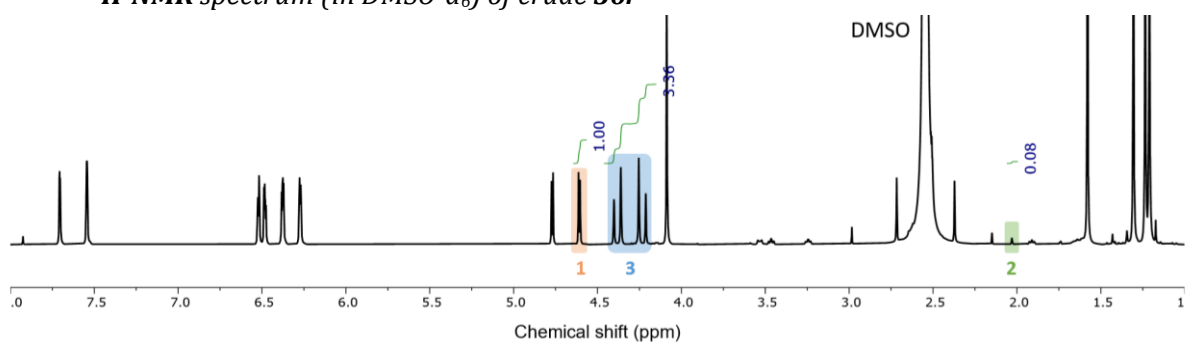
- $^1\text{H-NMR}$ spectrum (in DMSO-d_6) of crude **3m**.



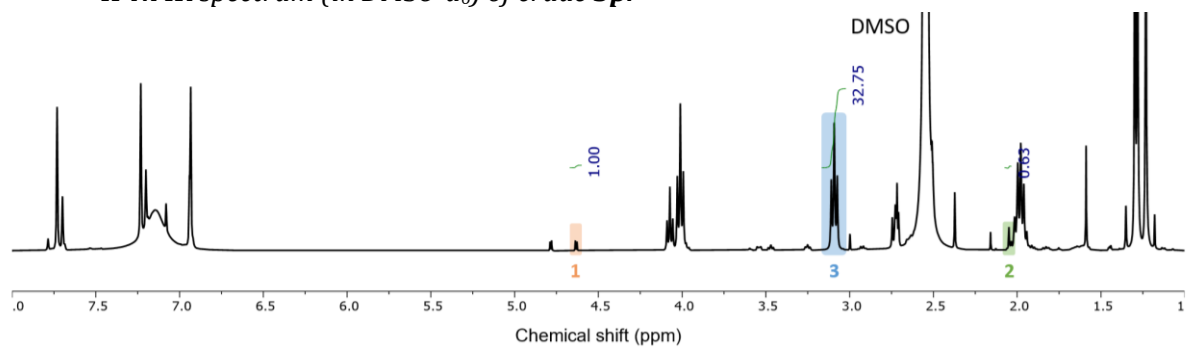
- $^1\text{H-NMR}$ spectrum (in DMSO-d_6) of crude **3n**.



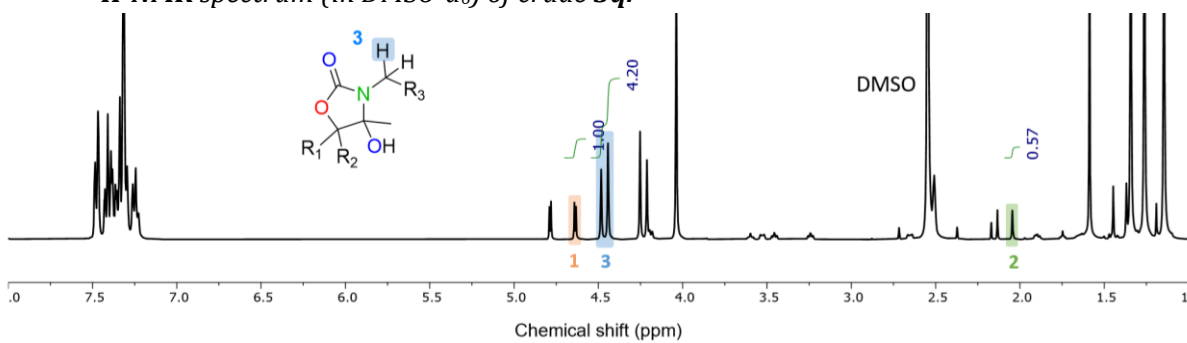
- $^1\text{H-NMR}$ spectrum (in DMSO-d_6) of crude **3o**.



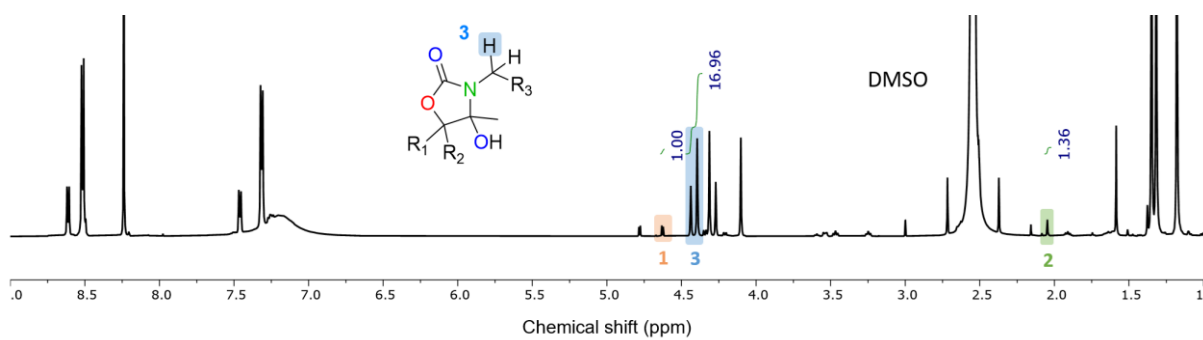
- $^1\text{H-NMR}$ spectrum (in DMSO-d_6) of crude **3p**.



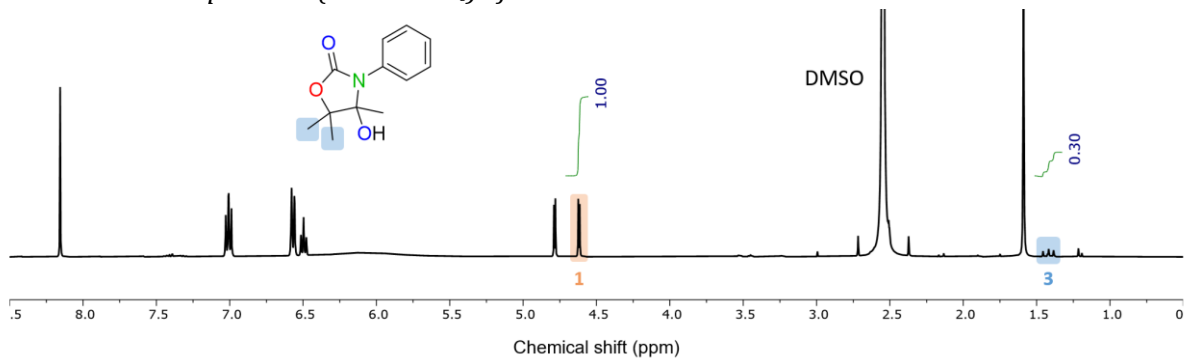
- $^1\text{H-NMR}$ spectrum (in DMSO-d_6) of crude **3q**.



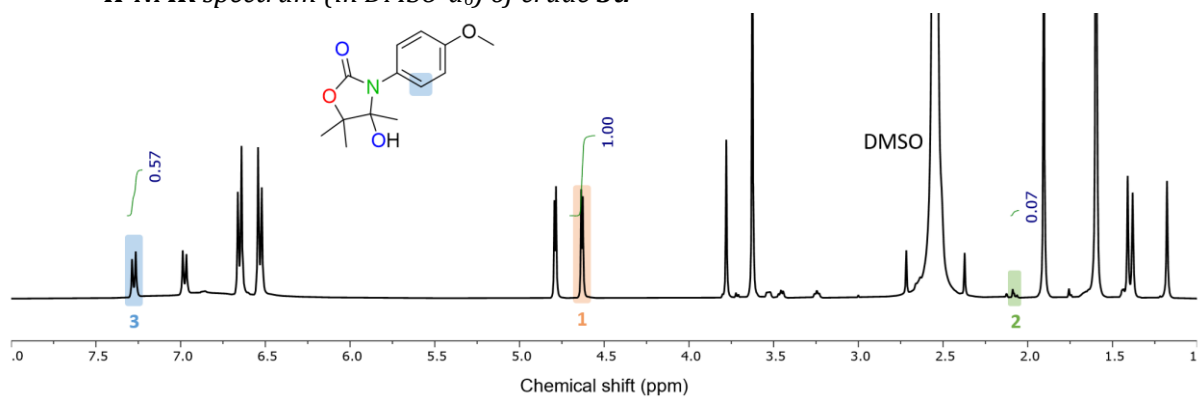
- $^1\text{H-NMR}$ spectrum (in DMSO-d_6) of crude **3r**.



- $^1\text{H-NMR}$ spectrum (in DMSO-d_6) of crude **3s**.



- $^1\text{H-NMR}$ spectrum (in DMSO-d_6) of crude **3t**.

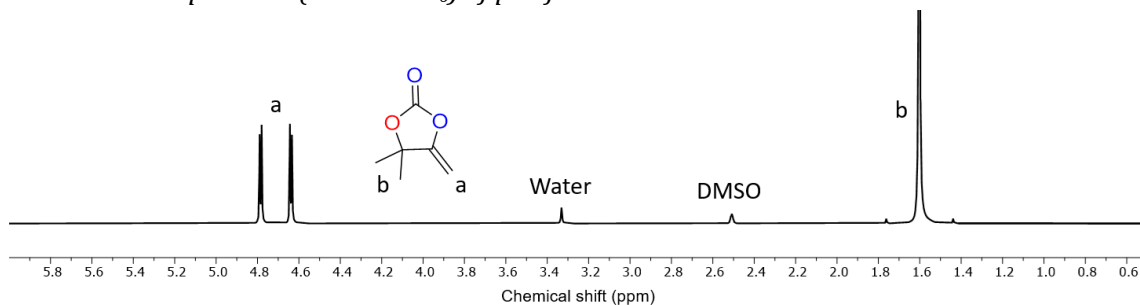


6. Structural characterisation

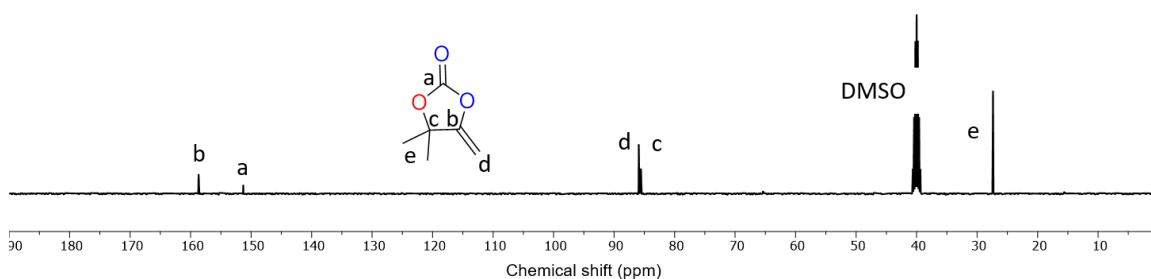
- $^1\text{H-NMR}$, and $^{13}\text{C-NMR}$ spectra of purified alpha cyclic carbonate (αCC)

4,4-dimethyl-5-methylene-1,3-dioxolan-2-one (1a): Synthesized according to the general procedure, white solid. $^1\text{H NMR}$ (400 MHz, DMSO-d_6) δ 4.72 (dd, $J = 57.5, 3.8$ Hz, 2H), 1.60 (s, 6H) ppm. $^{13}\text{C NMR}$ (400 MHz, DMSO-d_6) δ 158.7, 151.3, 86.0, 85.6, 27.4 ppm.

- $^1\text{H-NMR}$ spectrum (in DMSO-d_6) of purified **1a**.

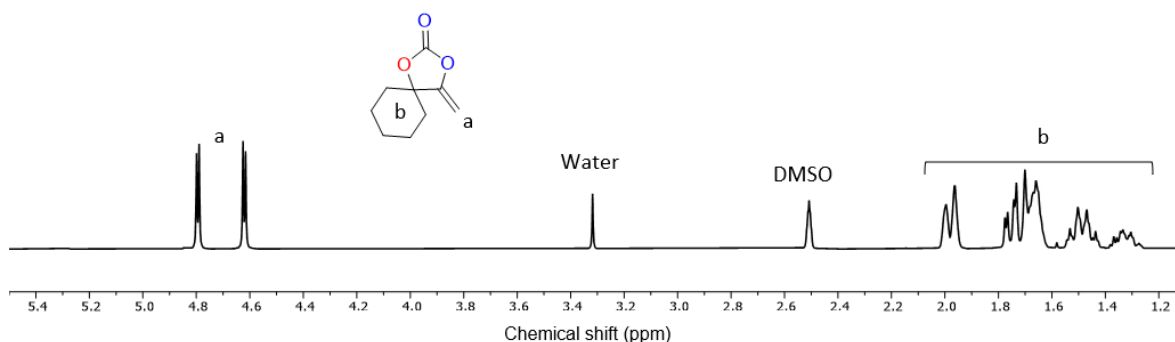


- $^{13}\text{C-NMR}$ spectrum (in DMSO-d_6) of purified **1a**.

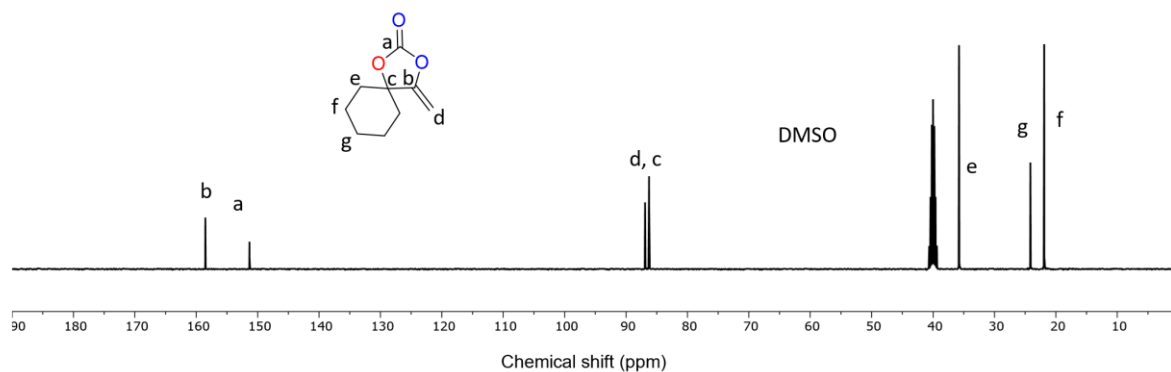


4-methylene-1,3-dioxaspiro[4.5]decan-2-one (1b): Synthesized according to the general procedure, colorless liquid. $^1\text{H NMR}$ (400 MHz, DMSO-d_6) δ 4.69 (dd, $J = 70.2, 3.9$ Hz, 2H), 2.02 – 1.92 (m, 2H), 1.81 – 1.69 (m, 3H), 1.66 (p, $J = 4.5, 3.2$ Hz, 2H), 1.58 – 1.42 (m, 2H), 1.42 – 1.25 (m, 1H) ppm. $^{13}\text{C NMR}$ (400 MHz, DMSO-d_6) δ 158.6, 151.3, 86.8, 86.1, 35.9, 24.1, 21.9 ppm.

- $^1\text{H-NMR}$ spectrum (in DMSO-d_6) of purified **1b**.

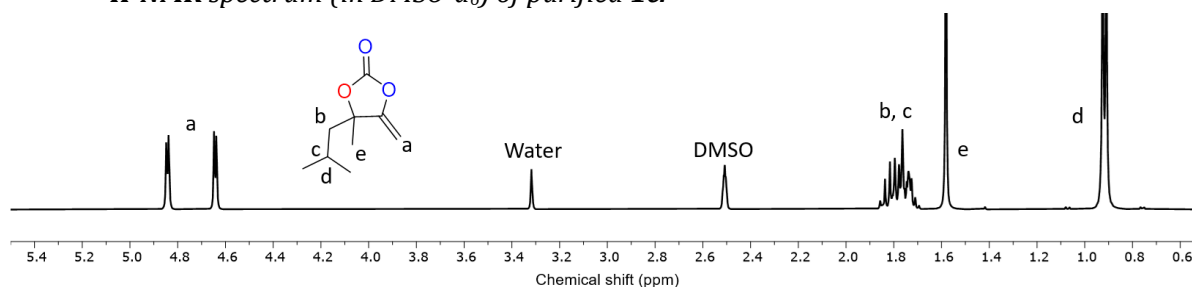


- $^{13}\text{C-NMR}$ spectrum (in DMSO-d_6) of purified **1b**.

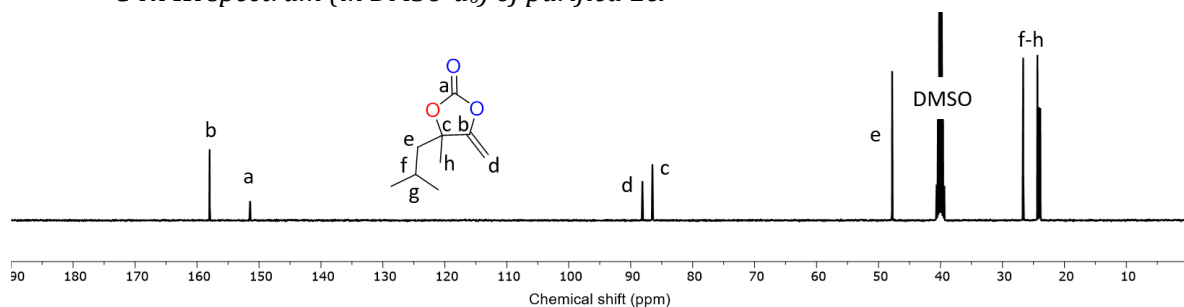


4-isobutyl-4-methyl-5-methylene-1,3-dioxolan-2-one (1c): Synthesized according to the general procedure, colorless liquid. $^1\text{H NMR}$ (400 MHz, DMSO-d_6) δ 4.74 (ddd, $J = 79.8, 3.9, 1.5$ Hz, 2H), 1.88 – 1.65 (m, 3H), 1.58 (s, 3H), 0.92 (d, $J = 6.2$ Hz, 6H) ppm. $^{13}\text{C NMR}$ (400 MHz, DMSO-d_6) δ 158.0, 151.5, 88.1, 86.5, 47.8, 26.7, 24.3, 24.1, 23.9 ppm.

- $^1\text{H-NMR}$ spectrum (in DMSO-d_6) of purified **1c**.

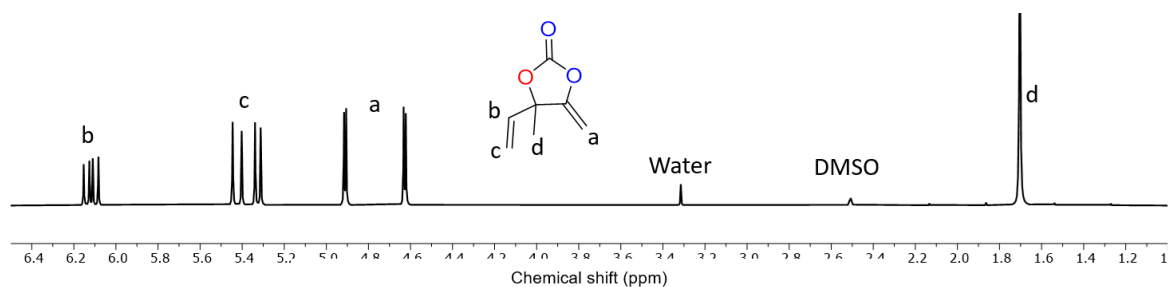


- $^{13}\text{C-NMR}$ spectrum (in DMSO-d_6) of purified **1c**.

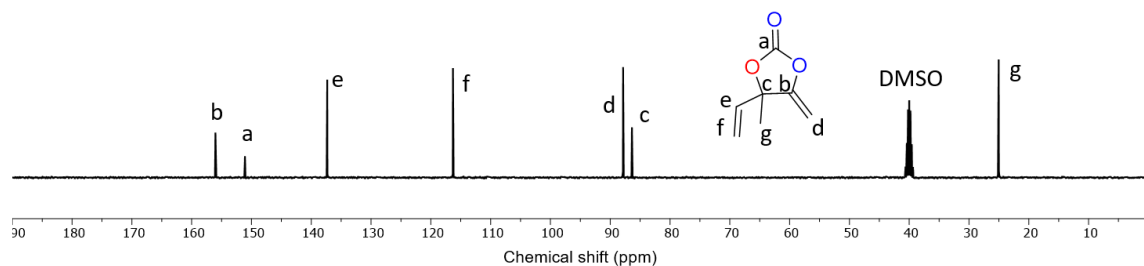


4-methyl-5-methylene-4-vinyl-1,3-dioxolan-2-one (1d): Synthesized according to the general procedure, colorless liquid. $^1\text{H NMR}$ (400 MHz, DMSO-d_6) δ 6.12 (dd, $J = 17.2, 10.7$ Hz, 1H), 5.42 (d, $J = 17.2$ Hz, 1H), 5.33 (d, $J = 10.7$ Hz, 1H), 4.91 (d, $J = 4.0$ Hz, 1H), 4.63 (d, $J = 4.0$ Hz, 1H), 1.70 (s, 3H) ppm. $^{13}\text{C NMR}$ (400 MHz, DMSO-d_6) δ 156.0, 151.1, 137.3, 116.3, 87.9, 86.4, 25.0 ppm.

- $^1\text{H-NMR}$ spectrum (in DMSO-d_6) of purified **1d**.

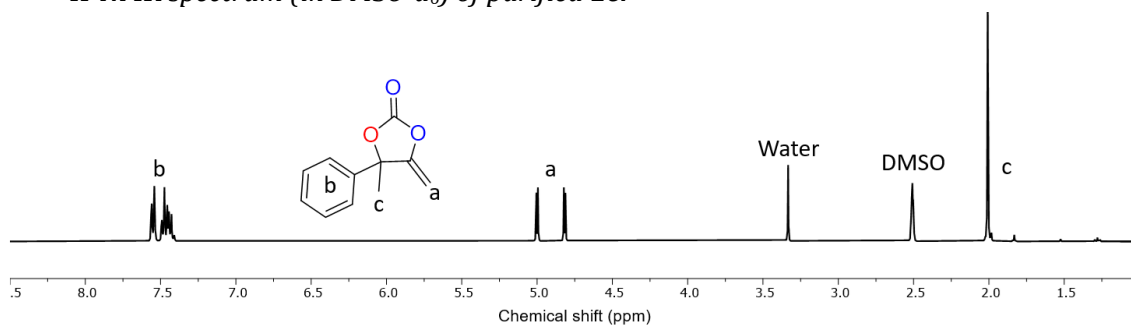


- $^{13}\text{C-NMR}$ spectrum (in DMSO-d_6) of purified **1d**.

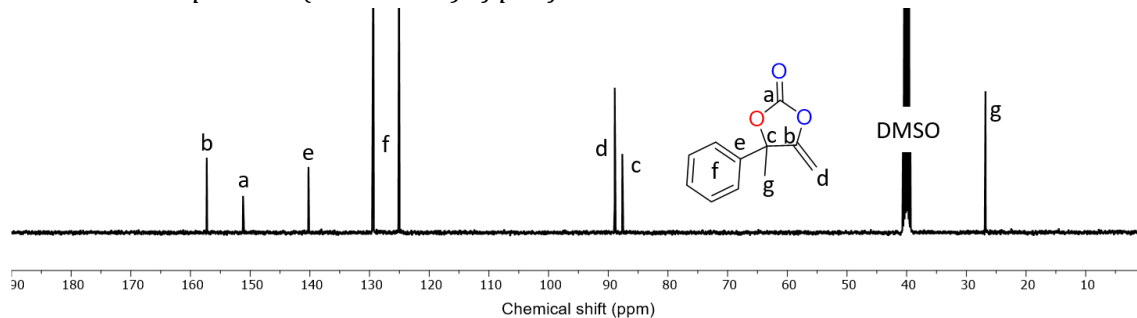


4-methyl-5-methylene-4-phenyl-1,3-dioxolan-2-one (1e): Synthesized according to the general procedure, white solid. $^1\text{H-NMR}$ (400 MHz, DMSO-d_6) δ 7.56 (dd, $J = 8.2, 1.6$ Hz, 2H), 7.51 – 7.43 (m, 2H), 7.46 – 7.37 (m, 1H), 5.00 (d, $J = 4.2$ Hz, 1H), 4.81 (dt, $J = 4.1, 1.2$ Hz, 1H), 2.01 (s, 3H) ppm. $^{13}\text{C-NMR}$ (400 MHz, DMSO-d_6) δ 157.3, 151.2, 140.2, 129.4, 125.1, 88.9, 87.6, 26.8 ppm.

- $^1\text{H-NMR}$ spectrum (in DMSO-d_6) of purified **1e**.



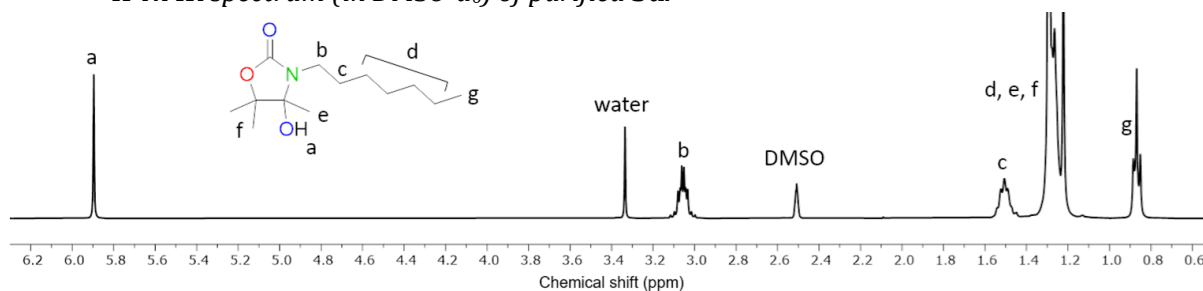
- $^{13}\text{C-NMR}$ spectrum (in DMSO-d_6) of purified **1e**.



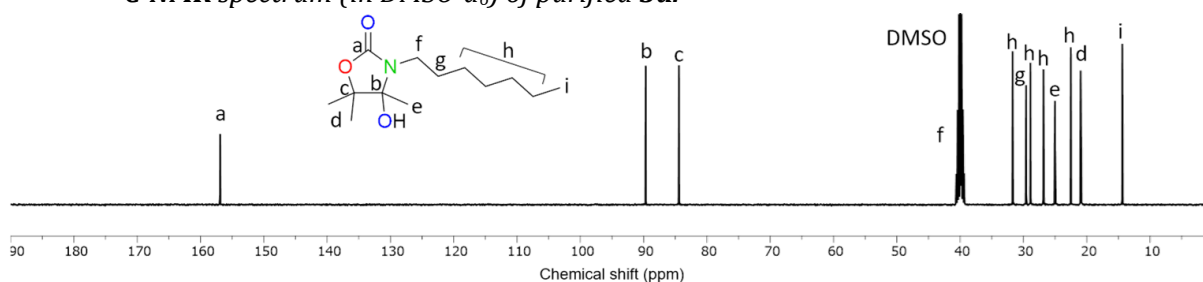
- ^1H , $^{13}\text{C-NMR}$, and ATR-IR spectra of purified oxazolidones

3-heptyl-4-hydroxy-4,5,5-trimethyloxazolidin-2-one (3a): Synthesized according to the general procedure, white solid. $^1\text{H NMR}$ (400 MHz, DMSO-d_6) δ 5.90 (s, 1H), 3.06 (td, $J = 7.3, 3.9$ Hz, 2H), 1.51 (p, $J = 7.2$ Hz, 2H), 1.28 (dd, $J = 8.5, 4.3$ Hz, 14H), 1.22 (s, 3H), 0.87 (t, $J = 6.8$ Hz, 3H) ppm. $^{13}\text{C NMR}$ (400 MHz, DMSO-d_6) δ 156.9, 89.7, 84.4, 39.9, 31.7, 29.6, 28.9, 26.8, 25.0, 22.5, 21.0, 20.9, 14.4 ppm. **FT-IR** (neat, ν in cm^{-1}): 3366 (O-H), 1724 (C=O).

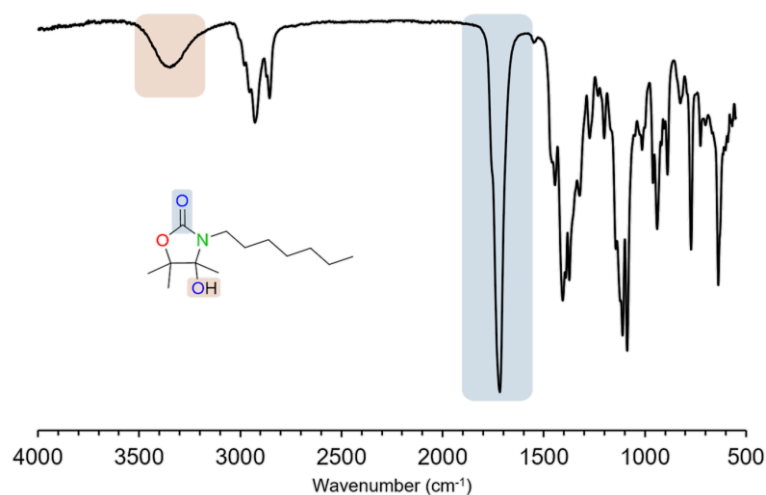
- $^1\text{H-NMR}$ spectrum (in DMSO-d_6) of purified **3a**.



- $^{13}\text{C-NMR}$ spectrum (in DMSO-d_6) of purified **3a**.



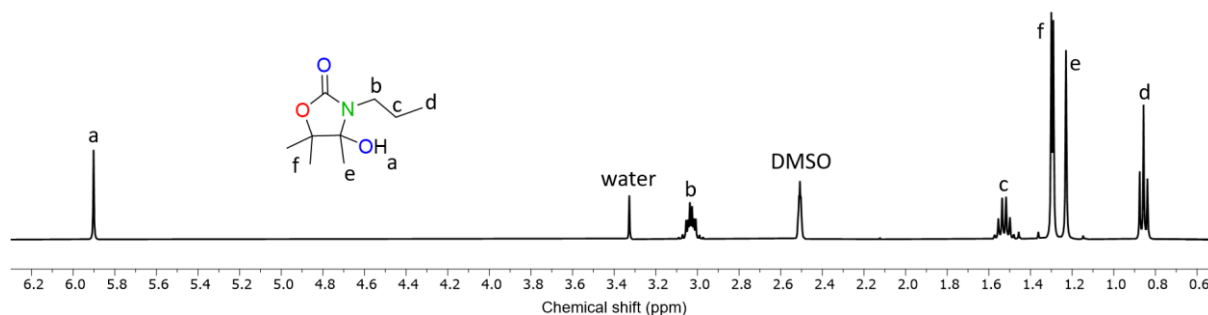
- **FT-IR** spectrum (in DMSO-d_6) of purified **3a**.



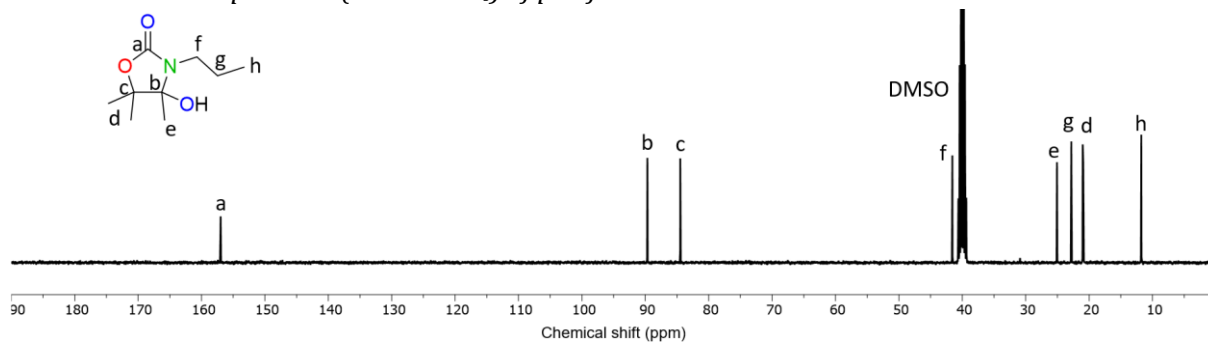
4-hydroxy-4,5,5-trimethyl-3-propyloxazolidin-2-one (3b): Synthesized according to the general procedure, white solid. $^1\text{H NMR}$ (400 MHz, DMSO-d_6) δ 5.90 (s, 1H), 3.03 (td, $J = 7.2, 3.7$ Hz, 2H), 1.53 (h, $J = 7.3$ Hz, 2H), 1.30 (d, $J = 3.9$ Hz, 6H), 1.23 (s, 3H), 0.86 (t, $J = 7.4$ Hz, 3H) ppm.

^{13}C NMR (400 MHz, DMSO-d_6) δ 157.0, 89.7, 84.5, 41.6, 25.1, 22.8, 21.0, 20.9, 11.8 ppm. FT-IR (neat, ν in cm^{-1}): 3366 (O-H), 1724 (C=O).

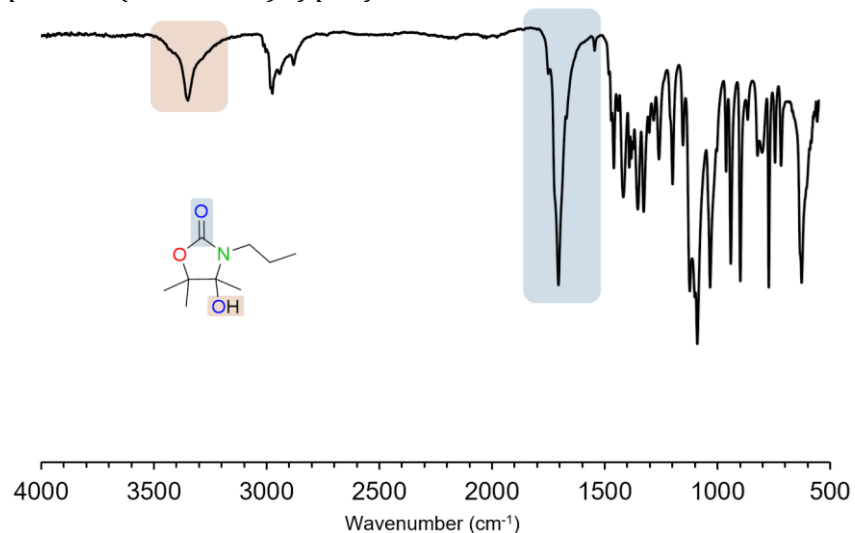
- ^1H -NMR spectrum (in DMSO-d_6) of purified **3b**.



- ^{13}C -NMR spectrum (in DMSO-d_6) of purified **3b**.



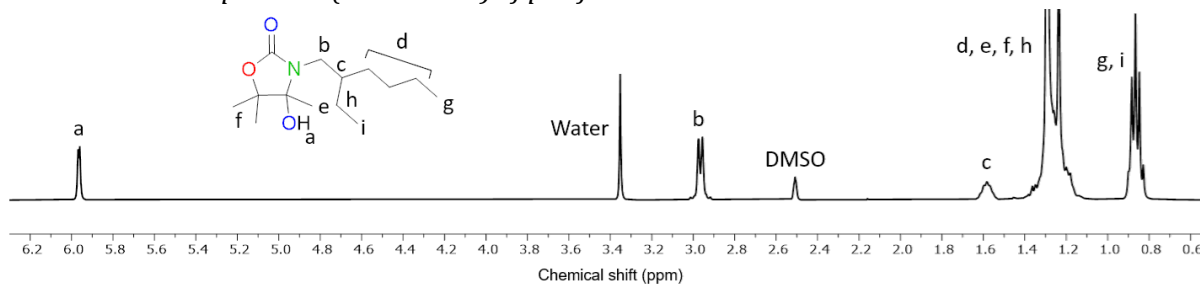
- FT-IR spectrum (in DMSO-d_6) of purified **3b**.



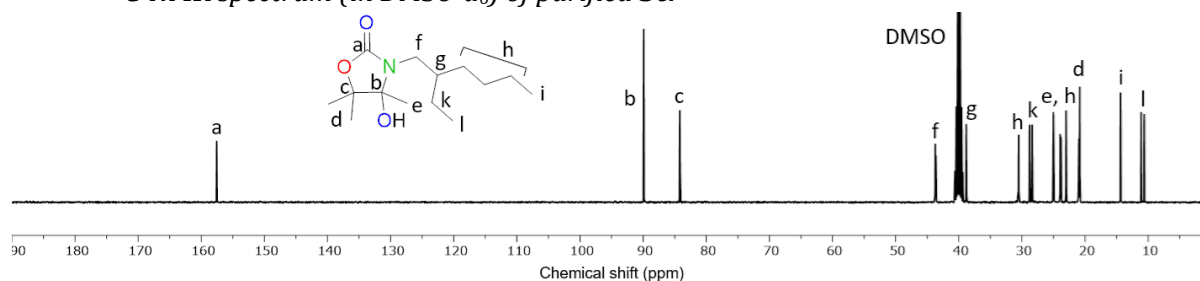
3-(2-ethylhexyl)-4-hydroxy-4,5,5-trimethyloxazolidin-2-one (3c): Synthesized according to the general procedure, white solid. ^1H NMR (400 MHz, DMSO-d_6) δ 5.96 (d, $J = 3.4$ Hz, 1H), 3.02 – 2.91 (m, 2H), 1.59 (h, $J = 6.6$ Hz, 1H), 1.42 – 1.11 (m, 16H), 0.87 (p, $J = 7.7, 7.0$ Hz, 7H) ppm. ^{13}C

NMR (400 MHz, DMSO- d_6) δ 157.6, 89.9, 84.2, 84.2, 43.7, 43.6, 38.8, 38.8, 30.6, 30.5, 28.8, 28.4, 25.0, 23.9, 23.8, 23.0, 23.0, 21.0, 21.0, 20.8, 14.4, 14.4, 11.1, 10.6 ppm. **FT-IR** (neat, ν in cm^{-1}): 3366 (O-H), 1724 (C=O). **HRMS** (ESI): $\text{C}_{14}\text{H}_{27}\text{NO}_3$ $[\text{M}+\text{Na}]^+$: calculated, 280.1889; found, 280.1885.

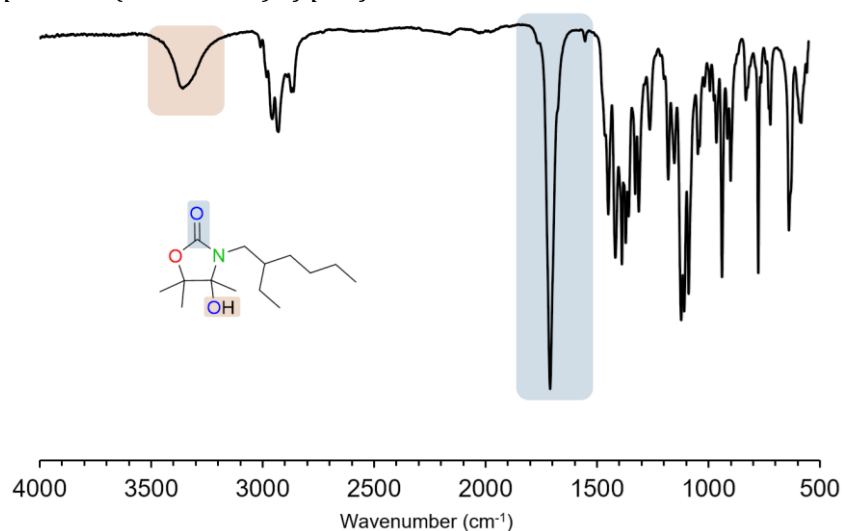
- $^1\text{H-NMR}$ spectrum (in DMSO- d_6) of purified **3c**.



- $^{13}\text{C-NMR}$ spectrum (in DMSO- d_6) of purified **3c**.



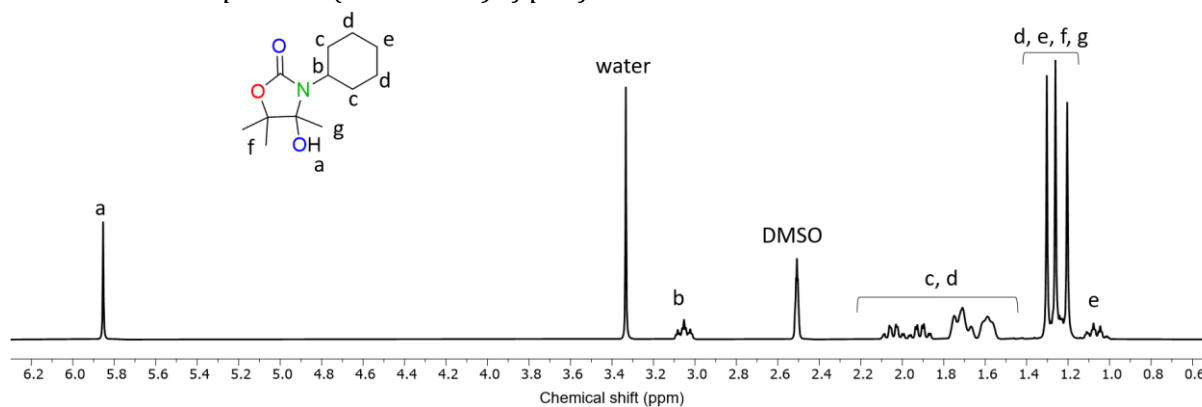
- **FT-IR** spectrum (in DMSO- d_6) of purified **3c**.



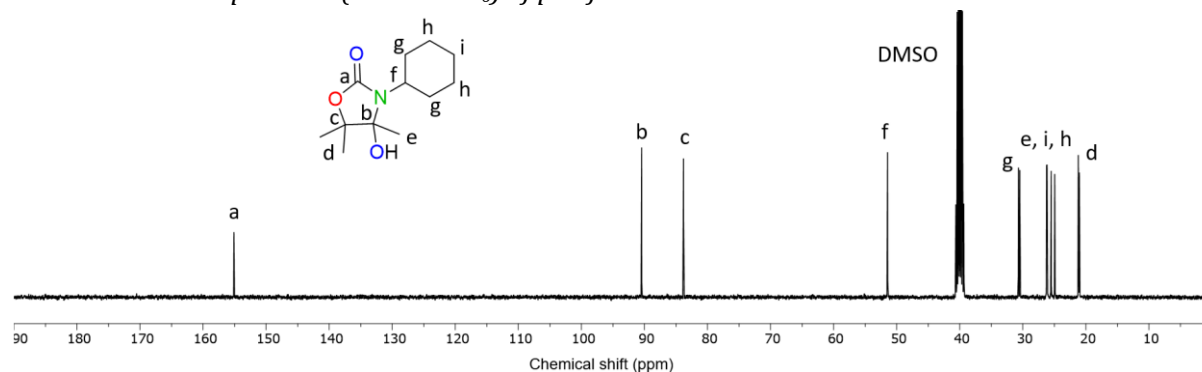
3-cyclohexyl-4-hydroxy-4,5,5-trimethyloxazolidin-2-one (3d): Synthesized according to the general procedure, white solid. $^1\text{H NMR}$ (400 MHz, DMSO- d_6) δ 5.85 (s, 1H), 3.05 (tt, $J = 11.9, 3.7$ Hz, 1H), 2.12 – 1.84 (m, 2H), 1.78 – 1.53 (m, 6H), 1.28 (d, $J = 16.7$ Hz, 7H), 1.20 (s, 3H), 1.06 (qt, $J =$

13.1, 3.5 Hz, 1H) ppm. **¹³C NMR** (400 MHz, DMSO-*d*₆) δ 155.1, 90.5, 83.8, 51.5, 30.7, 30.5, 26.2, 26.2, 25.5, 25.0, 21.2, 21.1 ppm. **FT-IR** (neat, ν in cm⁻¹): 3366 (O-H), 1724 (C=O).

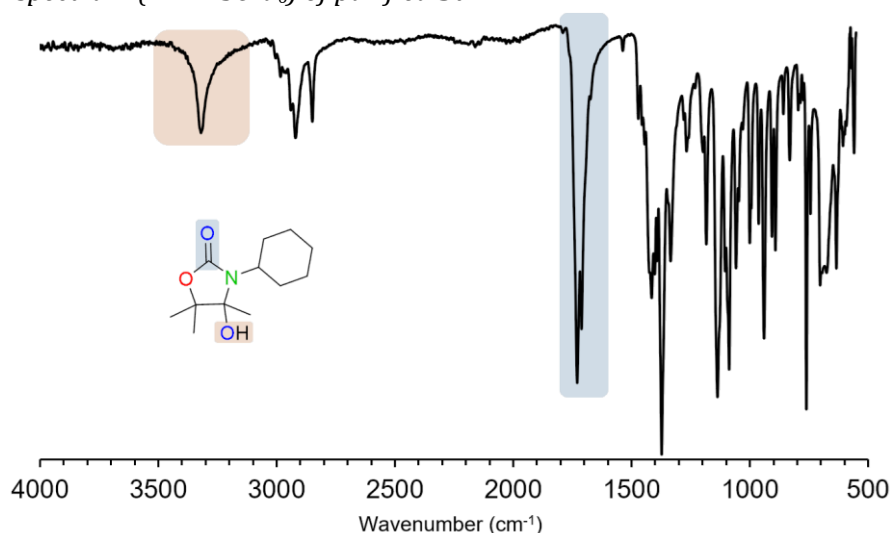
- **¹H-NMR spectrum (in DMSO-*d*₆) of purified 3d.**



- **¹³C-NMR spectrum (in DMSO-*d*₆) of purified 3d.**



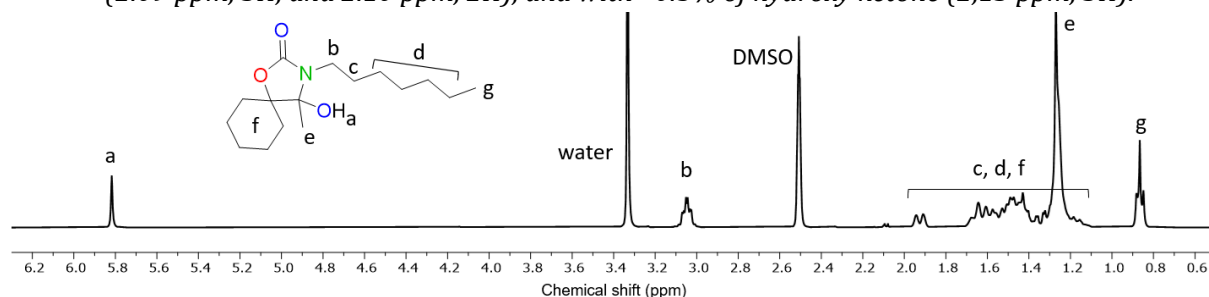
- **FT-IR spectrum (in DMSO-*d*₆) of purified 3d.**



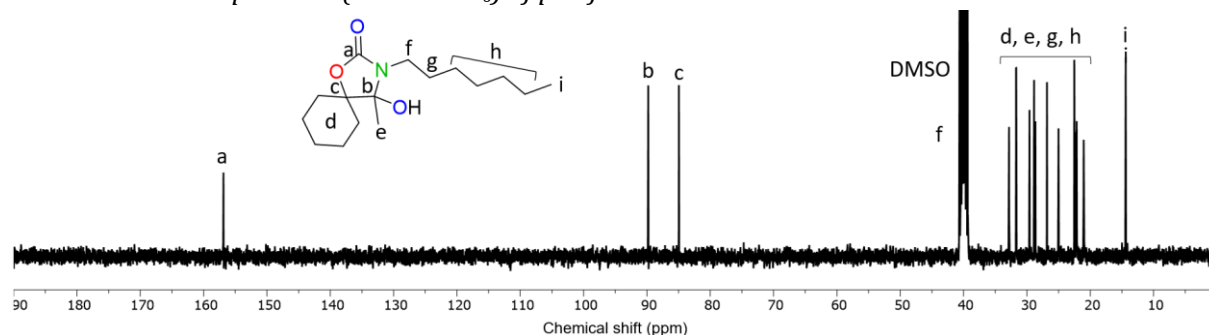
3-heptyl-4-hydroxy-4-methyl-1-oxa-3-azaspiro[4.5]decan-2-one (3e): Synthesized according to the general procedure, white solid. **¹H NMR** (400 MHz, DMSO-*d*₆) δ 5.82 (s, 1H), 3.05 (td, *J* = 7.1, 2.8 Hz, 2H), 1.97 – 1.88 (m, 2H), 1.63 (q, *J* = 13.1 Hz, 2H), 1.58 – 1.45 (m, 2H), 1.48 – 1.31 (m, 2H), 1.26 (d, *J* = 5.9 Hz, 15H), 0.90 – 0.83 (m, 3H) ppm. **¹³C NMR** (400 MHz, DMSO-*d*₆) δ

156.9, 89.8, 85.0, 40.0, 32.8, 31.7, 29.6, 28.9, 28.7, 26.8, 25.0, 22.5, 22.3, 22.1, 21.0, 14.4 ppm. **FT-IR** (neat, ν in cm^{-1}): 3366 (O-H), 1724 (C=O). **HRMS** (ESI): $\text{C}_{16}\text{H}_{29}\text{NO}_3$ $[\text{M}+\text{Na}]^+$: calculated, 306.2045; found, 306.2052.

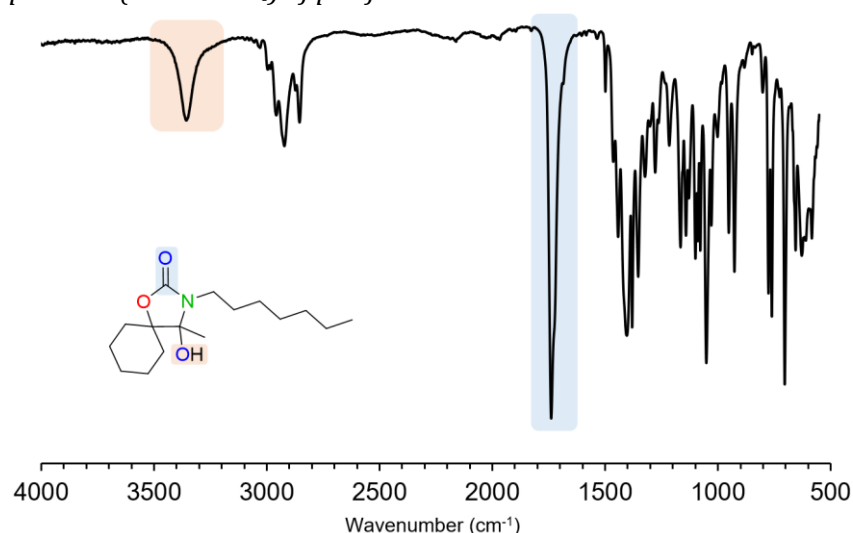
- $^1\text{H-NMR}$ spectrum (in DMSO-d_6) of purified **3e**. Purity level of 98% with 1.5% Intermediate (2.09 ppm, 3H, and 2.10 ppm, 2H), and with <0.5% of hydroxy ketone (2,13 ppm, 3H).



- $^{13}\text{C-NMR}$ spectrum (in DMSO-d_6) of purified **3e**.



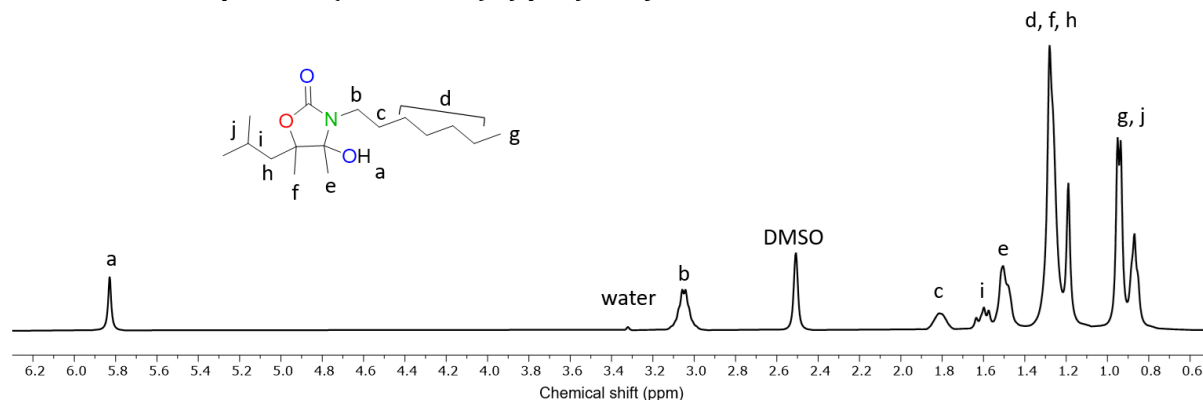
- **FT-IR** spectrum (in DMSO-d_6) of purified **3e**.



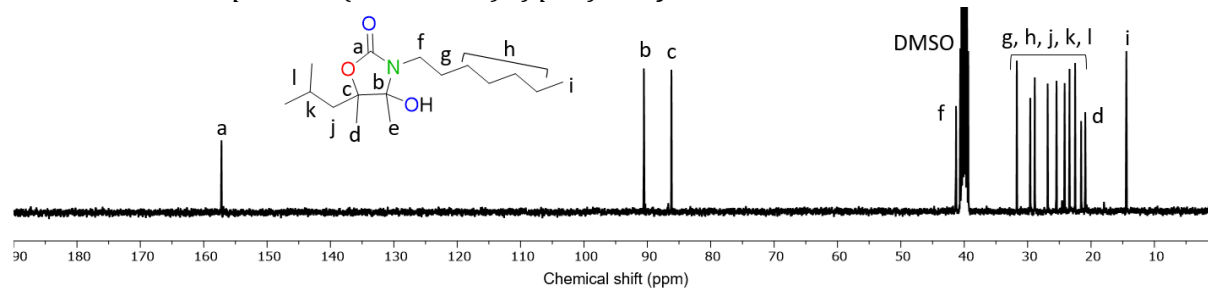
3-heptyl-4-hydroxy-5-isobutyl-4,5-dimethylloxazolidin-2-one (3f): Synthesized according to the general procedure, white solid. $^1\text{H NMR}$ (400 MHz, DMSO-d_6) δ 5.83 (s, 1H), 3.05 (h, $J = 7.2$ Hz, 2H), 1.81 (q, $J = 8.1$ Hz, 1H), 1.60 (dd, $J = 14.8, 9.3$ Hz, 1H), 1.54 – 1.44 (m, 3H), 1.27 (d, $J = 8.0$ Hz, 11H), 1.19 (s, 3H), 0.94 (d, $J = 6.6$ Hz, 6H), 0.88 (d, $J = 6.1$ Hz, 3H) ppm. $^{13}\text{C NMR}$ (400 MHz, DMSO-d_6)

δ 157.2, 90.6, 90.3, 86.7, 86.2, 41.3, 31.7, 29.6, 28.9, 28.8, 26.8, 25.5, 25.4, 24.6, 24.4, 24.2, 23.4, 22.5, 22.5, 21.6, 20.9, 18.0, 14.4 ppm. **FT-IR** (neat, ν in cm^{-1}): 3366 (O-H), 1724 (C=O). **HRMS** (ESI): $\text{C}_{16}\text{H}_{31}\text{NO}_3$ $[\text{M}+\text{Na}]^+$: calculated, 308.2202; found, 308.2212.

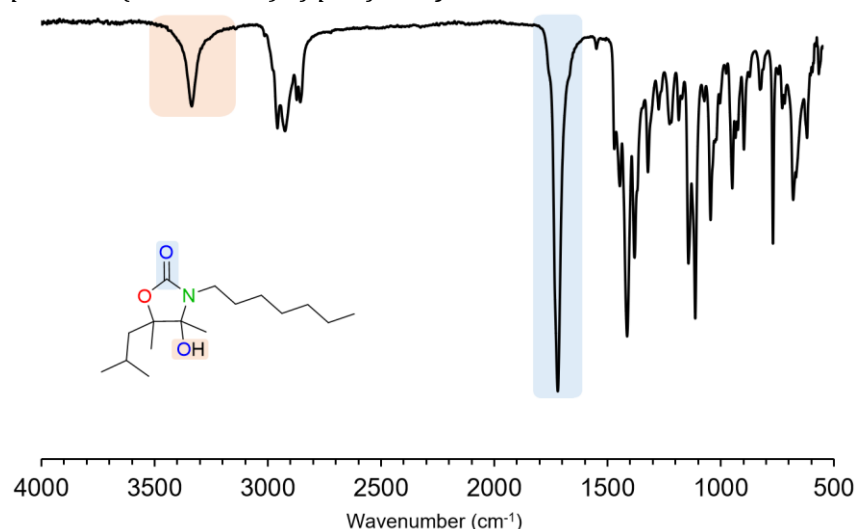
- $^1\text{H-NMR}$ spectrum (in $\text{DMSO-}d_6$) of purified **3f**.



- $^{13}\text{C-NMR}$ spectrum (in $\text{DMSO-}d_6$) of purified **3f**.



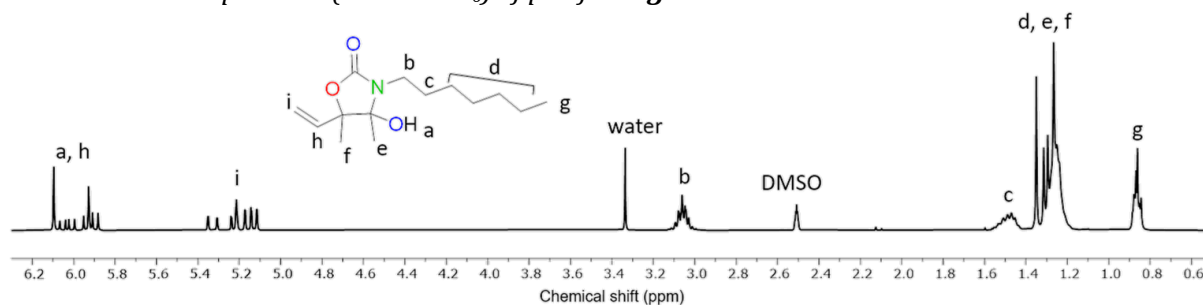
- **FT-IR** spectrum (in $\text{DMSO-}d_6$) of purified **3f**.



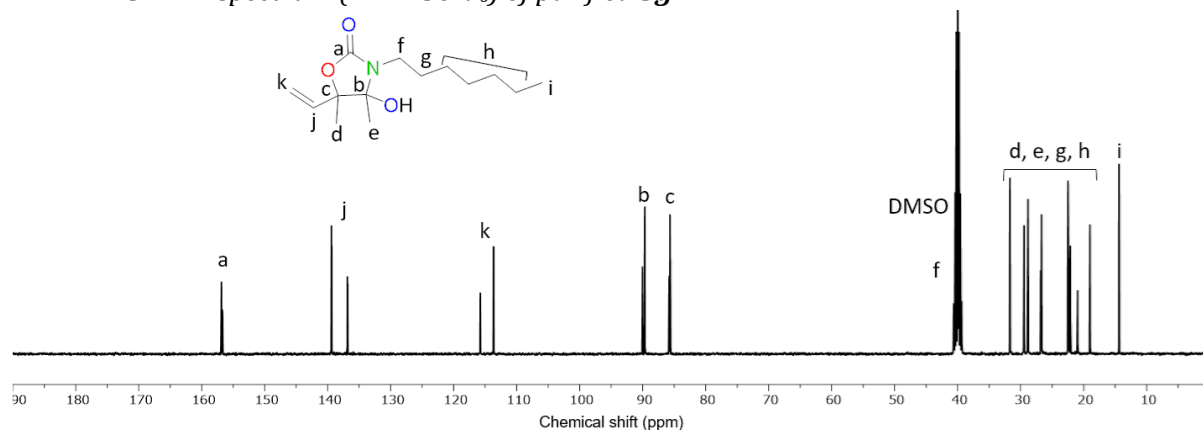
3-heptyl-4-hydroxy-4,5-dimethyl-5-vinyloxazolidin-2-one (3g): Synthesized according to the general procedure, white solid. $^1\text{H NMR}$ (400 MHz, $\text{DMSO-}d_6$) δ 6.12 – 5.86 (m, 2H), 5.26 – 5.09 (m, 2H), 3.06 (tt, $J = 7.3, 5.3$ Hz, 2H), 1.54 – 1.43 (m, 2H), 1.35 (s, 2H), 1.27 (dq, $J = 11.6, 6.4, 5.0$ Hz, 12H), 0.87 (td, $J = 6.9, 3.0$ Hz, 3H) ppm. $^{13}\text{C NMR}$ (400 MHz, $\text{DMSO-}d_6$) δ 156.9, 156.7, 139.4, 136.9, 115.8, 113.7, 90.0, 89.7, 85.8, 85.7, 40.0, 39.9, 31.7, 31.7, 29.5, 29.5, 28.9, 28.8, 26.8, 26.7, 22.5,

22.5, 22.4, 22.1, 21.0, 19.0, 14.4, 14.4 ppm. **FT-IR** (neat, ν in cm^{-1}): 3366 (O-H), 1724 (C=O). **HRMS** (ESI): $\text{C}_{14}\text{H}_{25}\text{NO}_3$ $[\text{M}+\text{Na}]^+$: calculated, 278.1732; found, 278.1734.

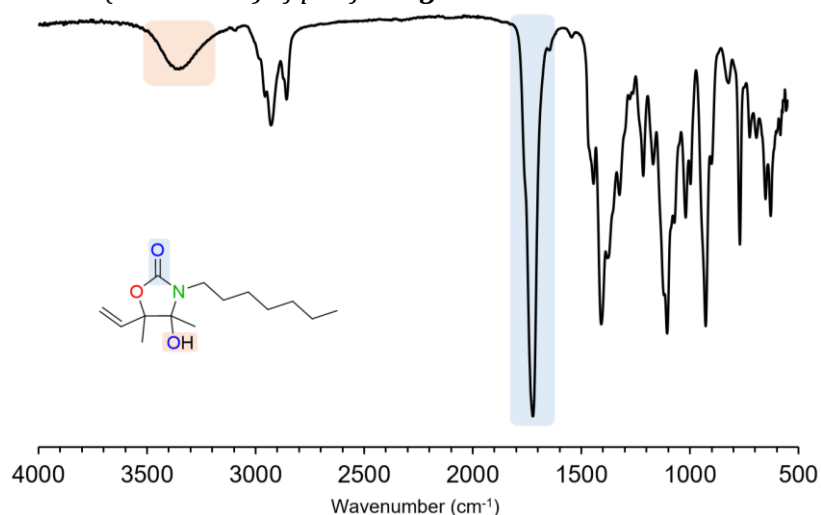
- $^1\text{H-NMR}$ spectrum (in DMSO-d_6) of purified **3g**.



- $^{13}\text{C-NMR}$ spectrum (in DMSO-d_6) of purified **3g**.

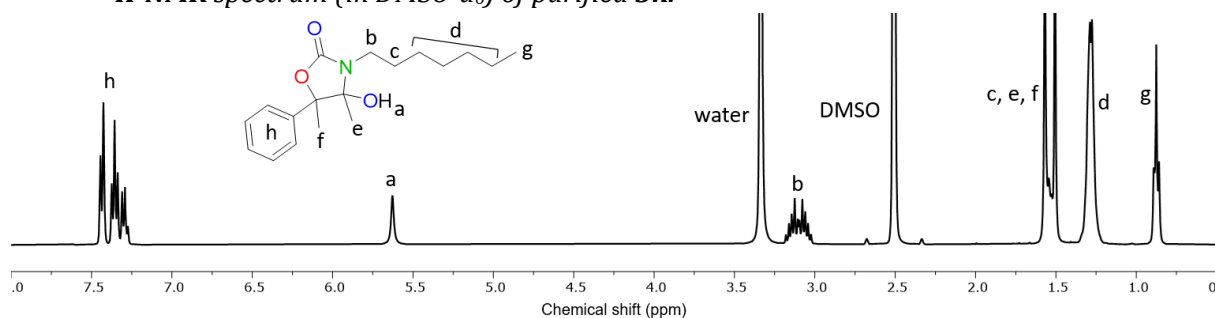


- **FT-IR** spectrum (in DMSO-d_6) of purified **3g**.

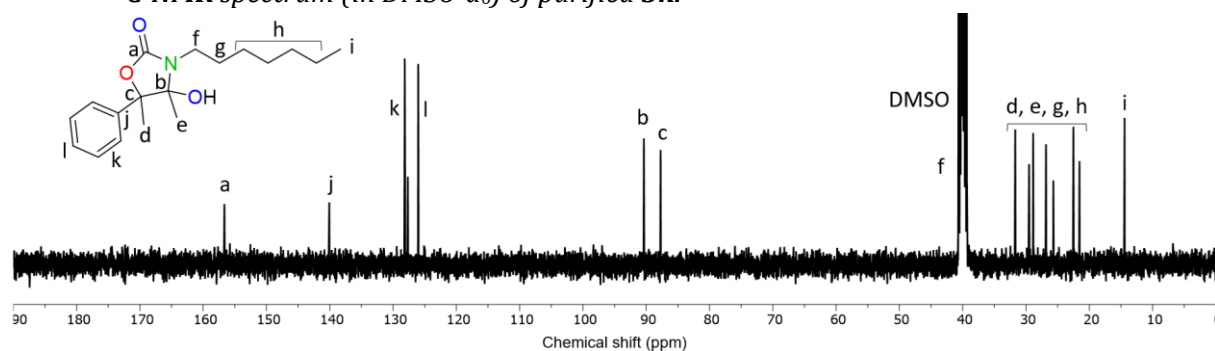


3-heptyl-4-hydroxy-4,5-dimethyl-5-phenyloxazolidin-2-one (3h): Synthesized according to the general procedure, white solid. $^1\text{H NMR}$ (400 MHz, DMSO-d_6) δ 7.40 – 7.27 (m, 3H), 5.63 (s, 1H), 3.20 – 3.00 (m, 2H), 1.54 (d, $J = 25.1$ Hz, 8H), 1.29 (dd, $J = 7.7, 4.4$ Hz, 8H), 0.91 – 0.84 (m, 3H) ppm. $^{13}\text{C NMR}$ (400 MHz, DMSO-d_6) δ 156.6, 140.1, 128.2, 127.7, 126.0, 90.4, 87.7, 40.0, 31.7, 29.5, 28.9, 26.8, 25.7, 22.5, 21.6, 14.4 ppm. **FT-IR** (neat, ν in cm^{-1}): 3366 (O-H), 1724 (C=O). **HRMS** (ESI): $\text{C}_{18}\text{H}_{27}\text{NO}_3$ $[\text{M}+\text{Na}]^+$: calculated, 328.1889; found, 328.1877.

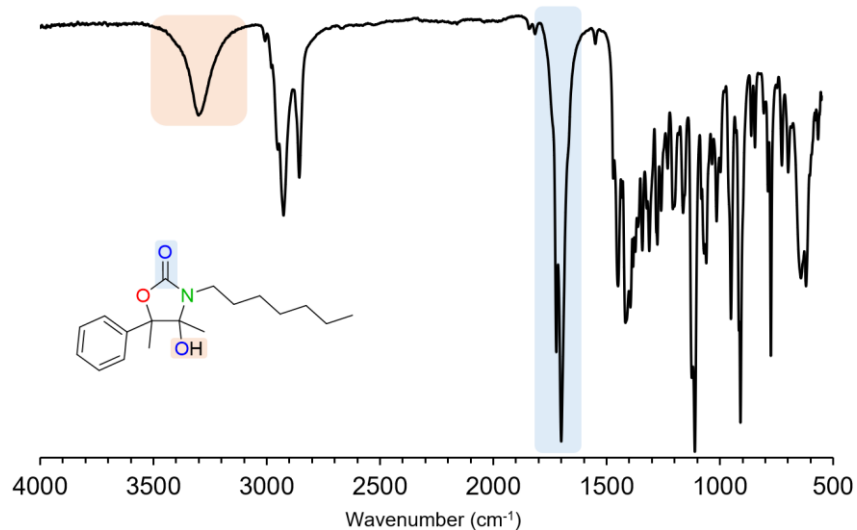
- $^1\text{H-NMR}$ spectrum (in DMSO-d_6) of purified **3h**.



- $^{13}\text{C-NMR}$ spectrum (in DMSO-d_6) of purified **3h**.

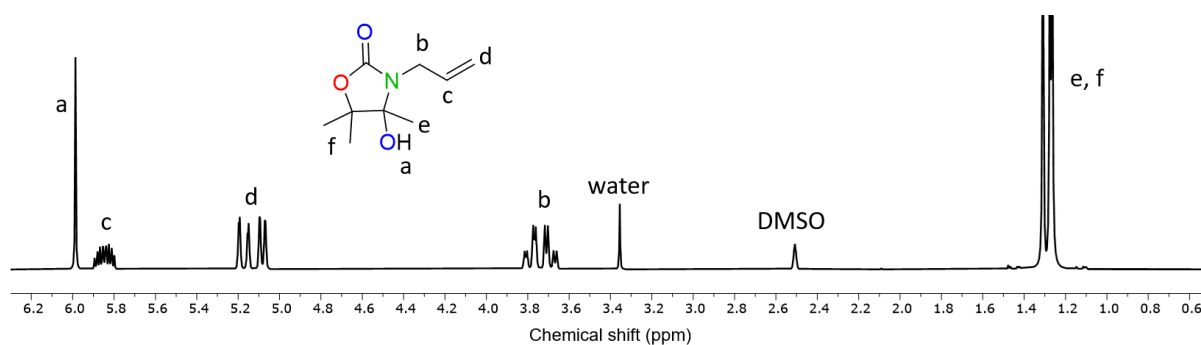


- FT-IR spectrum (in DMSO-d_6) of purified **3h**.

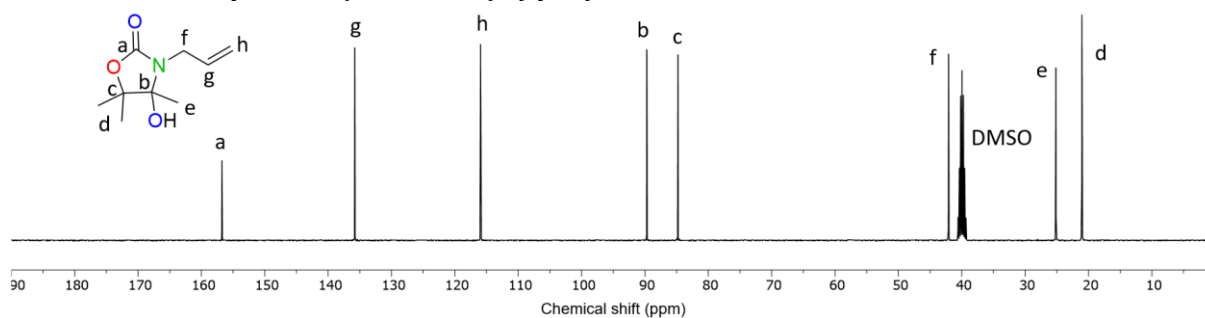


3-allyl-4-hydroxy-4,5,5-trimethyloxazolidin-2-one (3i): Synthesized according to the general procedure, white solid. $^1\text{H NMR}$ (400 MHz, DMSO-d_6) δ 5.99 (s, 1H), 5.85 (dddd, $J = 17.2, 10.5, 5.8, 4.8$ Hz, 1H), 5.17 (dq, $J = 17.2, 1.8$ Hz, 1H), 5.08 (dq, $J = 10.2, 1.6$ Hz, 1H), 3.79 (ddt, $J = 16.7, 4.9, 1.9$ Hz, 1H), 3.69 (ddt, $J = 16.7, 5.9, 1.6$ Hz, 1H), 1.31 (s, 3H), 1.27 (d, $J = 4.2$ Hz, 6H) ppm. $^{13}\text{C NMR}$ (400 MHz, DMSO-d_6) δ 156.8, 135.8, 115.9, 89.7, 84.8, 42.1, 25.2, 21.0, 21.0 ppm. FT-IR (neat, ν in cm^{-1}): 3366 (O-H), 1724 (C=O).

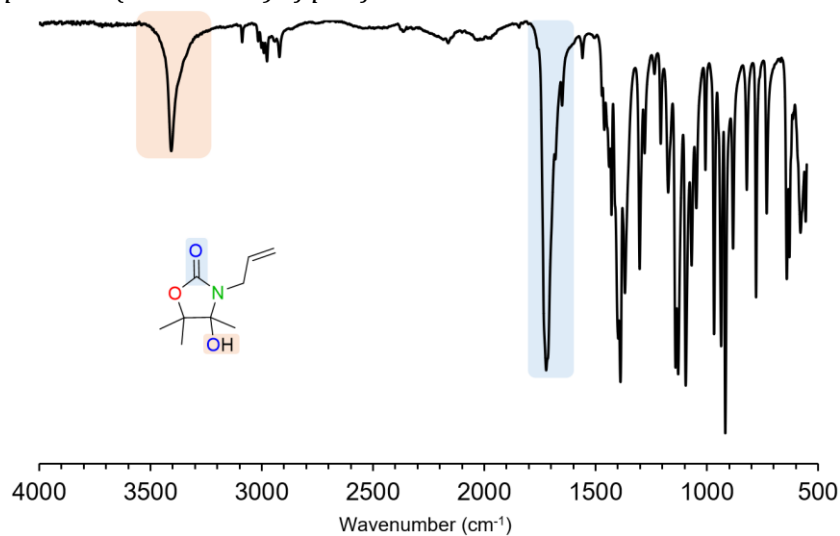
- $^1\text{H-NMR}$ spectrum (in DMSO-d_6) of purified **3i**.



- $^{13}\text{C-NMR}$ spectrum (in DMSO-d_6) of purified **3i**.

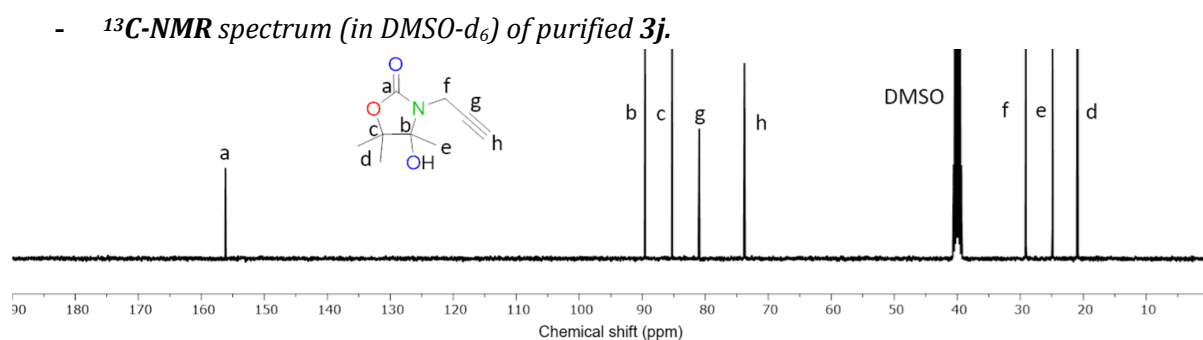
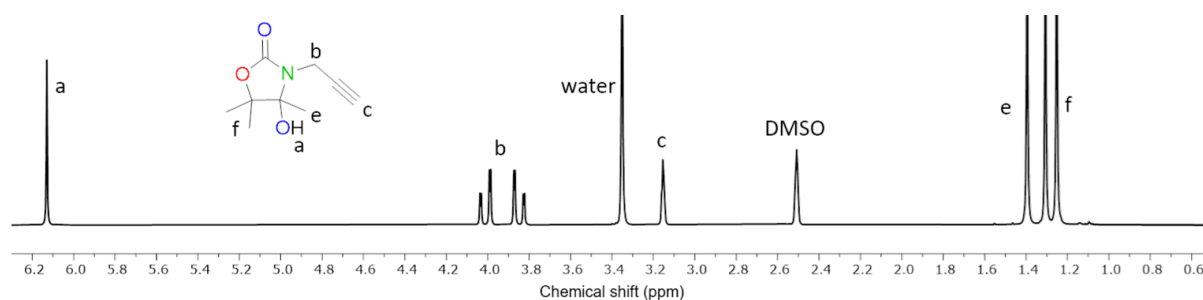


- **FT-IR** spectrum (in DMSO-d_6) of purified **3i**.

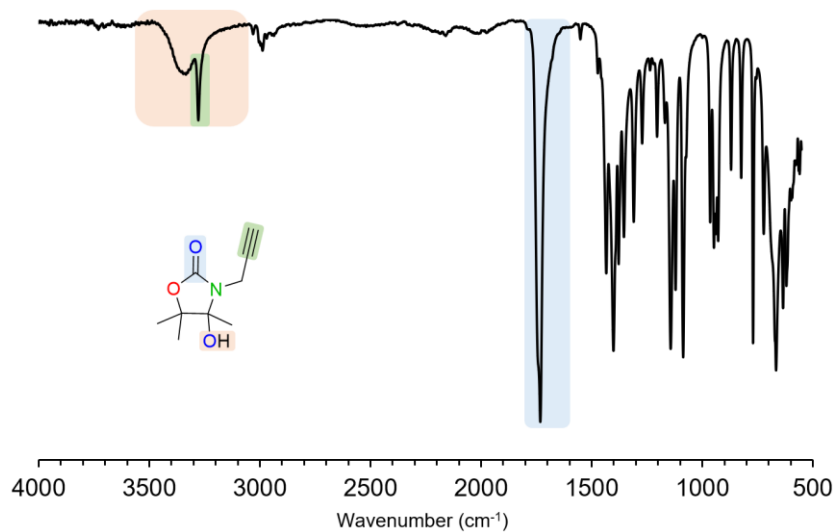


4-hydroxy-4,5,5-trimethyl-3-(prop-2-yn-1-yl)oxazolidin-2-one (3j): Synthesized according to the general procedure, white solid. $^1\text{H NMR}$ (400 MHz, DMSO-d_6) δ 6.13 (s, 1H), 4.01 (dd, $J = 18.2, 2.5$ Hz, 1H), 3.85 (dd, $J = 18.2, 2.5$ Hz, 1H), 3.15 (q, $J = 2.2$ Hz, 1H), 1.39 (s, 3H), 1.31 (s, 3H), 1.25 (s, 3H) ppm. $^{13}\text{C NMR}$ (400 MHz, DMSO-d_6) δ 156.2, 89.6, 85.3, 81.0, 73.8, 29.1, 24.9, 21.0, 20.9 ppm. **FT-IR** (neat, ν in cm^{-1}): 3366 (O-H), 3300 (Alkyne), 1724 (C=O).

- $^1\text{H-NMR}$ spectrum (in DMSO-d_6) of purified **3j**.

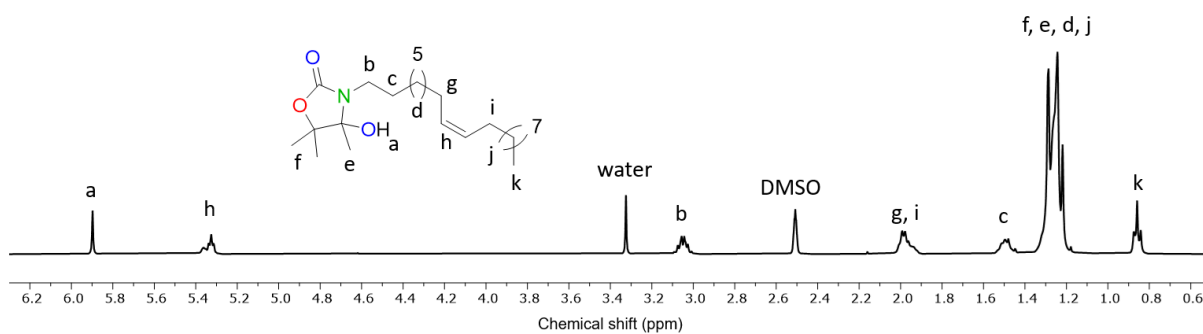


FT-IR spectrum (in DMSO-*d*₆) of purified **3j.**

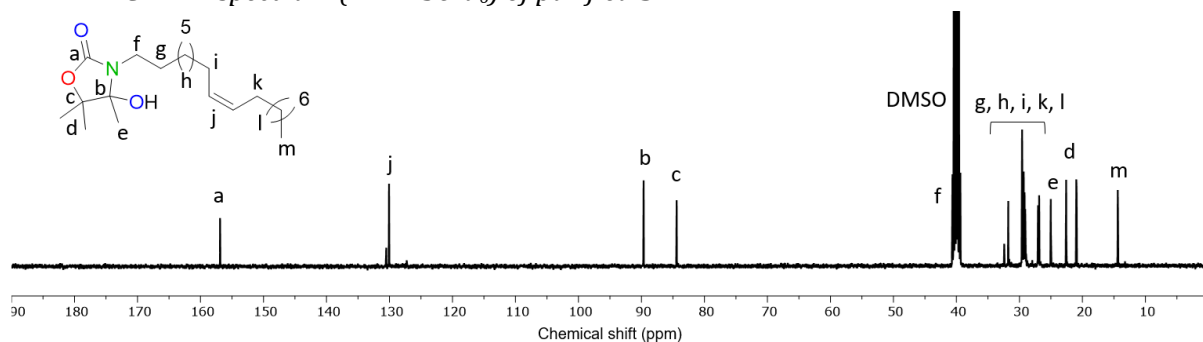


(Z)-4-hydroxy-4,5,5-trimethyl-3-(octadec-9-en-1-yl)oxazolidin-2-one (3k**):** Synthesized according to the general procedure, white solid. **¹H NMR** (400 MHz, DMSO-*d*₆) δ 5.90 (s, 1H), 5.34 (dt, $J = 14.9, 4.1$ Hz, 2H), 3.05 (td, $J = 7.2, 4.6$ Hz, 2H), 1.97 (dd, $J = 12.2, 5.9$ Hz, 4H), 1.55 – 1.42 (m, 2H), 1.34 – 1.20 (m, 31H), 0.86 (t, $J = 6.7$ Hz, 3H) ppm. **¹³C NMR** (400 MHz, DMSO-*d*₆) δ 156.9, 130.5, 130.1, 89.7, 84.4, 39.9, 32.4, 31.8, 29.6, 29.5, 29.5, 29.3, 29.2, 29.2, 29.1, 29.1, 27.1, 27.0, 26.9, 25.0, 22.6, 21.0, 20.9, 14.4 ppm. **FT-IR** (neat, ν in cm^{-1}): 3366 (O-H), 1724 (C=O).

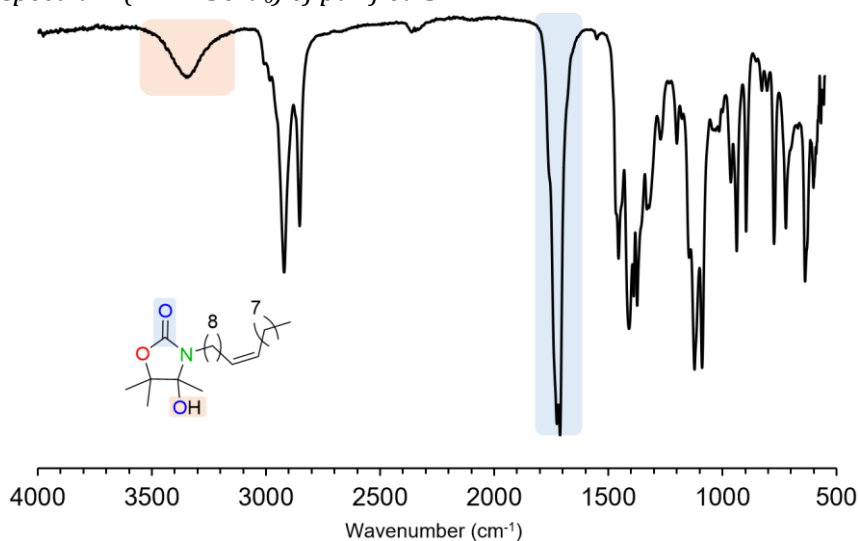
¹H-NMR spectrum (in DMSO-*d*₆) of purified **3k.**



- $^{13}\text{C-NMR}$ spectrum (in DMSO-d_6) of purified **3k**.

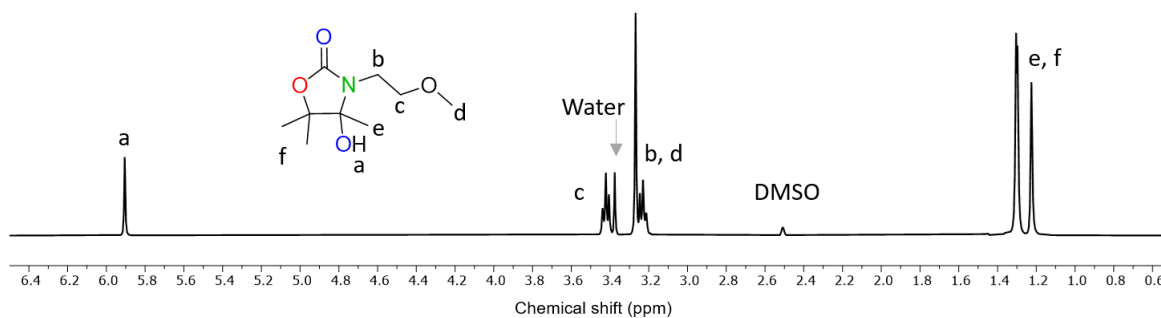


- **FT-IR** spectrum (in DMSO-d_6) of purified **3k**.

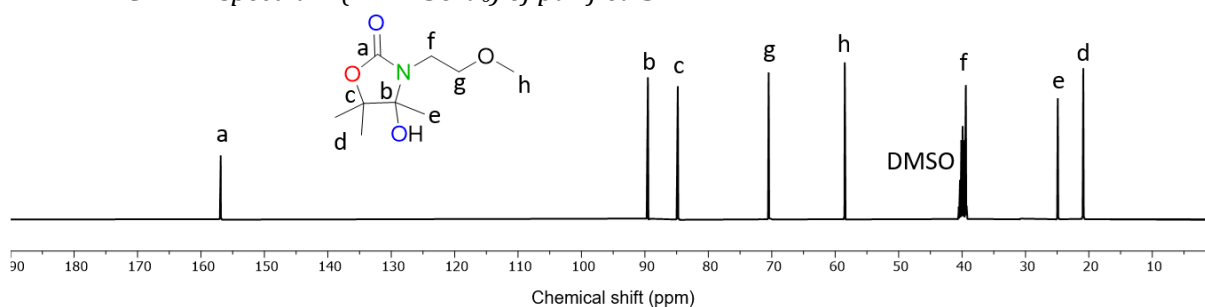


4-hydroxy-3-(2-methoxyethyl)-4,5,5-trimethyloxazolidin-2-one (3l): Synthesized according to the general procedure, white solid. $^1\text{H NMR}$ (400 MHz, DMSO-d_6) δ 5.91 (s, 1H), 3.42 (t, $J = 6.5$ Hz, 2H), 3.27 (s, 3H), 3.26 – 3.17 (m, 2H), 1.30 (d, $J = 3.2$ Hz, 6H), 1.22 (s, 3H) ppm. $^{13}\text{C NMR}$ (400 MHz, DMSO-d_6) δ 156.9, 89.5, 84.8, 70.5, 58.5, 39.4, 30.8, 24.9, 20.9, 20.9 ppm. **FT-IR** (neat, ν in cm^{-1}): 3366 (O-H), 1724 (C=O). **HRMS** (ESI): $\text{C}_9\text{H}_{17}\text{NO}_4$ $[\text{M}+\text{Na}]^+$: calculated, 226.1055; found, 226.1049.

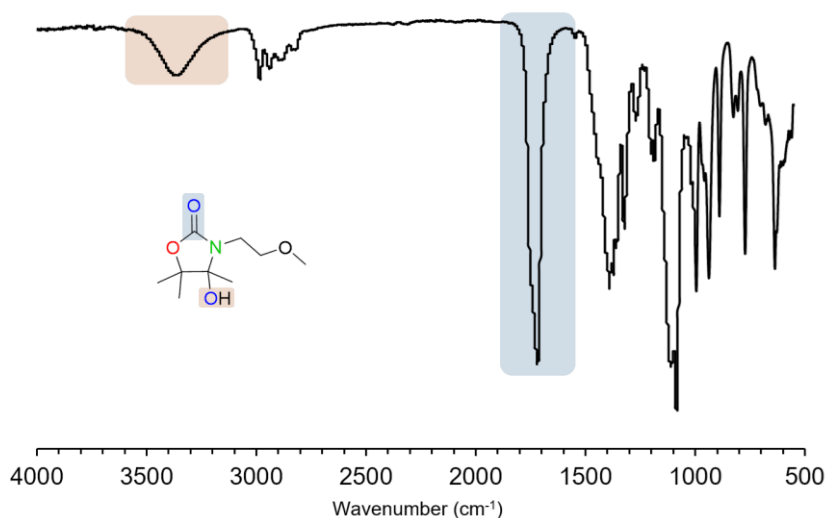
- $^1\text{H-NMR}$ spectrum (in DMSO-d_6) of purified **3l**.



- $^{13}\text{C-NMR}$ spectrum (in DMSO-d_6) of purified **3l**.



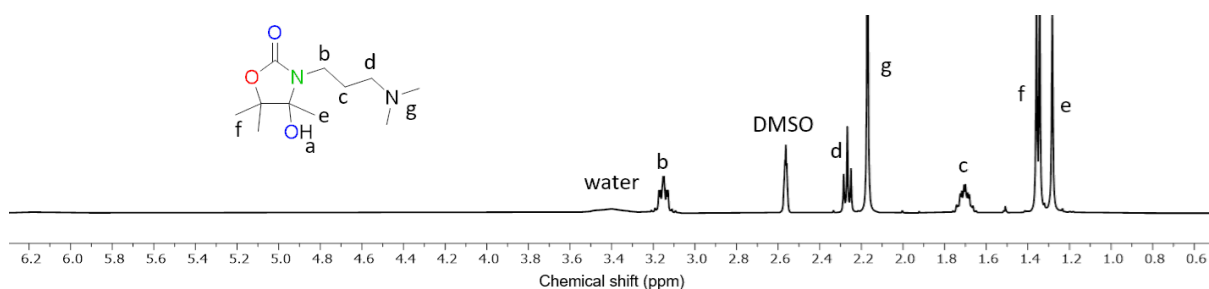
- **FT-IR** spectrum (in DMSO-d_6) of purified **3l**.



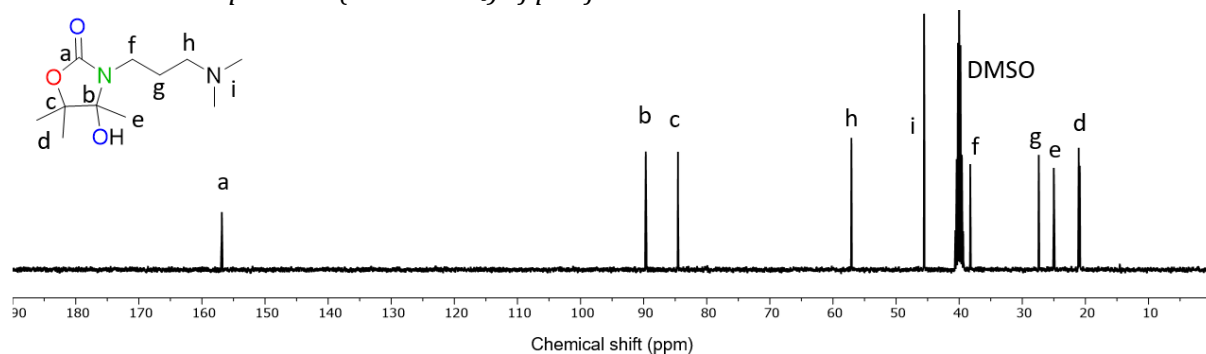
3-(3-(dimethylamino)propyl)-4-hydroxy-4,5,5-trimethyloxazolidin-2-one (3m):

Synthesized according to the general procedure, brown liquid. $^1\text{H NMR}$ (400 MHz, DMSO-d_6) δ 6.04 (s, 1H), 3.15 – 3.02 (m, 2H), 2.20 (t, J = 6.9 Hz, 2H), 2.11 (s, 6H), 1.70 – 1.58 (m, 2H), 1.29 (d, J = 6.1 Hz, 6H), 1.22 (s, 3H) ppm. $^{13}\text{C NMR}$ (400 MHz, DMSO-d_6) δ 156.9, 89.7, 84.6, 57.1, 45.6, 38.3, 27.4, 25.0, 21.1, 20.9 ppm. **FT-IR** (neat, ν in cm^{-1}): 3366 (O-H), 1724 (C=O).

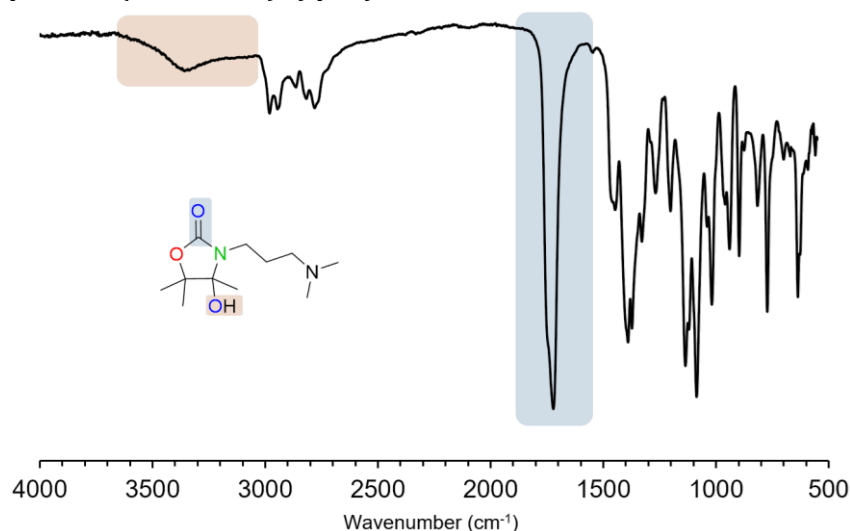
- $^1\text{H-NMR}$ spectrum (in DMSO-d_6) of purified **3m**. Purity level of 98 % with 1.5% of Intermediate (1.51 ppm, 6H), and <0.5% of ethyl acetate (1.99, 3H).



- $^{13}\text{C-NMR}$ spectrum (in DMSO-d_6) of purified **3m**.

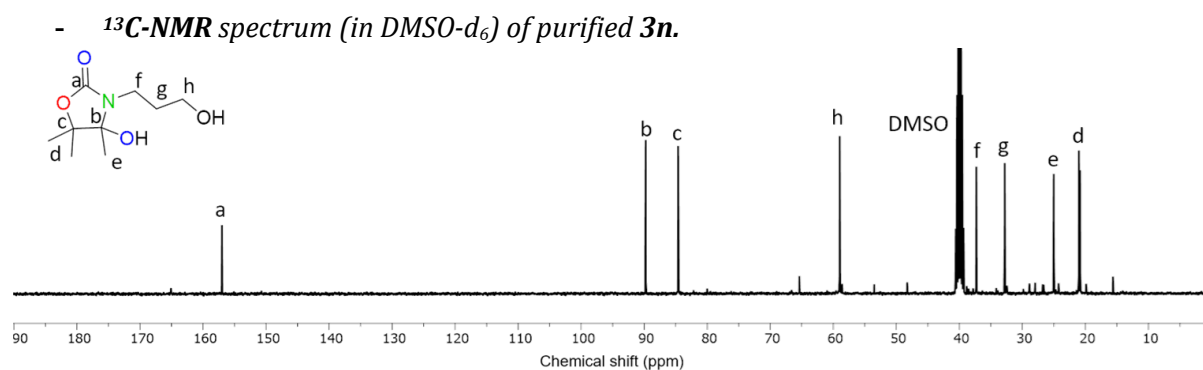
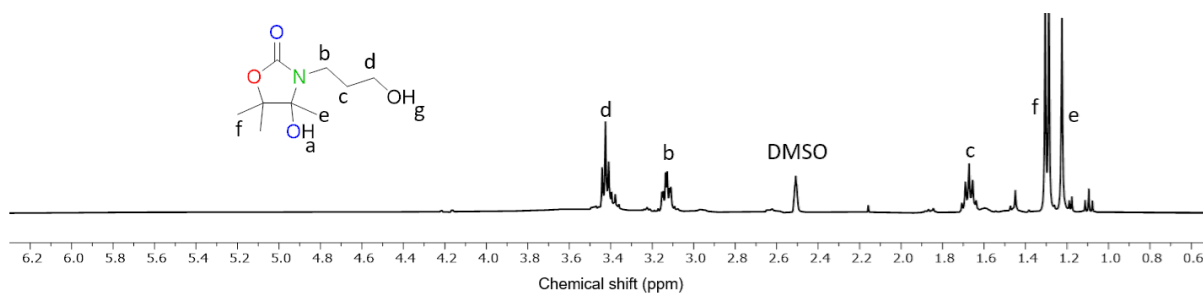


- **FT-IR** spectrum (in DMSO-d_6) of purified **3m**.

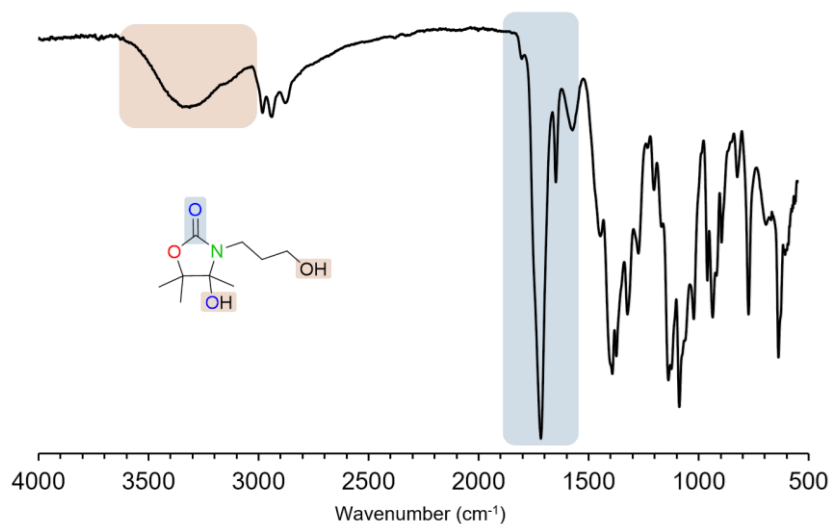


4-hydroxy-3-(3-hydroxypropyl)-4,5,5-trimethyloxazolidin-2-one (3n): Synthesized according to the general procedure, white solid. $^1\text{H NMR}$ (400 MHz, DMSO-d_6) δ 3.41 (dt, $J = 12.7, 6.7$ Hz, 2H), 3.13 (td, $J = 7.1, 2.7$ Hz, 2H), 1.73 – 1.61 (m, 2H), 1.30 (d, $J = 7.0$ Hz, 6H), 1.22 (s, 3H) ppm. $^{13}\text{C NMR}$ (400 MHz, DMSO-d_6) δ 157.0, 89.8, 84.6, 59.0, 37.3, 32.8, 25.0, 21.0, 20.8 ppm. **FT-IR** (neat, ν in cm^{-1}): 3366 (O-H), 1724 (C=O).

- $^1\text{H-NMR}$ spectrum (in DMSO-d_6) of purified **3n**. Purity level of 83 % with 4% Intermediate (1.44 ppm, 6H), with 2% of hydroxy ketone (2.15 ppm, 3H), and with 11% of diethyl ether (1.09 ppm, 3H).

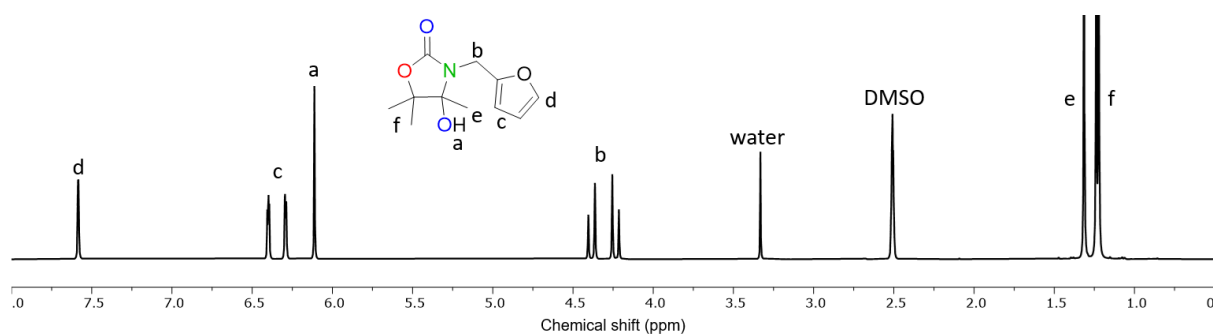


FT-IR spectrum (in DMSO-d₆) of purified **3n.**

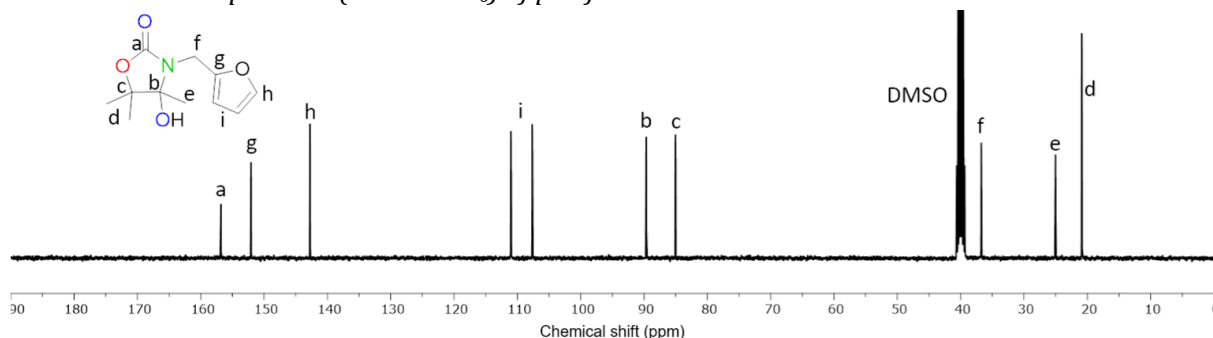


3-(furan-2-ylmethyl)-4-hydroxy-4,5,5-trimethyloxazolidin-2-one (3o**):** Synthesized according to the general procedure, white solid. **¹H NMR** (400 MHz, DMSO-d₆) δ 7.58 (dd, *J* = 1.8, 0.9 Hz, 1H), 6.40 (dd, *J* = 3.2, 1.8 Hz, 1H), 6.29 (dd, *J* = 3.0, 1.0 Hz, 1H), 6.11 (s, 1H), 4.38 (dd, *J* = 16.4, 1.0 Hz, 1H), 4.23 (d, *J* = 16.5 Hz, 1H), 1.31 (s, 3H), 1.23 (d, *J* = 6.2 Hz, 6H) ppm. **¹³C NMR** (400 MHz, DMSO-d₆) δ 156.8, 152.1, 142.7, 111.0, 107.7, 89.6, 85.0, 36.7, 25.0, 20.9 ppm. **FT-IR** (neat, ν in cm⁻¹): 3366 (O-H), 1724 (C=O).

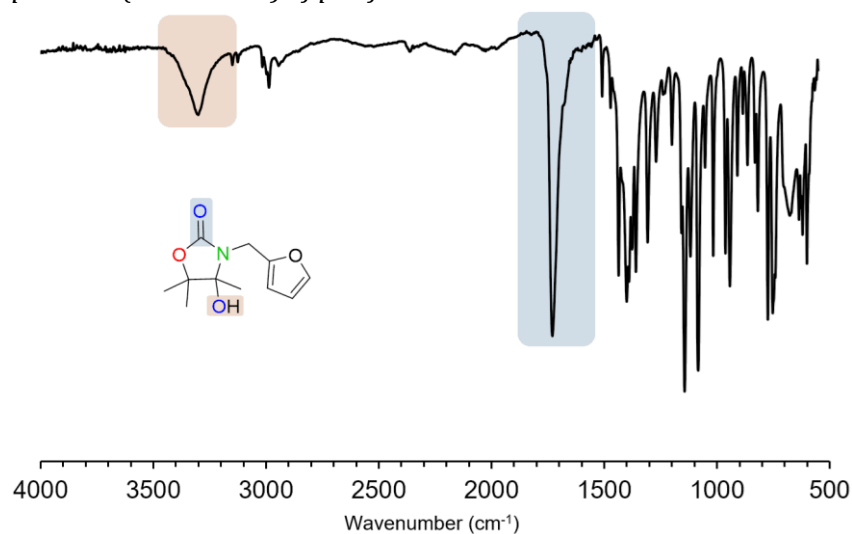
¹H-NMR spectrum (in DMSO-d₆) of purified **3o.**



- $^{13}\text{C-NMR}$ spectrum (in DMSO-d_6) of purified **3o**.



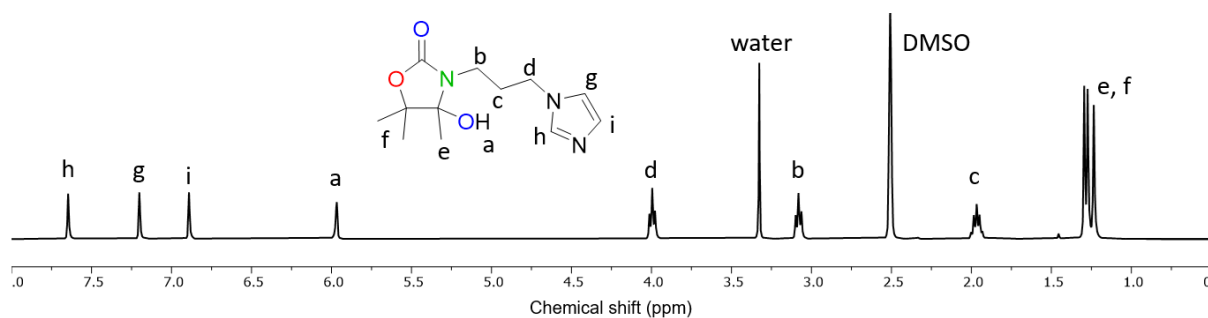
- **FT-IR** spectrum (in DMSO-d_6) of purified **3o**.



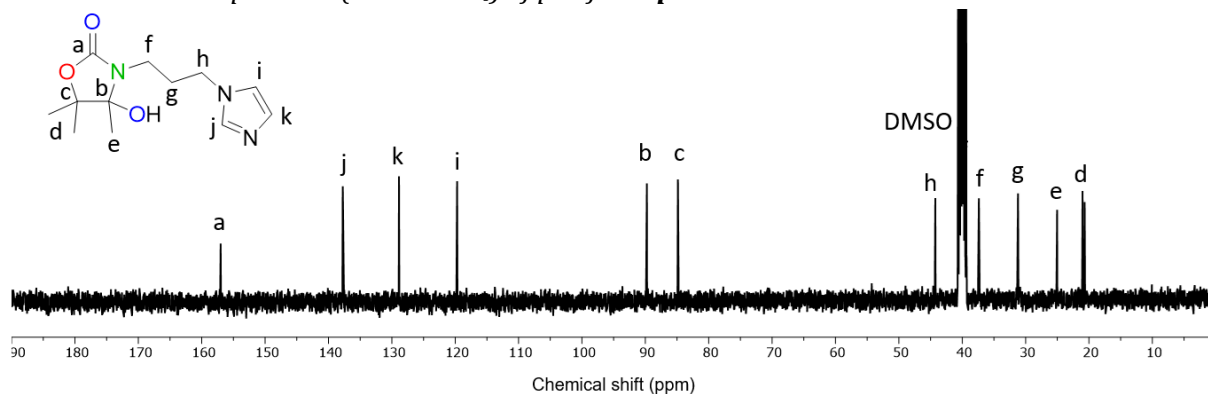
3-(3-(1H-imidazol-1-yl)propyl)-4-hydroxy-4,5,5-trimethyloxazolidin-2-one (3p):

Synthesized according to the general procedure, white solid. $^1\text{H NMR}$ (400 MHz, DMSO-d_6) δ 7.65 (d, $J = 1.2$ Hz, 1H), 7.20 (t, $J = 1.3$ Hz, 1H), 6.89 (d, $J = 1.2$ Hz, 1H), 5.98 (s, 1H), 4.00 (t, $J = 7.1$ Hz, 2H), 3.08 (t, $J = 7.2$ Hz, 2H), 1.97 (p, $J = 7.2$ Hz, 2H), 1.29 (d, $J = 8.6$ Hz, 6H), 1.24 (s, 3H) ppm. $^{13}\text{C NMR}$ (400 MHz, DMSO-d_6) δ 157.0, 137.7, 128.9, 119.7, 89.8, 84.9, 44.3, 37.4, 31.2, 25.0, 21.0, 20.7 ppm. **FT-IR** (neat, ν in cm^{-1}): 3366 (O-H), 1724 (C=O). **HRMS** (ESI): $\text{C}_{12}\text{H}_{19}\text{N}_3\text{O}_3$ $[\text{M}+\text{Na}]^+$: calculated, 254.1505; found, 254.1494.

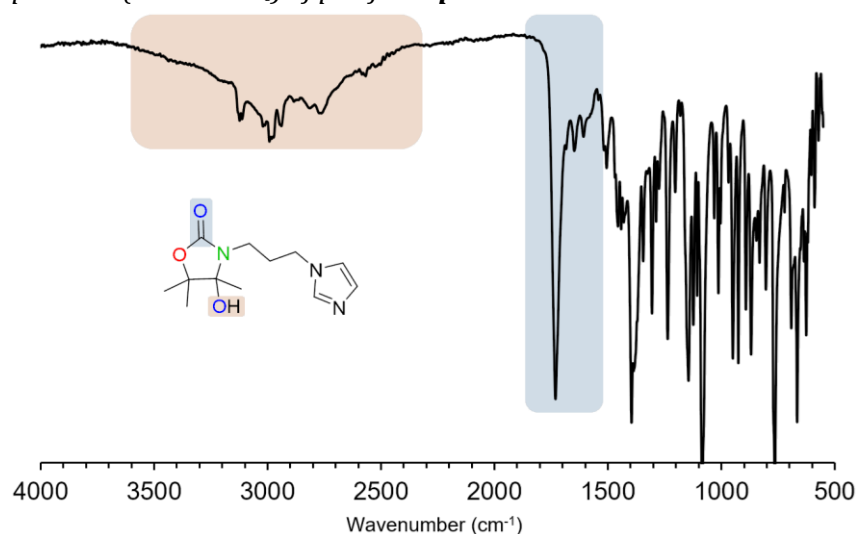
- $^1\text{H-NMR}$ spectrum (in DMSO-d_6) of purified **3p**.



- **¹³C-NMR spectrum (in DMSO-*d*₆) of purified **3p**.**

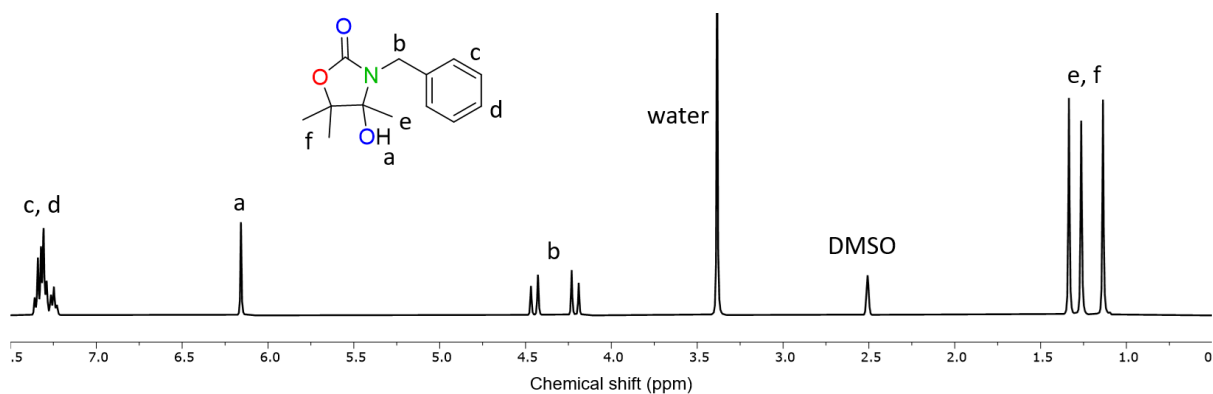


- **FT-IR spectrum (in DMSO-*d*₆) of purified **3p**.**

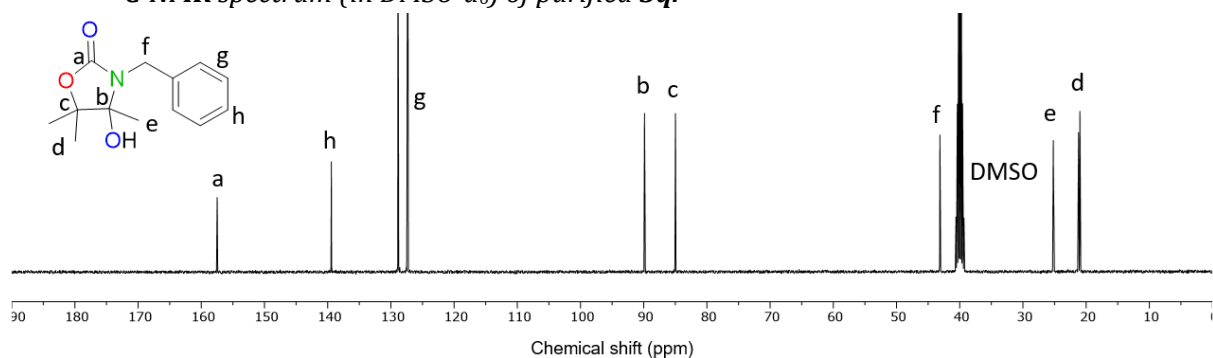


3-benzyl-4-hydroxy-4,5,5-trimethyloxazolidin-2-one (3q**):** Synthesized according to the general procedure, white solid. **¹H NMR** (400 MHz, DMSO-*d*₆) δ 7.34 (s, 1H), 7.31 (dd, $J = 7.6, 5.8$ Hz, 3H), 7.29 – 7.20 (m, 1H), 6.15 (s, 1H), 4.45 (d, $J = 16.2$ Hz, 1H), 4.21 (d, $J = 16.3$ Hz, 1H), 1.33 (s, 3H), 1.27 (s, 3H), 1.14 (s, 3H) ppm. **¹³C NMR** (400 MHz, DMSO-*d*₆) δ 157.5, 139.4, 128.9, 127.3, 89.9, 85.0, 43.1, 25.2, 21.2, 21.0 ppm. **FT-IR** (neat, ν in cm^{-1}): 3366 (O-H), 1724 (C=O).

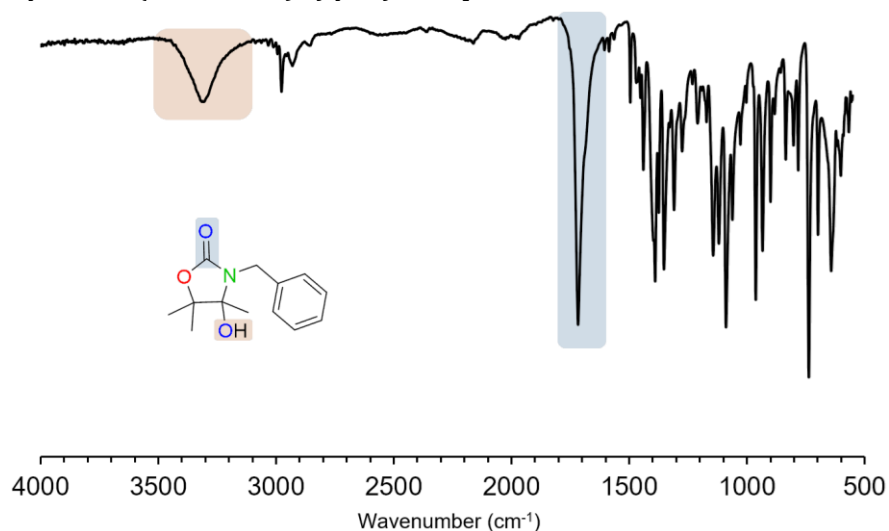
- **¹H-NMR spectrum (in DMSO-*d*₆) of purified **3q**.**



- $^{13}\text{C-NMR}$ spectrum (in DMSO-d_6) of purified **3q**.

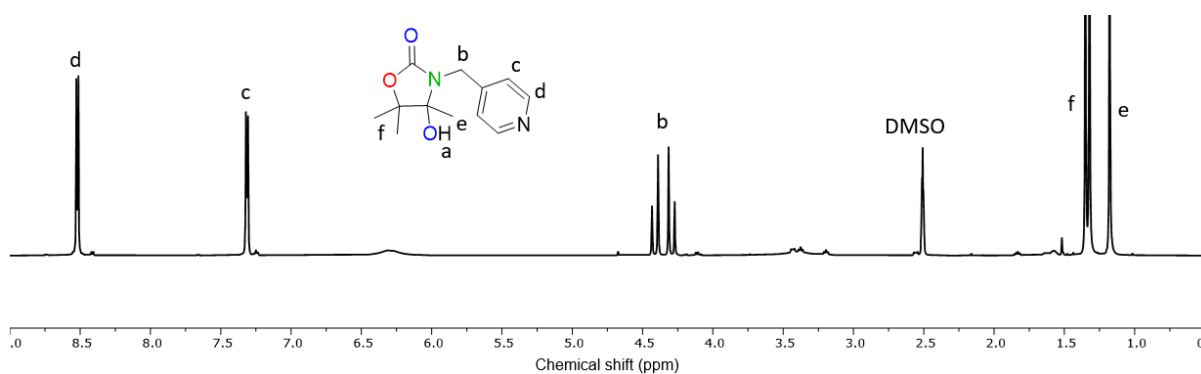


- **FT-IR** spectrum (in DMSO-d_6) of purified **3q**.

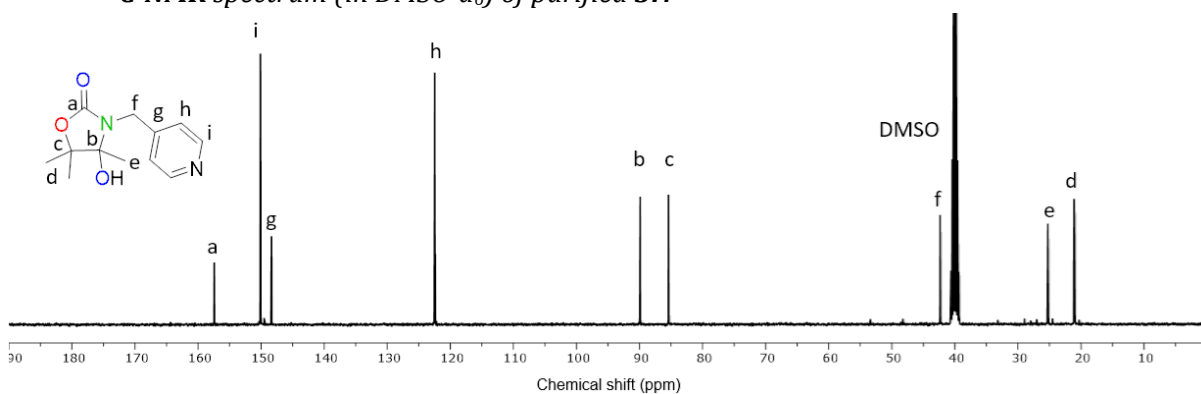


4-hydroxy-4,5,5-trimethyl-3-(pyridin-4-ylmethyl)oxazolidin-2-one (3r): Synthesized according to the general procedure, white solid. $^1\text{H NMR}$ (400 MHz, DMSO-d_6) δ 8.56 – 8.49 (m, 2H), 7.34 – 7.28 (m, 2H), 6.30 (s, 1H), 4.41 (d, $J = 17.0$ Hz, 1H), 4.29 (d, $J = 17.1$ Hz, 1H), 1.34 (d, $J = 11.5$ Hz, 6H), 1.18 (s, 3H) ppm. $^{13}\text{C NMR}$ (400 MHz, DMSO-d_6) δ 157.4, 150.1, 149.5, 148.4, 122.5, 89.9, 85.4, 42.3, 25.2, 21.1, 21.0 ppm. **FT-IR** (neat, ν in cm^{-1}): 3366 (O-H), 1724 (C=O). **HRMS** (ESI): $\text{C}_{12}\text{H}_{16}\text{N}_2\text{O}_3$ $[\text{M}+\text{Na}]^+$: calculated, 259.1059; found, 259.1066.

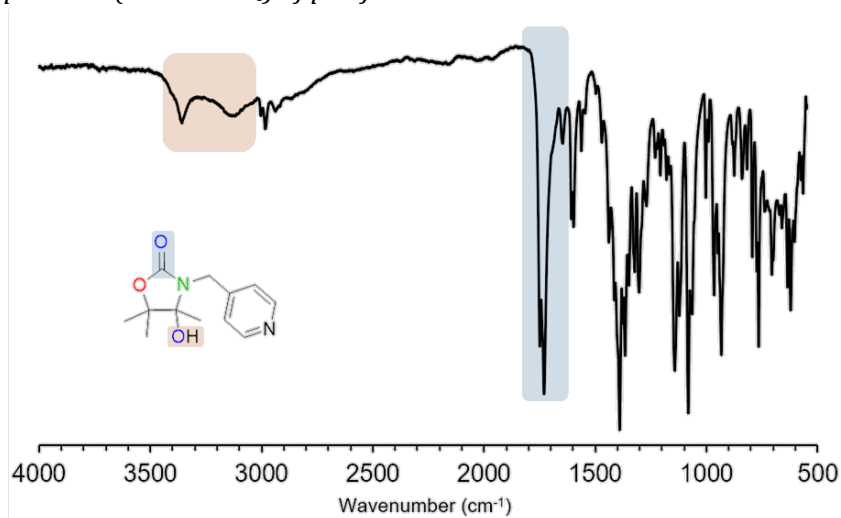
- $^1\text{H-NMR}$ spectrum (in DMSO-d_6) of purified **3r**.



- $^{13}\text{C-NMR}$ spectrum (in DMSO-d_6) of purified **3r**.

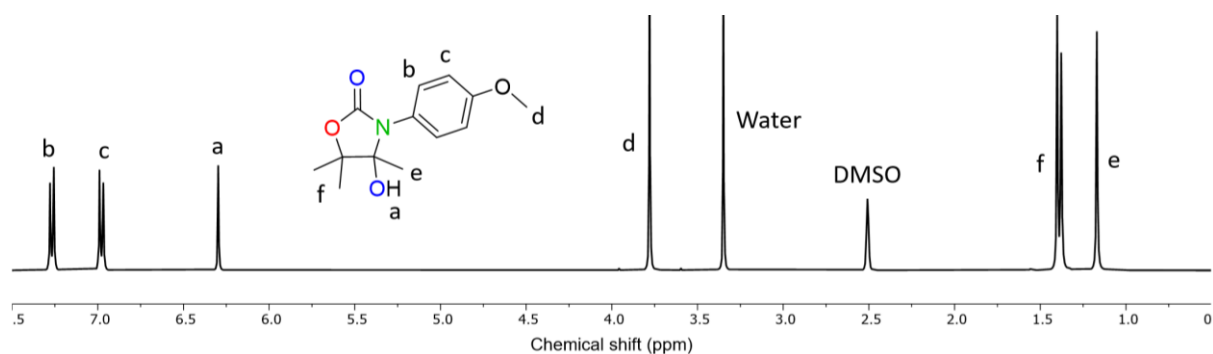


- **FT-IR** spectrum (in DMSO-d_6) of purified **3r**.

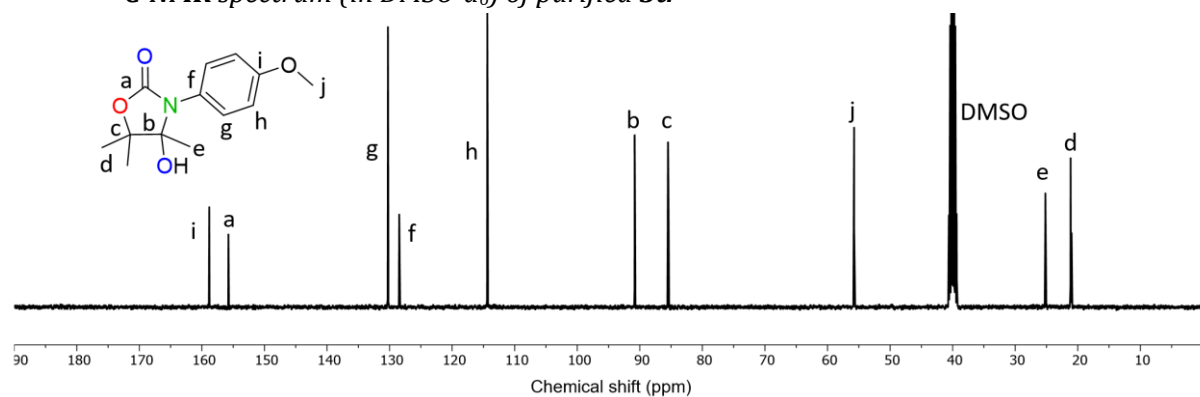


4-hydroxy-3-(4-methoxyphenyl)-4,5,5-trimethyloxazolidin-2-one (3t): Synthesized according to the general procedure, white solid. $^1\text{H NMR}$ (400 MHz, DMSO-d_6) δ 7.31 – 7.23 (m, 2H), 7.02 – 6.94 (m, 2H), 6.30 (s, 1H), 3.78 (s, 3H), 1.39 (d, $J = 9.5$ Hz, 6H), 1.17 (s, 3H) ppm. $^{13}\text{C NMR}$ (400 MHz, DMSO-d_6) δ 158.8, 155.8, 130.3, 128.5, 114.4, 90.8, 85.5, 55.8, 25.2, 21.1, 21.0 ppm. **FT-IR** (neat, ν in cm^{-1}): 3366 (O-H), 1724 (C=O).

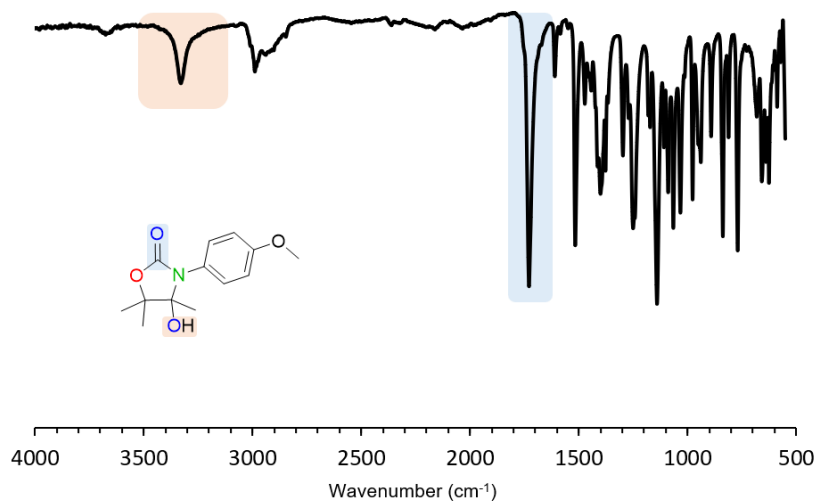
- $^1\text{H-NMR}$ spectrum (in DMSO-d_6) of purified **3t**.



- $^{13}\text{C-NMR}$ spectrum (in DMSO-d_6) of purified **3t**.



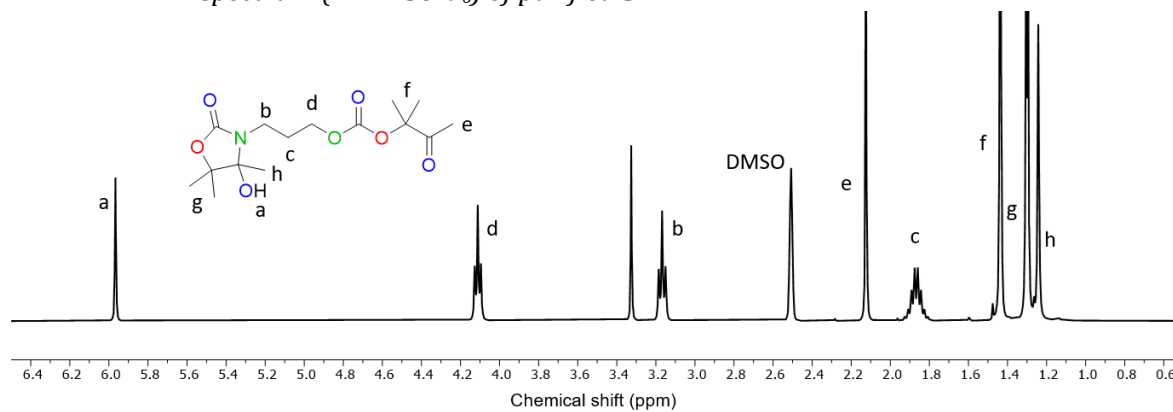
- *FT-IR* spectrum (in DMSO-d_6) of purified **3t**.



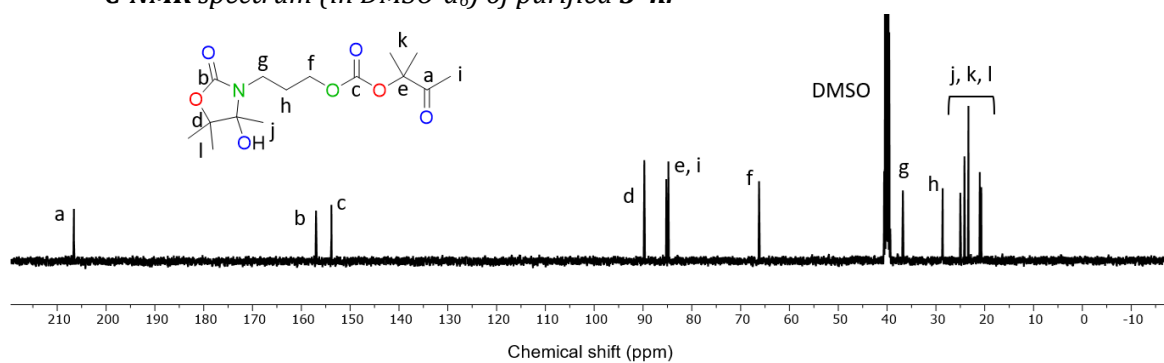
• ^1H , $^{13}\text{C-NMR}$ spectra of side product **3''n**

3-heptyl-4-hydroxy-4,5-dimethyl-5-vinylloxazolidin-2-one (3n): Synthesized according to the general procedure, white solid. $^1\text{H NMR}$ (400 MHz, DMSO-d_6) δ 5.97 (s, 1H), 4.11 (t, $J = 6.3$ Hz, 2H), 3.17 (d, $J = 14.0$ Hz, 2H), 2.12 (s, 3H), 1.95 – 1.79 (m, $J = 7.0$ Hz, 2H), 1.44 (s, 6H), 1.33 – 1.22 (m, 9H) ppm. $^{13}\text{C NMR}$ (400 MHz, DMSO-d_6) δ 206.6, 157.0, 153.8, 89.8, 85.2, 84.8, 66.2, 36.8, 28.6, 25.0, 24.2, 23.4, 21.0, 20.7 ppm.

- $^1\text{H-NMR}$ spectrum (in DMSO-d_6) of purified $3''\text{n}$.



- $^{13}\text{C-NMR}$ spectrum (in DMSO-d_6) of purified $3''\text{n}$.



7. References

- (1) Habets, T.; Siragusa, F.; Grignard, B.; Detrembleur, C. Advancing the Synthesis of Isocyanate-Free Poly(Oxazolidones)s: Scope and Limitations. *Macromolecules* **2020**, *53* (15), 6396–6408. <https://doi.org/10.1021/acs.macromol.0c01231>.
- (2) Frisch, M. J.; Trucks, G. W.; Schlegel, H. B.; Scuseria, G. E.; Robb, M. A.; Cheeseman, J. R.; Scalmani, G.; Barone, V.; Petersson, G. A.; Nakatsuji, H. Gaussian 16, Revision C.02; Gaussian, Inc. *Wallingford, CT* **2019**.
- (3) Chai, J.-D.; Head-Gordon, M. Long-Range Corrected Hybrid Density Functionals with Damped Atom–Atom Dispersion Corrections. *Phys. Chem. Chem. Phys.* **2008**, *10* (44), 6615. <https://doi.org/10.1039/b810189b>.
- (4) Ouhib, F.; Grignard, B.; Van Den Broeck, E.; Luxen, A.; Robeyns, K.; Van Speybroeck, V.; Jerome, C.; Detrembleur, C. A Switchable Domino Process for the Construction of Novel CO₂-Sourced Sulfur-Containing Building Blocks and Polymers. *Angewandte Chemie* **2019**, *131* (34), 11894–11899. <https://doi.org/10.1002/ange.201905969>.
- (5) Habets, T.; Olmedo-Martínez, J. L.; del Olmo, R.; Grignard, B.; Mecerreyes, D.; Detrembleur, C. Facile Access to CO₂-Sourced Polythiocarbonate Dynamic Networks And Their Potential As Solid-State Electrolytes For Lithium Metal Batteries. *ChemSusChem* **2023**, *16* (14), e202300225. <https://doi.org/10.1002/cssc.202300225>.
- (6) Siragusa, F.; Van Den Broeck, E.; Ocando, C.; Müller, A. J.; De Smet, G.; Maes, B. U. W.; De Winter, J.; Van Speybroeck, V.; Grignard, B.; Detrembleur, C. Access to Biorenewable and CO₂-Based Polycarbonates from Exovinylene Cyclic Carbonates. *ACS Sustainable Chem. Eng.* **2021**, *9* (4), 1714–1728. <https://doi.org/10.1021/acssuschemeng.0c07683>.
- (7) Mardirossian, N.; Head-Gordon, M. Thirty Years of Density Functional Theory in Computational Chemistry: An Overview and Extensive Assessment of 200 Density Functionals. *Molecular Physics* **2017**, *115* (19), 2315–2372. <https://doi.org/10.1080/00268976.2017.1333644>.
- (8) Cossi, M.; Rega, N.; Scalmani, G.; Barone, V. Energies, Structures, and Electronic Properties of Molecules in Solution with the C-PCM Solvation Model. *Journal of Computational Chemistry* **2003**, *24* (6), 669–681. <https://doi.org/10.1002/jcc.10189>.
- (9) Fukui, K. The Path of Chemical Reactions - the IRC Approach. *Acc. Chem. Res.* **1981**, *14* (12), 363–368. <https://doi.org/10.1021/ar00072a001>.
- (10) Hratchian, H. P.; Schlegel, H. B.; Dykstra, C. E.; Frenking, G.; Kim, K. S.; Scuseria, G. Theory and Applications of Computational Chemistry: The First 40 Years. *Dykstra, CE* **2005**, 195.

- (11) Hratchian, H. P.; Schlegel, H. B. Accurate Reaction Paths Using a Hessian Based Predictor–Corrector Integrator. *The Journal of Chemical Physics* **2004**, *120* (21), 9918–9924. <https://doi.org/10.1063/1.1724823>.
- (12) Hratchian, H. P.; Schlegel, H. B. Using Hessian Updating To Increase the Efficiency of a Hessian Based Predictor-Corrector Reaction Path Following Method. *J. Chem. Theory Comput.* **2005**, *1* (1), 61–69. <https://doi.org/10.1021/ct0499783>.
- (13) Zhao, Y.; Truhlar, D. G. Exploring the Limit of Accuracy of the Global Hybrid Meta Density Functional for Main-Group Thermochemistry, Kinetics, and Noncovalent Interactions. *J. Chem. Theory Comput.* **2008**, *4* (11), 1849–1868. <https://doi.org/10.1021/ct800246v>.
- (14) Luchini, G.; Alegre-Requena, J. V.; Funes-Ardoiz, I.; Paton, R. S. GoodVibes: Automated Thermochemistry for Heterogeneous Computational Chemistry Data. F1000Research April 24, 2020. <https://doi.org/10.12688/f1000research.22758.1>.
- (15) Bursch, M.; Mewes, J.-M.; Hansen, A.; Grimme, S. Best-Practice DFT Protocols for Basic Molecular Computational Chemistry. *Angewandte Chemie International Edition* **2022**, *61* (42), e202205735. <https://doi.org/10.1002/anie.202205735>.
- (16) Habets, T.; Méreau, R.; Siragusa, F.; Grignard, B.; Detrembleur, C. Fast, Regioselective Aminolysis of Tetrasubstituted Cyclic Carbonates and Application to Recyclable Thermoplastics and Thermosets. *ACS Macro Lett.* **2024**, *13* (11), 1425–1432. <https://doi.org/10.1021/acsmacrolett.4c00570>.